MECHANISTIC-EMPIRICAL PAVEMENT DESIGN GUIDE CALIBRATION FOR PAVEMENT REHABILITATION

Final Report

SPR 718

MECHANISTIC-EMPIRICAL PAVEMENT DESIGN GUIDE CALIBRATION FOR PAVEMENT REHABILITATION

Final Report

SPR 718

by

Dr R. Chris Williams and R. Shaidur
Institute for Transportation
Iowa State University,
2711 South Loop Drive, Suite 4700
Ames, IA 50010-8664

for

Oregon Department of Transportation
Research Section
555 13th St
Salem OR 97301

and

Federal Highway Administration
400 Seventh Street, SW
Washington, DC 20590-0003

January 2013

Technical Report Documentation Page

1. Report No.	2. Government Accession No.	3. Recipient's Catalog No.

4. Title and Subtitle	5. Report Date
Mechanistic-Empirical Pavement Design Guide Calibration for Pavement Rehabilitation	January 2013
	6. Performing Organization Code
7. Author(s)	8. Performing Organization Report No.
Dr R. Chris Williams and R. Shaidur	
9. Performing Organization Name and Address	10. Work Unit No. (TRAIS)
Institute for Transportation Iowa State University, 2711 South Loop Drive, Suite 4700 Ames, IA 50010-8664	
	11. Contract or Grant No.
	SPR 718
12. Sponsoring Agency Name and Address	13. Type of Report and Period Covered
Oregon Department of Transportation Research Section and Federal Highway Administration 200 Hawthorne Ave. SE, Suite B-240 400 Seventh Street, SW Salem, OR 97301-5192 Washington, DC 20590-0003	Final Report
	14. Sponsoring Agency Code
15. Supplementary Notes	

16. Abstract

The Oregon Department of Transportation (ODOT) is in the process of implementing the recently introduced AASHTO Mechanistic-Empirical Pavement Design Guide (MEPDG) for new pavement sections. The majority of pavement work conducted by ODOT involves rehabilitation of existing pavements. Hot mix asphalt (HMA) overlays are preferred for both flexible and rigid pavements. However, HMA overlays are susceptible to fatigue cracking (alligator and longitudinal cracking), rutting, and thermal cracking. This study conducted work to calibrate the design process for rehabilitation of existing pavement structures. Forty-four pavement sections throughout Oregon were included. A detailed comparison of predictive and measured distresses was made using MEPDG software Darwin M-E (Version 1.1). It was found that Darwin M-E predictive distresses did not accurately reflect measured distresses, calling for a local calibration of performance prediction models. Darwin M-E over predicted total rutting compared to the measured total rutting and most of the rutting predicted by Darwin M-E occurs in the subgrade. For alligator (bottom-up) and thermal cracking, Darwin M-E underestimated the amount of cracking considerably as compared to in-field measurements. A high amount of variability between predicted and measured values was observed for longitudinal (top-down) cracking. The performance (punch-out) model was also assessed for continuously reinforced concrete pavement (CRCP) using Darwin M-E's default (nationally calibrated) coefficients.

Four distress prediction models (rutting, alligator, longitudinal, and thermal cracking) of the HMA overlays were calibrated for Oregon conditions. It was found that the locally calibrated models for rutting, alligator, and longitudinal cracking provided better predictions with lower bias and standard error than the nationally (default) calibrated models. However, there was a high degree of variability between the predicted and measured distresses, especially for longitudinal and transverse cracking, even after the calibration. It is believed that there is a significant lack-of-fit modeling error for the occurrence of longitudinal cracks. The Darwin M-E calibrated models of rutting and alligator cracking can be implemented, however, it is recommended that additional sites be established and included in the future calibration efforts to improve the accuracy of the prediction models.

17. Key Words	18. Distribution Statement
Pavement, hot mix asphalt, HMA, overlays, MEPDG, Darwin M-E, calibration, rutting, alligator cracking, longitudinal cracking, thermal cracking	Copies available from NTIS, and online at http://www.oregon.gov/ODOT/TD/TP_RES/

19. Security Classification (of this report)	20. Security Classification (of this page)	21. No. of Pages	22. Price
Unclassified	Unclassified		

SI* (MODERN METRIC) CONVERSION FACTORS

APPROXIMATE CONVERSIONS TO SI UNITS

Symbol	When You Know	Multiply By	To Find	Symbol
	LENGTH			
in	inches	25.4	millimeters	mm
ft	feet	0.305	meters	m
yd	yards	0.914	meters	m
mi	miles	1.61	kilometers	km
	AREA			
in^2	square inches	645.2	millimeters squared	mm^2
ft^2	square feet	0.093	meters squared	m^2
yd^2	square yards	0.836	meters squared	m^2
ac	acres	0.405	hectares	ha
mi^2	square miles	2.59	kilometers squared	km^2
	VOLUME			
fl oz	fluid ounces	29.57	milliliters	ml
gal	gallons	3.785	liters	L
ft^3	cubic feet	0.028	meters cubed	m^3
yd^3	cubic yards	0.765	meters cubed	m^3
	NOTE: Volumes greater than 1000 L shall be shown in m^3.			
	MASS			
oz	ounces	28.35	grams	g
lb	pounds	0.454	kilograms	kg
T	short tons (2000 lb)	0.907	megagrams	Mg
	TEMPERATURE (exact)			
°F	Fahrenheit	(F-32)/1.8	Celsius	°C

APPROXIMATE CONVERSIONS FROM SI UNITS

Symbol	When You Know	Multiply By	To Find	Symbol
	LENGTH			
mm	millimeters	0.039	inches	in
m	meters	3.28	feet	ft
m	meters	1.09	yards	yd
km	kilometers	0.621	miles	mi
	AREA			
mm^2	millimeters squared	0.0016	square inches	in^2
m^2	meters squared	10.764	square feet	ft^2
m^2	meters squared	1.196	square yards	yd^2
ha	hectares	2.47	acres	ac
km^2	kilometers squared	0.386	square miles	mi^2
	VOLUME			
ml	milliliters	0.034	fluid ounces	fl oz
L	liters	0.264	gallons	gal
m^3	meters cubed	35.315	cubic feet	ft^3
m^3	meters cubed	1.308	cubic yards	yd^3
	MASS			
g	grams	0.035	ounces	oz
kg	kilograms	2.205	pounds	lb
Mg	megagrams	1.102	short tons (2000 lb)	T
	TEMPERATURE (exact)			
°C	Celsius	1.8C+32	Fahrenheit	°F

*SI is the symbol for the International System of Measurement

ACKNOWLEDGEMENTS

This research was sponsored by the Oregon Department of Transportation (ODOT) and the Federal Highway Administration (FHWA) under this project titled "Mechanistic Design Guide Calibration for Pavement Rehabilitation". The authors gratefully acknowledge Oregon State University (OSU) and ODOT engineers for all the technical assistance and data provided. This research study would not have been possible without the contribution of a number of individuals. The authors would like to acknowledge the significant efforts of Tim Link from OSU and the technical advisory panel members Justin G. Moderie (Chair), John Coplantz, Larry Ilg, and Anthony Bosen. The authors would also like to extend their gratitude toward Jon Lazarus (project coordinator) for his cooperation and assistance provided throughout this research. The contents of this paper reflect the views of the authors, who are responsible for the accuracy of the facts and data presented herein, and do not necessarily reflect the official policies of the ODOT and FHWA. This paper does not constitute a standard, specification, or regulation.

DISCLAIMER

TABLE OF CONTENTS

LIST OF TABLES

LIST OF PHOTOS/FIGURES

1.0 INTRODUCTION

1.1 BACKGROUND

The new Mechanistic-Empirical Pavement Design Guide (MEPDG) and software were developed through the National Cooperative Highway Research Program (NCHRP) 1-37A project in recognition of the limitations of the current American Association of State Highway and Transportation Officials (AASHTO) Design Guide (*NCHRP 2004*). It represents a transitioning of the empirically-based pavement design to a mechanistic-empirical procedure that combines the strengths of advanced analytical modeling and observed field performance. The pavement performance prediction models in the MEPDG were calibrated primarily using design inputs and performance data largely from the national Long-Term Pavement Performance (LTPP) database. However, these performance prediction models warrant detailed validation and calibration because of potential differences between national and local conditons. Therefore, it is necessary to calibrate these performance prediction models for implementation in local conditions by taking into account local material properties, traffic patterns, environmental conditions, construction, and maintenance activities.

The importance of local calibration of performance prediction models contained in MEPDG is well-documented by different transportation agencies throughout the United States. Hall (*Hall et al. 2011*) conducted a local calibration of performance prediction models in MEPDG for Arkansas. Rutting and alligator (bottom-up) cracking models were successfully calibrated, however, longitudinal (top-down) cracking and thermal (transverse) cracking models were not calibrated due to the nature of data. Souliman (*Souliman et al. 2010*) calibrated distress models for alligator cracking, longitudinal cracking, rutting, and roughness for hot mix asphalt (HMA) pavements for Arizona using 39 LTPP pavement sections. It was found that national calibrated MEPDG under predicted alligator cracking and AC rutting while the longitudinal cracking and the subgrade rutting were over predicted. Significant improvement of performance prediction for alligator cracking and AC rutting resulted after calibration; however, only marginal improvement was realized for longitudinal cracking and roughness models. Hoegh (*Hoegh et al. 2010*) conducted a local calibration of the rutting model for MnROAD test sections. They concluded that the locally calibrated model greatly improved the MEPDG rutting prediction for various pavement designs in MnROAD conditions. A study by Von Quintus (*Von Quintus 2008*) found that the measurement error of the performance data had the greatest effect on the precision of MEPDG performance models. MEPDG performance models were verified for Iowa using Pavement Management Information System (PMIS) data (*Kim et al. 2010*). Systematic differences were observed for rutting and cracking models. Muthadi and Kim (*Muthadi and Kim 2008*) performed the MEPDG calibration for HMA pavements located in North Caorlina (NC) using version 1.0 of the MEPDG software. Two distress models, rutting and alligator cracking, were used for this effort. This study concluded that the standard error for the rutting model and the alligator cracking model was significantly lower after the calibration.

The properly calibrated MEPDG will enable more economical designs as well as potentially linking pavement design with actual material characteristics-, and construction processes. Further, as newer technologies and materials are developed, characterization of their material properties will expedite their use in the MEPDG. Several examples exist including the use of warm mix asphalt, post consumer asphalt roofing shingles in asphalt mixtures, and the evaluation of other technologies such as additives and modifiers.

It is imperative that performace prediction models contained in MEPDG be properly calibrated to local conditions prior to adopting and using them for design purposes (*ARA 2007*). The local calibration process involves three important steps: verification, calibration, and validation. The term verification refers to assessing the accuracy of the nationally (default) calibrated prediction models for local conditions. The term calibration refers to the mathematical process through which the total error or difference between observed and predicted values of performance is minimized. The term validation refers to the process to confirm that the locally calibrated performance prediction models can produce robust and accurate predictions for cases other than those used for model calibration.

1.2 THE NEED FOR LOCAL CALIBRATION

The Oregon Department of Transportation (ODOT) is in the process of implementing the new Mechanistic-Empirical pavement design guide (MEPDG) for new pavement sections. Internally, ODOT has been evaluating the MEPDG for new sections for both hot mix asphalt and Portland cement concrete interstate pavement sections. Work is also currently being conducted at Oregon State University to develop design inputs and evaluate the three principal pavement performance models (e.g., fatigue cracking, rutting, and thermal cracking models) that are integral to the design process of new work sections for asphalt concrete (AC) pavement structures. However, the vast majority of pavement work conducted by ODOT involves rehabilitation of existing pavements. Additional work is therefore needed to calibrate the design process for rehabilitation of existing pavement structures.

Asphalt mix overlays are the preferred rehabilitation treatment for both hot mix asphalt (HMA) and Portland cement concrete (PCC) pavements in Oregon. However, like new work sections, overlays are also susceptible to fatigue cracking (both alligator and longitudinal cracking), rutting, and thermal cracking (transverse cracking) - thus, the need to include these forms of distress in the calibration process.

1.3 REPORT ORGANIZATION

The overall objective of the research is to provide ODOT with pavement performance models for AC overlays that can predict alligator (bottom-up) cracking, longitudinal (top-down) cracking, rutting, and thermal (transverse) cracking calibrated to Oregon conditions. And, verification runs on the CRCP pavement sections will also be done to assess the nationally calibrated performance prediction model. The tasks toward the accomplishment of the objective are presented step by step in the next seven chapters. The background and the need for local calibration were presented in Chapter 1. Chapter 2 summarizes literature review with regard to implementing the MEPDG and local calibration at national and local research levels. It also discusses the local calibration methodology employed in this study. Chapter 3 discusses the development of a calibration plan

and pavement sections to be included in the new ODOT-calibration process. Chapter 4 describes the input parameters needed for Darwin M-E, the design software that was developed for use of the MEPDG models. Chapter 4 also summarizes the survey results conducted on the Oregon pavement sections which were included in the calibration study. The verification run results using the nationally (default) calibrated coefficients are summarized in Chapter 5. This chapter also contains the summary of the sensitivity analysis conducted on Oregon's select pavement sections. Chapter 6 presents the results and analysis of the local calibration effort with 44 Oregon case examples. Validation results are also included. Finally, the conclusions and recommendations for future research are given in Chapter 7.

2.0 LITERATURE REVIEW

The national calibration-validation process was successfully completed for Mechanistic-Empirical Pavement Design Guide (MEPDG) in 2004 (*NCHRP 2004*). Although this effort was comprehensive, a further validation study is highly recommended as a prudent step in implementing a new design procedure that is so different from current procedures. The objective of this task is to review available existing literature with regard to implementing the MEPDG and local calibration at national and local research levels. A comprehensive literature review was undertaken specifically to identify the following information:

- Identify local calibration steps detailed in National Cooperative Highway Research Program (NCHRP) projects for local calibration.
- Examine how State agencies apply the NCHRP projects' local calibration procedures in their pavement systems.
- Summarize MEPDG pavement performance models' local calibration coefficients reported in literature.

2.1 SUMMARY OF NCHRP PROJECTS FOR MEPDG LOCAL CALIBRATION

At the request of the American Association of State Highway and Transportation Officials (AASHTO) Joint Task Force on Pavements (JTFP), the NCHRP initiated the project, 1-40 "*Facilitating the Implementation of the Guide for the Design of New and Rehabilitated Pavement Structures*" following NCHRP 1- 37A (*NCHRP 2004*) for implementation and adoption of the recommended MEPDG (*TRB 2009*). A key component of the NCHRP 1-40 is an independent, third-party review to test the design guide's underlying assumptions, evaluate its engineering reasonableness and design reliability, and to identify opportunities for its implementation in day-to-day design production work. Beyond this immediate requirement, NCHRP 1-40 includes a coordinated effort to acquaint state DOT pavement designers with the principles and concepts employed in the recommended guide, assist them with the interpretation and use of the guide and its software and technical documentation. NCHRP 1-40 also includes step-by-step procedures to help State DOT engineers calibrate distress models on the basis of local and regional conditions for use in the recommended guide, and perform other activities to facilitate its acceptance and adoption.

There are two NCHRP research projects that are closely related to local calibration of MEPDG performance predictions. They are:

(1) NCHRP 9-30 project (*NCHRP 2003a; NCHRP 2003b*), "*Experimental Plan for Calibration and Validation of Hot Mix Asphalt Performance Models for Mix and Structural Design"*, and

(2) NCHRP 1-40B (*Von Quintus et al. 2005; NCHRP 2007; Von Quintus et al. 2009a; Von Quintus et al. 2009b; NCHRP 2009; TRB 2010*), "*User Manual and Local Calibration Guide for the Mechanistic-Empirical Pavement Design Guide and Software*".

Under the NCHRP 9-30 project, pre-implementation studies involving verification and recalibration have been conducted in order to quantify the bias and residual error of the flexible pavement distress models included in the MEPDG (*Muthadi 2007*). Based on the findings from the NCHRP 9-30 study, the NCHRP 1-40B project has focused on preparing (i) a user manual for the MEPDG and software and (ii) detailed, practical guide for highway agencies for local or regional calibration of the distress models in the MEPDG and software. The manual and guide have been presented in the form of a draft AASHTO recommended practices; the guide shall contain two or more examples or case studies illustrating the step-by-step procedures. It was also noted that the longitudinal cracking model be dropped from the local calibration guide development in NCHRP 1-40B study due to lack of accuracy in the predictions (*Muthadi 2007; Von Quintus and Moulthrop 2007*). NCHRP 1-40 B was completed in 2009 and the draft of report was transferred to the AASHTO Joint Technical Committee on Pavements for review and future action (*TRB 2010*).

NCHRP 1-40B study (*NCHRP 2007*) initially provided three primary steps for calibrating the MEPDG to local conditions and materials as follows:

Step. 1. *Verification of MEPDG performance models with national calibration factors*: Run the current version of the MEPDG software for new field sections using the best available materials and performance data. The accuracy of the prediction models was evaluated using the bias (defined as average over or under prediction) and the residual error (defined as the predicted minus observed distress) as illustrated in Figure 2.1. If there is a significant bias and residual error, it is recommended to calibrate the models to local conditions leading to the second step.

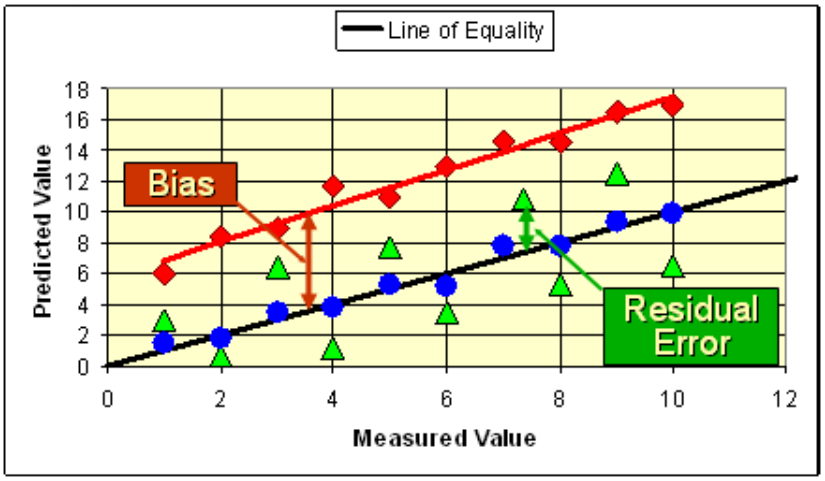

Figure 2.1: The Bias and the Residual Error (*Von Quintus 2008a*)

Step. 2. *Calibration of the model coefficients*: eliminate the bias and minimize the standard error between the predicted and measured distresses.

Step. 3. *Validation of MEPDG performance models with local calibration factors*: Once the bias is eliminated and the standard error is within the agency's acceptable level after the calibration, validation is performed on the models to check for the reasonableness of the performance predictions.

NCHRP 1-40B study (*NCHRP 2009*) continued on the work from the 2007 study and detailed the initial three steps into 11 steps for local calibration of the MEPDG. These 11 steps are depicted in Figure 2.2 and Figure 2.3 below and each of the 11 steps are summarized in the following subsections. Please note that the Accelerated Pavement Testing (APT) has been cross-hatched to reflect this is not viable as APT facilities do not exist in Oregon.

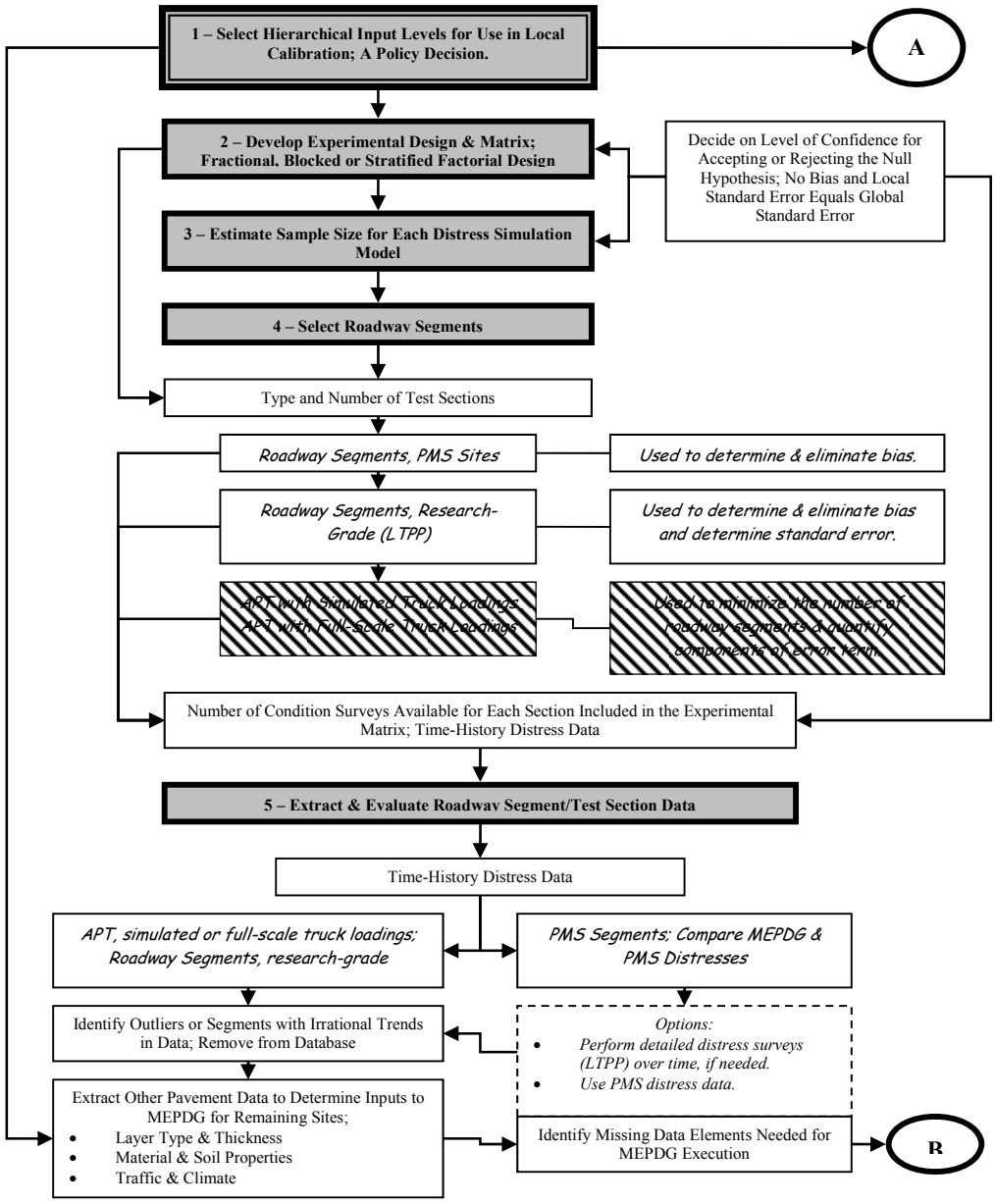

Figure 2.2: Flow Chart for the Procedure and Steps Suggested for Local Calibration: Steps 1-5 (*NCHRP 2009*)

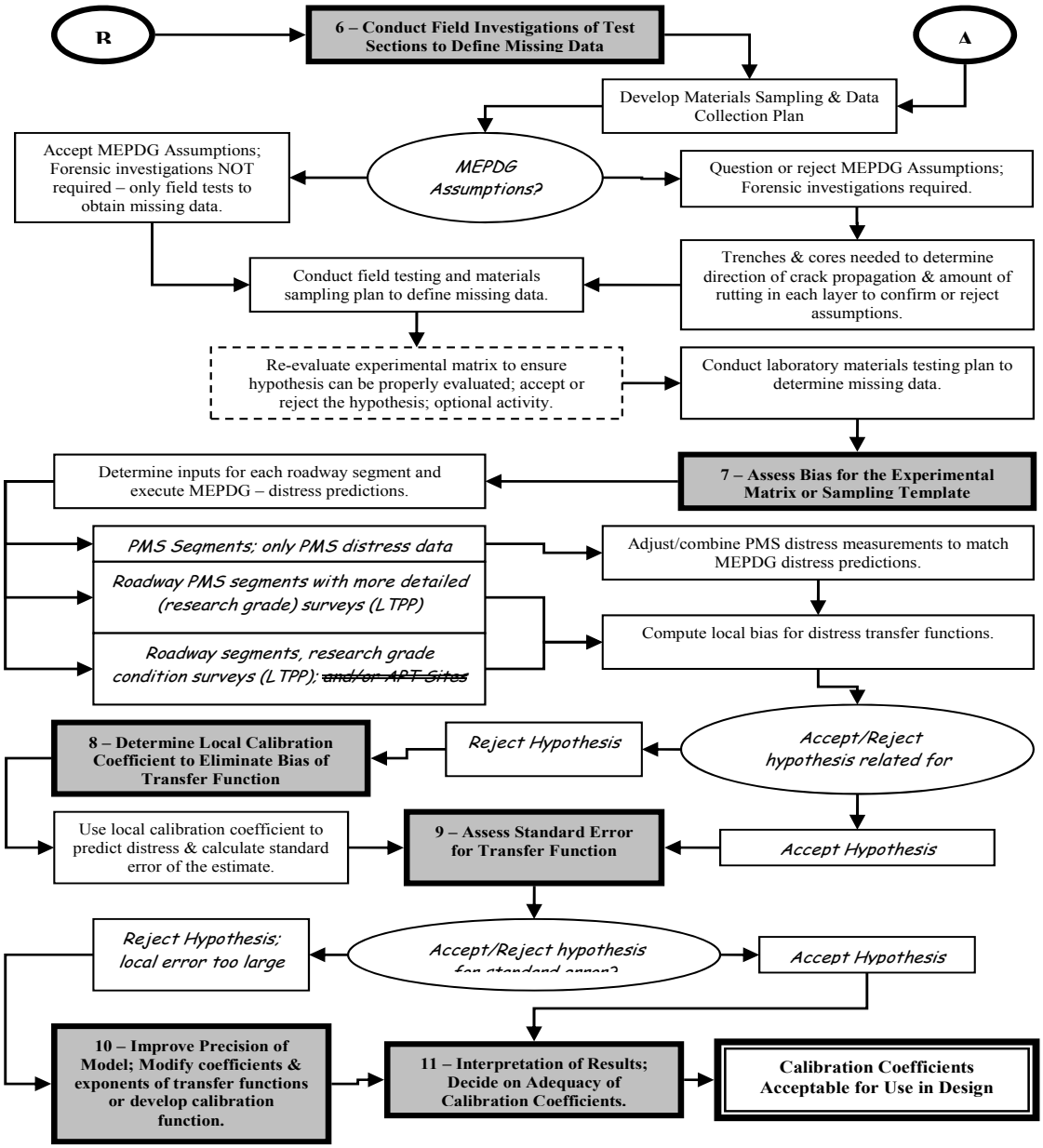

Figure 2.3: Flow Chart for the Procedure and Steps Suggested for Local Calibration: Steps 6-11 (*NCHRP 2009*)

Step 1: Select Hierarchical Input Level

The MEPDG provides the user with the highest flexibility in obtaining the design inputs for a design project based on its importance and the available resources. In general, the MEPDG considers three hierarchical levels of inputs. Level 1 input represents the highest level of accuracy and lowest level of input errors. Level 1 material input requires laboratory or field testing, such as the dynamic modulus testing of hot mix asphalt concrete, site-specific axle load spectra data collections, or nondestructive deflection testing. Level 1 input is more representative of the agency or project specific materials, traffic, and climatic inputs, thus requiring more resources and time than other levels. Level 2 input represents an intermediate level of accuracy.

Inputs are estimated from correlations based on limited laboratory test results or selected from an agency database. Examples include estimating HMA dynamic modulus from binder, aggregate, and mix properties, estimating PCC elastic moduli from compressive strength tests, or using site-specific traffic volume and traffic classification data in conjunction with agency-specific axle load spectra. Level 3 inputs provide the lowest level of accuracy. Inputs typically represent user-selected values or typical averages for the region. Examples include default unbound materials resilient modulus values or default HMA Poisson's ratio for a given mix classes and aggregates used by an agency.

The hierarchical input level to be used in the local validation-calibration process should be consistent with the way the agency intends to determine the inputs for day-to-day use. Some of input level 3 data could be available in the state Department of Transportation (DOT) pavement management system (PMS). It is also important to point out that the calibration using level 1 and 2 input data is dependent upon material and mixture characteristics. Further the linkage of material and mixture characteristics to pavement performance is critical to the level 1 and 2 calibrations. The general information from which the inputs were determined for each input category is discussed in Step 5.

Step 2: Experimental Factorial & Matrix or Sampling Template

A detailed sampling template should be created considering traffic, climate, pavement structure and materials representing local conditions. The number of roadway segments selected for the sampling template should result in a balanced factorial with the same number of replicates within each category.

Step 3: Estimate Sample Size for Each Performance Indicator Prediction Model

The sample size (total number of roadway segments or projects) can be estimated with statistical confidence level of significance. The selection of higher confidence levels can provide more reliable data but increase the number of segments needed. The number of distress observations per segment is dependent on the measurement error or within segment data variability over time (i.e.; higher the within project data dispersion or variability, larger the number of observations needed for each distress). The number of distress measurements made within a roadway segment is also dependent on the within project variability of the design features and site conditions. NCHRP 1-40B project report (*NCHRP 2009*) provided the following equation in determination of the number of distress observations:

$$N = \left(\frac{z_\alpha \left(s_y \right)}{e_t} \right)^2 \qquad \textbf{(2.1)}$$

where, z_α = 1.282 for a 90 percent confidence interval; s_y = standard deviation of the maximum true or observed values; and e_t = tolerable bias. The tolerable bias will be estimated from the levels that are expected to trigger some major rehabilitation activity, which are agency dependent. The s_e/s_y value (ratio of the standard error and standard deviation of the measured values) will also be agency dependent.

Step 4: Select Roadway Segments

Roadway segments should be selected to cover a range of distress values that are of similar ages within the sampling template. Roadway segments exhibiting premature or accelerated distress levels, as well as those exhibiting superior performance (low levels of distress over long periods of time), can be used, but with caution. The roadway segments selected for the sampling template when using hierarchal input level 3 data should represent average performance conditions. It is important that the same number of performance observations per age per each roadway segment be available in selecting roadway segments for the sampling template. It would not be good practice to have some segments with ten observations over 10 years with other segments having only two or three observations over 10 years. The segments with one observation per year would have a greater influence on the validation-calibration process than the segments with less than one observation per year.

Step 5: Extract and Evaluate Roadway Segment/Test Section Data

This step is grouped into four activities:

(1) extracting and reviewing the performance data;
(2) comparing the performance indicator magnitudes to the trigger values;
(3) evaluating the distress data to identify anomalies and outliers; and
(4) determining the inputs to the MEPDG.

First, measured time-history distress data should be made from accelerated pavement testing (APT) or extracted from the agency's PMS. In the case of the Oregon DOT, the distress data was extracted from the agency's PMS. The extraction of data from agency PMS should require a prior step of reviewing PMS database to determine whether the measured values are consistent with the values predicted by the MEPDG. NCHRP 1-40B project report (*NCHRP 2009*) demonstrated the conversion procedures of pavement distress measurement units between PMS and MEPDG for flexible pavements PMS database of Kansas Department of Transportation (KSDOT) and rigid pavements PMS database of Missouri Department of Transportation (MODOT). These examples in NCHRP 1-40B project report (*NCHRP 2009*) are reproduced below.

2.1.1 Kansas DOT (KSDOT) Data Interpretation for MEPDG Use

For the HMA pavement performance data in KSDOT, the measured cracking values are different, while the rutting and International Roughness Index (IRI) values are similar and assumed to be the same. The cracking values and how they were used in the local calibration process are defined below.

Fatigue Cracking. KSDOT measures fatigue cracking in number of wheel path feet per 100 foot sample by crack severity, but do not distinguish between alligator cracking and longitudinal cracking in the wheel path. In addition, reflection cracks are not distinguished separately from the other cracking distresses. The PMS data were converted to a percentage value similar to what is reported in the Highway Performance Monitoring System (HPMS) system from Kansas. In summary, the following equation was used to convert KSDOT cracking measurements to a

percentage value that is predicted by the MEPDG

$$FC = \left(\frac{FCR_1(0.5) + FCR_2(1.0) + FCR_3(1.5) + FCR_4(2.0)}{8.0} \right) \quad \textbf{(2.2)}$$

All load related cracks are included in one value. Thus, the MEPDG predictions for load related cracking were combined into one value by simply adding the length of longitudinal cracks and reflection cracks for Hot Mix Asphalt (HMA) overlays, multiplying by 1.0 ft, dividing that product by the area of the lane and adding that value to the percentage of alligator cracking predicted by the MEPDG.

Thermal Cracking. Another difference is that KSDOT records thermal cracks as the number of cracks by severity level. The following equation has been used by KSDOT to convert their measured values to the MEPDG predicted value of ft/mile.

$$TC = \left(\frac{TCR_o + TCR_1 + TCR_2 + TCR_3}{(10)(12)(52.8)} \right) \quad \textbf{(2.3)}$$

The value of 10 in the above equation is needed because the data are stored with an implied decimal. The value of 12 ft is the typical lane width, and the value of 52.8 coverts from 100 foot sample to a per mile basis. Prior to 1999, KSDOT did not record the number or amount of sealed thermal cracking incidents (TCR_0). As a result, the amount of thermal cracks sometimes goes to "0".

2.1.2 Missouri DOT (MODOT) Data Interpretation for MEPDG Use

For the PCC pavement performance data in MODOT, the measured thermal cracking values are different from the MEPDG, while the thermal joint faulting and IRI values are similar and assumed to be the same. The thermal cracking values and how they were used in the local calibration process are defined below.

Thermal Cracking. The MEPDG requires the percentage of all Portland Cement Concrete (PCC) slabs with mid panel fatigue thermal cracking. Both MODOT and LTPP describe thermal cracking as cracks that are predominantly perpendicular to the pavement slab centerline. Measured cracking is reported in 3 severity levels (low, medium, and high) and provides distress maps showing the exact location of all thermal cracking identified during visual distress surveys. Thus, the databases contain, for a given number of slabs within a 500-ft pavement segment, the total number of low, medium, and high severity thermal cracking. Since LTPP does not provide details on whether a given slab has multiple cracks, as shown in Figure 2.4, a simple computation of percent slabs with this kind of data can be misleading. Therefore, in order to produce an accurate estimate of percent slab cracked, distress maps or videos prepared as part of

distress data collection were reviewed to determine the actual number of slabs with thermal "fatigue" cracking for the 500-ft pavement segments. The total number of slabs was also counted with the percent slabs cracked was defined as follows:

$$Percent\ Slabs\ Cracked = \left(\frac{Number\ of\ cracked\ slabs}{Total\ number\ of\ slabs} \right) * 100 \quad \textbf{(2.4)}$$

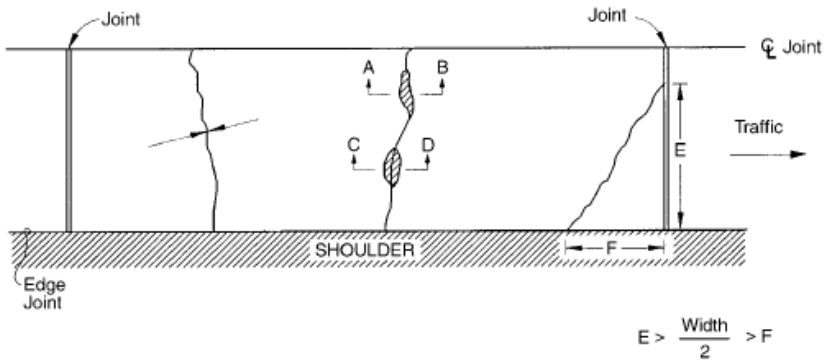

Figure 2.4: LTPP Thermal Cracking (*Miller and Bellinger 2003*)

Thermal Joint Faulting. It is measured and reported by MODOT and LTPP as the difference in elevation to the nearest 1 mm between the pavement surfaces on either side of a thermal joint. The mean joint faulting for all joints within a 500-ft pavement section is reported. This is comparable to the MEPDG predicted faulting.

IRI. The values included in the MODOT PMS database are comparable to the MEPDG predicted IRI.

The second activity of step 5 is to compare the distress magnitudes to the trigger values for each distress. In other words, answer the following question—does the sampling template include values close to the design criteria or trigger value? This comparison is important to provide an answer if the collected pavement distress data could be properly utilized to validate and accurately determine the local calibration values. For example, low values of fatigue cracking measurements comparing to agency criteria is difficult to validate and accurately determine the local calibration values or adjustments for predicting the increase in cracking over time.

The distress data for each roadway segment included in the sampling template should be evaluated to ensure that the distress data are reasonable time-history plots. Any zeros that represent non-entry values should be removed from the local validation-calibration database. Distress data that return to zero values within the measurement period may indicate some type of maintenance or rehabilitation activity. Measurements taken after structural rehabilitation should be removed from the database or the observation period should end prior to the rehabilitation activity. Distress values that are zero as a result of some maintenance or pavement preservation activity, which is a part of the agency's management policy, should be removed but future distress observation values after that activity should be used. If the outliers or anomalies of data

can be explained and are a result of some non-typical condition, they should be removed. If the outlier or anomaly cannot be explained, they should remain in the database.

The MEPDG pavement input database related to each selected roadway segment should be prepared to execute the MEPDG software. The existing resource of these input data for level 3 analyses are agency PMS, traffic database, as-built plans, construction database files, etc. If data for level 3 were unavailable or inadequate, the mean value from the specifications was used or the average value determined for the specific input from other projects with similar conditions. The default values of the MEPDG could also be utilized in this case.

Step 6: Conduct Field and Forensic Investigations

Field and forensic investigations could be conducted to check the assumptions and conditions included in the MEPDG for the global (national) calibration effort. These field and forensic investigations include measuring the rutting in the individual layers, determining where the cracks initiated or the direction of crack propagation, and determining permanent curl/warp effective temperature, etc. The field and forensic investigations is not necessary if the agency accepts the assumptions and conditions included in the MEPDG.

Step 7: Assess Local Bias from Global Calibration Factors

The MEPDG software is executed using the global calibration values to predict the performance indicators for each roadway segment selected. The null hypothesis is first checked for the entire sampling matrix. The null hypothesis in equation below is that the average residual error ($e_r = y_{Measured} - x_{predicted}$) or bias is zero for a specified confidence level or level of significance.

$$H_O : \sum_{i=1}^{n} \left(y_{Measured} - x_{\Pr edicted} \right)_i = 0 \tag{2.5}$$

It is helpful for assessment through making plots of a comparison between the predicted ($x_{predicted}$) and the measured values ($y_{Measured}$) and a comparison between the residual errors (e_r) and the predicted values ($x_{predicted}$) for each performance indicator (See Figure 2.5).

Two other model parameters can be also used to evaluate model bias—the intercept (b_o) and slope (m) estimators using the following fitted linear regression model between the measured ($y_{Measured}$) and predicted ($x_{predicted}$) values.

$$\hat{y}_i = b_o + m(x_i) \tag{2.6}$$

The intercept (b_o) and slope (m) estimators can provide not only accuracy of each prediction but also identification of dependent factors such as pavement structure (new construction versus rehabilitation) and HMA mixture type (conventional HMA versus Superpave mixtures) to each prediction. For illustration, Figure 2.6 presents comparison of the intercept and slope estimators to the line of equality for the predicted and measured rut depths using the global calibration values.

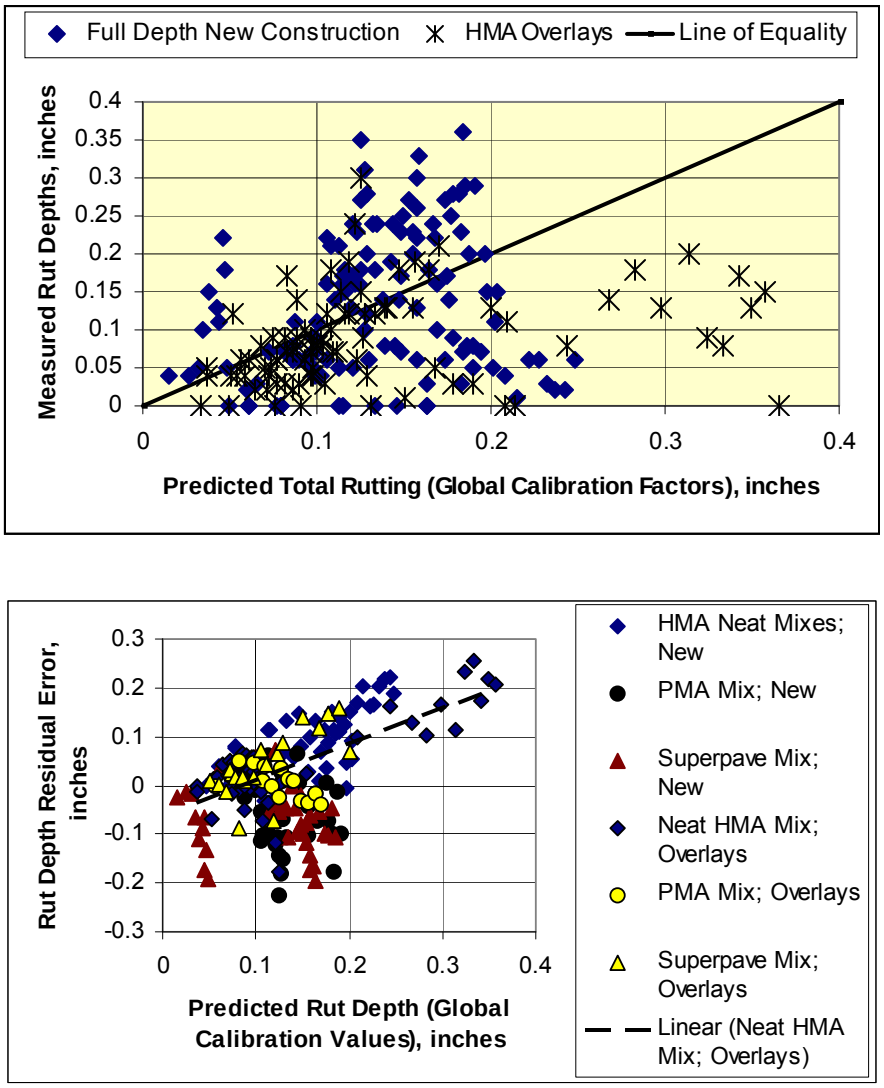

Figure 2.5: Comparison of Predicted and Measured Rut Depths Using the Global Calibration in KSDOT Study (*NCHRP 2009*)

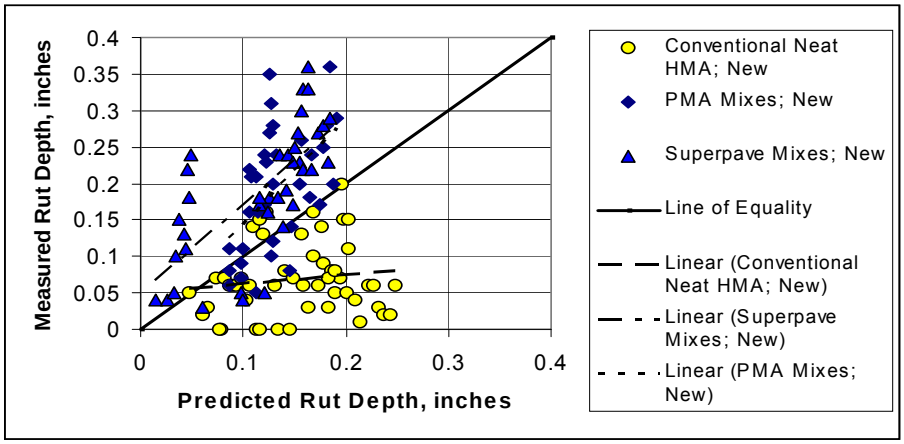

a. Intercept and slope estimators that are dependent on mixture type for the new construction PMS segments.

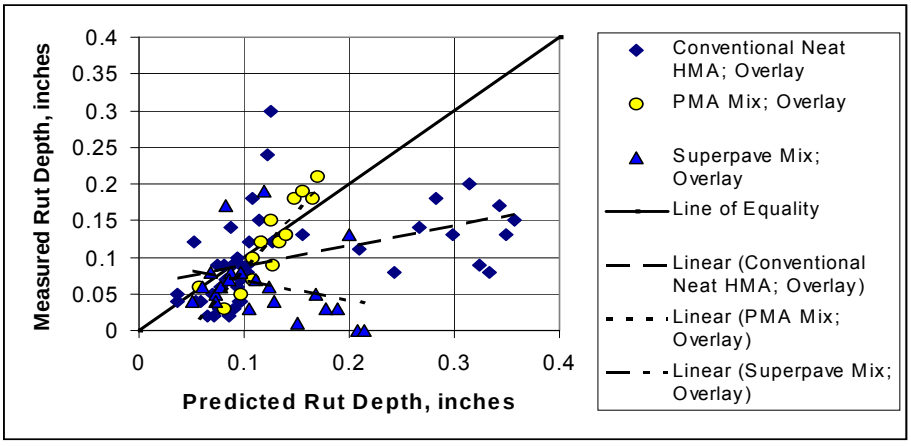

b. Intercept and slope estimators that are dependent on mixture type for the rehabilitation PMS segments

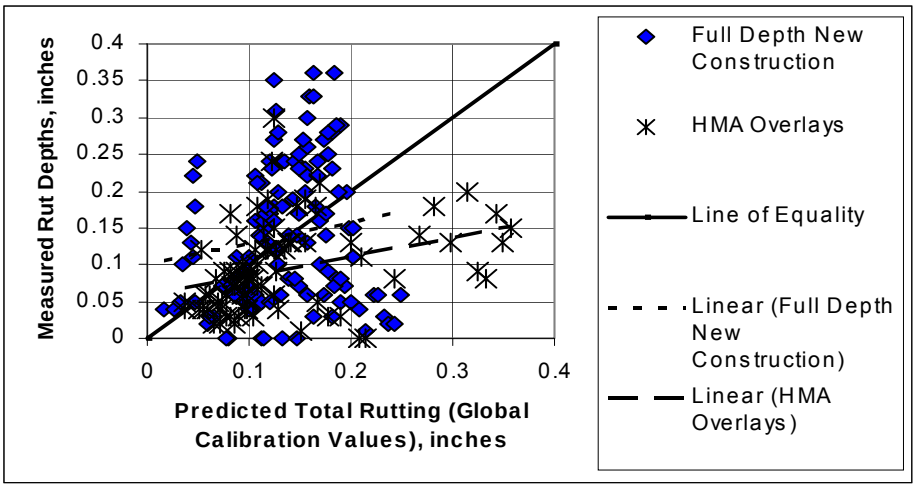

c. Intercept and slope estimators that are structure dependent for the PMS segments.

Figure 2.6: Comparison of the Intercept and Slope Estimators to the Line of Equality for the Predicted and Measured Rut Depths Using the Global Calibration Values in KSDOT Study (*NCHRP 2009*)

Step 8: Eliminate Local Bias of Distress Prediction Models

The MPEDG software includes two sets of parameters for local calibration of most performance indicator transfer functions. One set is defined as agency specific values and the other set as local calibration values. Figure 2.7 shows a screen shot of the tools section where these values can be entered into the software for each performance indicator on a project basis. The default values of the MEPDG performance indicator transfer functions are global calibration values for agency specific values (k_1, k_2, and k_3 in Figure 2.7) and are one for local calibration values (β_1, β_2, and β_3 in Figure 2.7). These parameters are used to make adjustments to the predicted values so that the difference between the measured and predicted values, defined as the residual error, is minimized. Either one can be used with success.

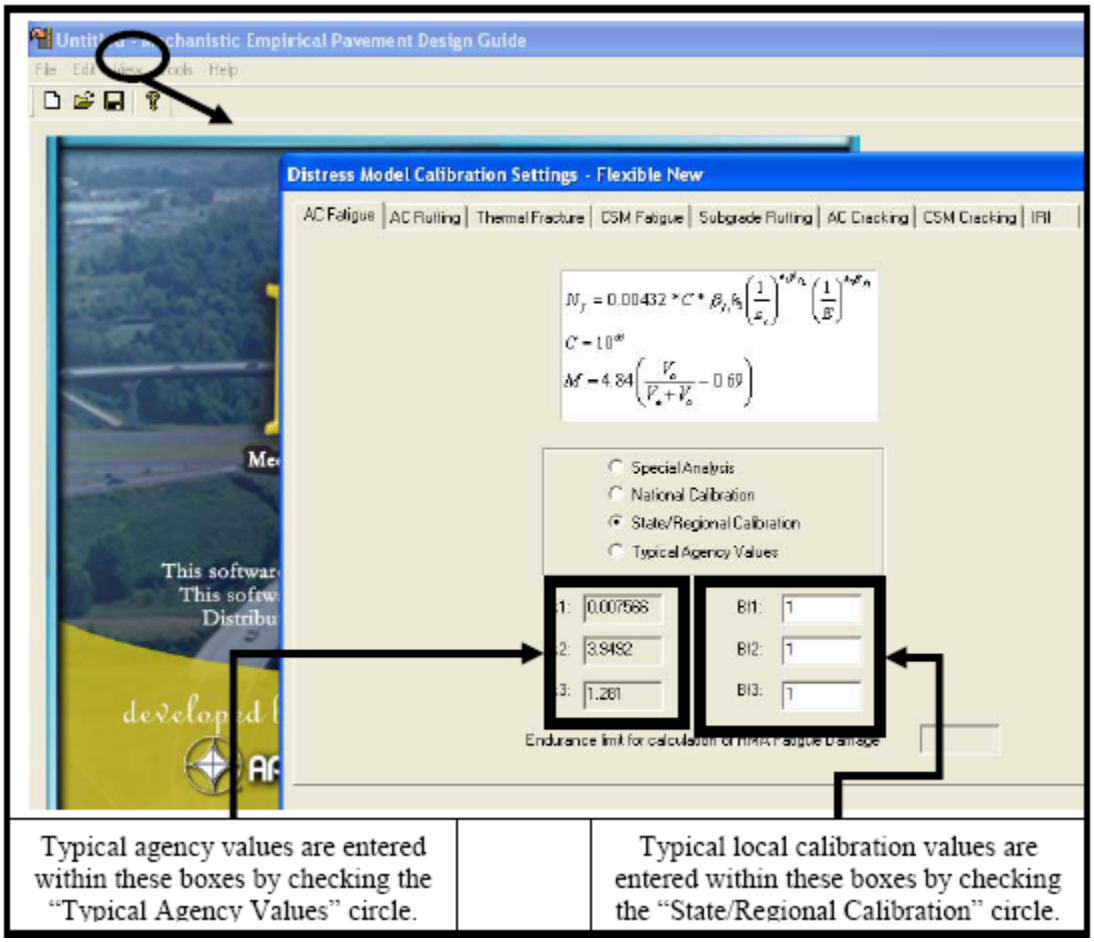

Figure 2.7 Screen Shot of the MEPDG Software for the Local Calibration and Agency Specific Values (*Von Quintus 2008b*)

NCHRP 1-40B project study (*NCHRP 2009*) lists the coefficients of the MEPDG transfer functions or distress and IRI prediction models that should be considered for revising the predictions to eliminate model bias for flexible pavements and HMA overlays. Table 2.1 from NCHRP 1-40B project study (*NCHRP 2009*) was prepared to provide guidance in eliminating any local model bias in the predictions. The distress specific parameters can be dependent on site factors, layer parameters, or policies of the agency.

Table 2.1: Calibration Parameters to Be Adjusted for Eliminating Bias and Reducing the Standard error of the Flexible Pavement Transfer Functions (*NCHRP 2009*)

Distress		Eliminate Bias	Reduce Standard Error
Total Rutting	Unbound Materials & HMA Layers	k_1, β_{s1}, or β_{r1}	k_2, k_3, and β_{r2}, β_{r3}
Load Related Cracking	Alligator Cracking	C_2 or k_1	k_2, k_3, and C_1
	Longitudinal Cracking	C_2 or k_1	k_2, k_3, and C_1
	Semi-Rigid Pavements	C_2 or β_{c1}	C_1, C_2, C_4
Non-Load Related Cracking	Traverse Cracking	β_{t3}	β_{t3}
IRI		C_4	C_1, C_2, C_3

The process to eliminate the bias is applied to the globally calibrated pavement performance transfer functions found to result in bias from step 7. The process used to eliminate the bias depends on the cause of that bias and the accuracy desired by the agency. NCHRP 1-40B project study (*NCHRP 2009*) addresses three possibilities of bias and the bias elimination procedures corresponding to each possibility reproduced below.

The residual errors are, for the most part, always positive or negative with a low standard error of the estimate in comparison to the trigger value, and the slope of the residual errors versus predicted values is relatively constant and close to zero. In other words, the precision of the prediction model is reasonable but the accuracy is poor. In this case, the local calibration coefficient is used to reduce the bias. This condition generally requires the least level of effort and the fewest number of runs or iterations of the MEPDG with varying the local calibration values to reduce the bias. The statistical assessment described in step 7 should be conducted to the local calibrated pavement performance to check obtaining agency acceptable bias.

The bias is low and relatively constant with time or number of loading cycles, but the residual errors have a wide dispersion varying from positive to negative values. In other words, the accuracy of the prediction model is reasonable, but the precision is poor. In this case, the coefficient of the prediction equation is used to reduce the bias but the value of the local calibration coefficient is probably dependent on some site feature, material property, and/or design feature included in the sampling template. This condition generally requires more runs and a higher level of effort to reduce dispersion of the residual errors. The statistical assessment described in step 7 should be conducted to the local calibrated pavement performance to check obtaining agency acceptable bias.

The residual errors versus the predicted values exhibit a significant and variable slope that is dependent on the predicted value. In other words, the precision of the prediction model is poor and the accuracy is time or number of loading cycles dependent—there is poor correlation between the predicted and measured values. This condition is the most difficult to evaluate because the exponent of the number of loading cycles needs to be considered. This condition also requires the highest level of effort and many more MEPDG runs with varying the local calibration values to reduce bias and dispersion. The statistical assessment described in step 7

should be conducted to the local calibrated pavement performance to check obtaining agency acceptable bias.

Step 9: Assess Standard Error of the Estimate

After the bias is reduced or eliminated for each of the transfer functions, the standard error of the estimate (SEE, S_e) from the local calibration is evaluated in comparison to the SEE from the global calibration. The standard error of the estimate for each globally calibrated transfer function is included under the "Tools" section of the MEPDG software. Figure 2.8 illustrates the comparison of the SEE for the globally calibrated transfer functions to the SEE for the locally calibrated transfer functions.

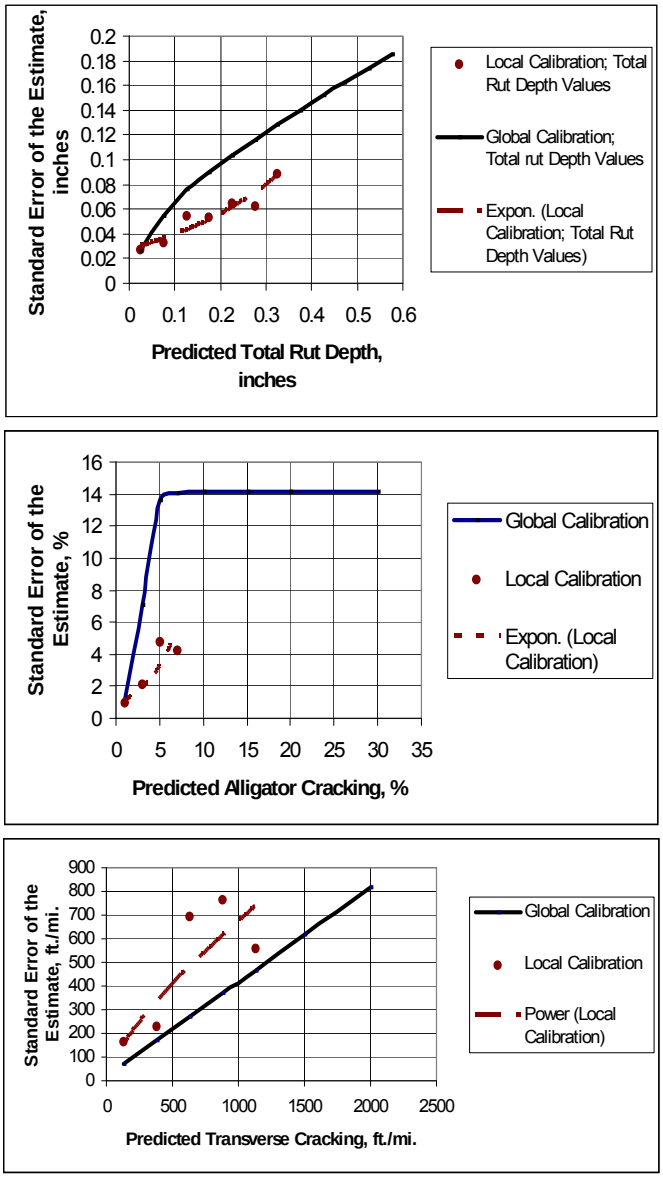

Figure 2.8: Comparison of the Standard Error of the Estimate for the Global-Calibrated and Local-Calibrated Transfer Function in KSDOT Study (*NCHRP 2009*)

Step 10: Reduce Standard Error of the Estimate

If the SEE from the local calibration is found in step 9 to be statistically different in comparison to the SEE included in the MEPDG for each performance indicator, an statistical analysis of variance (ANOVA) can be conducted to determine if the residual error or bias is dependent on some other parameter or material/layer property for the selected roadway segments. If no correlation would be identified, the local calibration factors determined from step 8 and the SEE values obtained from step 9 could be considered as the final products for the selected roadway segments. If some correlation to some parameters (for example, HMA mixture volumetric properties) would be identified, the local calibration values should be determined for each type in correlated parameters or new calibration function should be developed. NCHRP Project 1-40B and Von Quintus (*2008b*) documented HMA mixture specific factors used to modify or adjust the MEPDG global calibration factors for the rut depth and the alligator (bottom-up) cracking transfer functions where sufficient data are available.

Step 11: Interpretation of Results and Deciding on Adequacy of Calibration Factors

The purpose of this step is to decide whether to adopt the local calibration values or continue to use the global values that were based on data included in the LTPP program from around the U.S. To make that decision, an agency should identify major differences between the LTPP projects and the standard practice of the agency to specify, construct, and maintain their roadway network. More importantly, the agency should determine whether the local calibration values can explain those differences. The agency should evaluate any change from unity for the local calibration parameters to ensure that the change provides engineering reasonableness.

2.2 MEPDG LOCAL CALIBRATION STUDIES AT THE STATE LEVEL

As apart to NCHRP projects, multiple State level research efforts have been being conducted regarding the local calibration of the MEPDG involving each step described in NCHRP 1-40B study. However, not many research studies for MEPDG validation in local sections have been finalized because the MEPDG has constantly been updated through NCHRP projects (*2006a; 2006b*) after the release of the initial MEPDG software (Version 0.7). This section summarizes up to date MEPDG local calibration research efforts at the State level.

Hot Mix Asphalt Pavements

A study by Galal and Chehab (*Galal and Chehab 2005*) in Indiana compared the distress measures of existing HMA overlays over a rubblized PCC slab section using AASHTO 1993 design with the MEPDG (Version 0.7) performance prediction results using the same design inputs. The results indicated that MEPDG provide good estimation to the distress measure except longitudinal (top–down) cracking. They also emphasized the importance of local calibration of performance prediction models.

The Montana DOT conducted the local calibration study of MEPDG for flexible pavements (*Von Quintus and Moulthrop 2007*). In this study, results from the NCHRP 1-40B (*Von Quintus et al. 2005*) verification runs were used to determine any bias and the standard error, and compare that

error to the standard error reported from the original calibration process that was completed under NCHRP Project 1-37A (*NCHRP 2004*). Bias was found for most of the distress transfer functions. National calibration coefficients included in Version 0.9 of the MEPDG were used initially to predict the distresses and smoothness of the Montana calibration refinement test sections to determine any prediction model bias. These runs were considered a part of the validation process, similar to the process used under NCHRP Projects 9-30 and 1-40B. The findings from this study are summarized for each performance model as shown below:

- *Rutting prediction model*: the MEPDG over-predicted total rut depth because significant rutting was predicted in unbound layers and embankment soils.
- *Alligator cracking prediction model*: the MEPDG fatigue cracking model was found to be reasonable.
- *Longitudinal cracking prediction model*: no consistent trend in the predictions could be identified to reduce the bias and standard error, and improve the accuracy of this prediction model. It is believed that there is a significant lack-of-fit modeling error for the occurrence of longitudinal cracks.
- *Thermal cracking prediction model*: the MEPDG prediction model with the local calibration factor was found to be acceptable for predicting thermal cracks in HMA pavements and overlays in Montana.
- *Smoothness prediction model*: the MEPDG prediction equations are recommended for use in Montana because there are too few test sections with higher levels of distress in Montana and adjacent States to accurately revise this regression equation.

Von Quintus (*Von Quintus 2008b*) summarized the flexible pavement local calibration value results of the MEPDG from NCHRP project 9-30, 1-40 B, and Montana DOT studies listed in Table 2.2. These results originally from Von Quintus (*Von Quintus 2008b*) are presented in Table 2.3 to Table 2.5 for the rut depth, fatigue cracking, and thermal cracking transfer functions, respectively. These could be useful reference for states having similar conditions of studied sites. The detailed information of studied sites is described elsewhere by Von Quintus (*Von Quintus 2008b*).

Table 2.2: Listing of Local Validation-Calibration Projects (*Von Quintus 2008b*)

Project Identification	Transfer Functions Included in the Local Validation and/or Calibration Efforts for Each Project				
	Rut Depth	**Area Cracking**	**Longitudinal Cracking**	**Thermal Cracking**	**Smoothness or IRI**
NCHRP Projects 9-30 & 1-40B; *Local Calibration Adjustments for HMA Distress Prediction Models in MEPDG Software, (*Von Quintus, et al., 2005a & b)	√	√	√		
Montana DOT, *MEPDG Flexible Pavement Performance Prediction Models for Montana, (*Von Quintus & Moulthrop, 2007a and b)	√	√	√	√	√
NCHRP Project 1-40B, *Examples Using Recommended Practice for Local Calibration of MEPDG Software,* Kansas Pavement Management Data, (Von Quintus, et al., 2008b)	√	√		√	√
NCHRP Project 1-40B, *Examples Using Recommended Practice for Local Calibration of MEPDG Software*,LTPP SPS-1 and SPS-5 Projects, (Von Quintus, et al., 2008b)	√	√		√	√

Table 2.3: Summary of Local Calibration Values for the Rut Depth Transfer Function (*Von Quintus 2008b*)

Project Identification		Unbound Materials/Soils, $\beta s1$		HMA Calibration Values		
		Fine-Grained	**Coarse-Grained**	$\beta r1$	$\beta r3$	$\beta r2$
NCHRP Projects 9-30 & 1-40B; Verification Studies, Version 0.900 of the MEPDG		0.3	0.3	Values dependent on volumetric properties of HMA; the values below represent the overall range.		
		Insufficient information to determine effect of varying soil types		6.9 to 10.8	0.65 to 0.90	0.90 to 1.10
Montana DOT; Based on version 0.900 of the MEPDG		0.3	0.3	Values dependent on volumetric properties of HMA; the values below represent the overall range.		
				7	0.7	1.13
Kansas DOT; PM Segments; HMA Overlay Projects; All Mixtures (Version 1.0)		0.5	0.5	1.5	0.95	1
Kansas PM Segments; New Construction	Conventional	0.5	0.5	1.5	0.9	1
	Superpave			1.5	1.2	1
	PMA			2.5	1.15	1
LTPP SPS-1 & SPS-5 Projects built in accordance with specification; conventional HMA mixtures (Version 1.0)		0.5	0.5			1
				1.25 to 1.60	0.90 to 1.15	1
LTPP SPS-1 Projects with anomalies or construction difficulties, unbound layers.		Values dependent on density and moisture content; values below represent the range found.		---	---	---
		0.50 to 1.25	0.50 to 3.0			

Table 2.4: Summary of Local Calibration Values for the Area Fatigue Cracking Transfer Function (*Von Quintus 2008b*)

Project Identification		*βf1*	*βf2*	*βf3*	C2
NCHRP Projects 9-30 & 1-40B; Verification Studies, Version 0.900 of the MEPDG		Values dependent on the volumetric properties.			
		0.75 to 10.0	1	0.70 to 1.35	1.0 to 3.0
Montana DOT; Based on version 0.900 of the MEPDG, with pavement preservation treatments		Values dependent on the volumetric properties.			
		13.21	1	1.25	1
Northwest Sites; Located in States Adjacent to Montana, without pavement preservation treatments		Values dependent on the volumetric properties.			
		1.0 to 5.0	1	1	1.0 to 3.0
Kansas DOT; PM Segments; HMA Overlay Projects; All HMA Mixtures		0.05	1	1	1
Kansas DOT; PM Segments; New Construction	Conventional HMA Mixes	0.05	1	1	1
	PMA	0.005	1	1	1
	Superpave	0.0005	1	1	1
Mid-West Sites	LTPP SPS-1 Projects built in accordance with specifications	0.005	1	1	1
	LTPP SPS-1 Projects with anomalies or production difficulties	1	1	1	1.0 to 4.0
	LTPP SPS-5 Projects; Debonding between HMA Overlay and Existing Surface	0.005	1	1	1.0 to 4.0

Table 2.5: Summary of the Local Calibration Values for the Thermal Cracking Transfer Function (*Von Quintus 2008b*)

Project Identification		*βt1*	*βt2*	*βt3*
Montana DOT; application of pavement preservation treatments.		---	---	0.25
Northwest Sites, located in states adjacent to Montana, but without pavement preservation treatments; appears to be agency dependent.		---	---	1.0 to 5.0
Kansas PM Segments; Full-Depth Projects	PMA	---	---	2
	Conventional	---	---	2
	Superpave	---	---	3.5
Kansas PM Segments; HMA Overlay Projects	PMA	---	---	2
	Conventional	---	---	7.5
	Superpave	---	---	7.5
LTPP Projects; HMA produced in accordance with specifications	Conventional	---	---	Dependent on Asphalt Content & Air Voids
LTPP Projects; Severely aged asphalt	Conventional	---	---	7.5 to 20.0

Kang (*Kang et al. 2007*) prepared a regional pavement performance database for a Midwest implementation of the MEPDG. They collected input data required by the MEPDG as well as measured fatigue cracking data of flexible and rigid pavements from Michigan, Ohio, Iowa and Wisconsin State transportation agencies. They reported that the gathering of data was labor-intensive because the data resided in various and incongruent data sets. Furthermore, some pavement performance observations included temporary effects of maintenance and those observations must be removed through a tedious data cleaning process. Due to the lack of reliability in collected pavement data, the calibration factors were evaluated based on Wisconsin data and the distresses predicted by national calibration factors were compared to the field collected distresses for each state except Iowa. This study concluded that the default national calibration values do not predict the distresses observed in the Midwest. Therefore, this reinforces the reason to collect local data from Oregon for the purpose of this study and calibrate the MEPDG for local conditions. The collection of more reliable pavement data is recommended for a future study.

Schram and Abdelrahman (*Schram and Abdelrahman 2006*) attempted to calibrate two of the MEPDG IRI models for the Jointed Plain Concrete Pavement (JPCP) and the HMA overlays of PCC pavements at the local project-level using Nebraska Department of Roads (NDOR) pavement management data. The focused dataset was categorized by annual daily truck traffic (ADTT) and surface layer thickness. Three categories of ADTT were considered: low (0 – 200 trucks/day), medium (201 – 500 trucks/day), and high (over 500 trucks/day). The surface layer thicknesses considered ranged from 6 inches to 14 inches for JPCP and 0 to 8 inches for HMA layers. Results showed that project-level calibrations reduced default model prediction error by

nearly twice that of network-level calibration. Table 2.6 and Table 2.7, as reported from this study, contain coefficients for the smoothness model of HMA overlays of rigid pavements and JPCP.

Table 2.6: HMA Overlaid Rigid Pavements' IRI Calibration Coefficients for Surface Layer Thickness within ADTT (*Schram and Abdelrahman 2006*)

				Frequency, HZ					
			Test Temp., C	0.1	0.5	1	5	10	25
5.8% Binder, 4.0% Air, 100 Gyrations	PG 64-22	Series 1-1	-10	2623	3097	3260	3554	3649	3750
			4.4	945	1533	1807	2424	2662	2943
			21.1	143	308	423	818	1042	1377
			37.8	27	47	63	130	180	279
			54.4	13	17	19	29	36	51
	PG 70-22	Series 1-2	-10	2696	3236	3442	3849	3994	4159
			4.4	1118	1664	1921	2527	2778	3091
			21.1	272	483	611	1008	1219	1530
			37.8	67	109	137	243	312	433
			54.4	30	40	46	70	86	114
	PG 70-28	Series 1-3	-10	2681	3207	3398	3754	3873	4004
			4.4	958	1522	1793	2427	2685	2998
			21.1	183	351	463	836	1048	1367
			37.8	46	74	93	171	225	327
			54.4	24	30	34	48	58	77
	PG 76-22	Series 1-4	-10	2612	2967	3093	3313	3386	3466
			4.4	1208	1722	1946	2428	2611	2825
			21.1	294	527	667	1081	1291	1585
			37.8	73	118	150	269	347	483
			54.4	35	44	51	75	92	123
5.8% Binder, 7.0% Air, Gyrations, as required	PG 64-22	Series 2-1	-10	1891	2349	2527	2886	3016	3165
			4.4	657	1052	1248	1730	1938	2203
			21.1	119	235	311	563	708	930
			37.8	24	43	56	109	146	215
			54.4	9	13	16	26	33	46
	PG 70-22	Series 2-2	-10	2246	2659	2806	3078	3168	3267
			4.4	853	1337	1563	2077	2281	2524
			21.1	153	306	408	742	928	1203
			37.8	32	54	70	135	183	272
			54.4	15	19	22	33	41	56
	PG 70-28	Series 2-3	-10	1897	2349	2525	2878	3005	3151
			4.4	652	1032	1222	1696	1902	2165
			21.1	138	251	324	566	704	918
			37.8	37	59	73	128	166	233
			54.4	18	23	27	38	46	61
	PG 76-22	Series 2-4	-10	2647	3056	3200	3464	3552	3647
			4.4	1100	1637	1879	2417	2626	2875
			21.1	237	442	571	972	1184	1489
			37.8	56	91	117	215	283	404
			54.4	26	34	39	57	70	95

Table 2.7: JPCP IRI Calibration Coefficients for Surface Layer Thickness within ADTT (*Schram and Abdelrahman 2006*)

AADTT	Thickness	C1	C2	C3	C4	N	R2	SEE (in/mi)
Low	6"-7"	0	0	1.0621	74.8461	33	0.434	26.885
	7"-8"	0	0	1.9923	46.9256	37	0.961	8.235
	8"-9"	0.8274	0	0	86.9721	39	0.904	14.465
	9"-10"	0.3458	0	1.5983	64.3453	110	0.537	26.23
	10"-11"	0.03	0	3.4462	10.7893	37	0.893	17.28
	11"-12"	--	--	--	--	--	--	--
	12"-13"	--	--	--	--	--	--	--
	13"-14"	--	--	--	--	--	--	--
	14"-15"	--	--	--	--	--	--	--
Medium	6"-7"	0	0	4.1422	0	3	0.966	5.094
	7"-8"	0	1.5628	0	71.9009	22	0.968	9.952
	8"-9"	0	0	1.7162	53.0179	122	0.291	40.537
	9"-10"	0.191	0	0.9644	89.399	609	0.686	24.945
	10"-11"	0	0	2.0945	73.1246	314	0.812	18.535
	11"-12"	0	0.009	1.3617	100	27	0.792	10.166
	12"-13"	--	--	--	--	--	--	--
	13"-14"	0	0.01	2.2226	24.9354	4	0.924	3.948
	14"-15"	--	--	--	--	--	--	--
High	6"-7"	--	--	--	--	--	--	--
	7"-8"	--	--	--	--	--	--	--
	8"-9"	0	0.1376	0.4352	79.5526	46	0.151	48.576
	9"-10"	0.1561	0	1.1024	62.9556	81	0.333	31.255
	10"-11"	0	0	1.6344	100	228	0.653	22.295
	11"-12"	0.1125	1.8207	1.1678	100	29	0.739	13.366
	12"-13"	0	0	1.5331	100	151	0.719	17.724
	13"-14"	0.01	0.01	0.5184	0	4	0.623	1.728
	14"-15"	0.1904	0	2.1387	51.4053	146	0.838	9.018

Muthadi and Kim (*Muthadi and Kim 2008*) performed the calibration of the MEPDG for HMA pavements located in North Carolina (NC) using version 1.0 of the MEPDG software. Two distress models, rutting and alligator cracking, were used for this effort. A total of 53 pavement

sections were selected from the LTPP program and the NC DOT databases for the calibration and validation process. Based on calibration procedures suggested by the NCHRP 1-40B study, the flow chart was made for this study. The verification results of the MEPDG performance models with national calibration factors showed bias (systematic difference) between the measured and predicted distress values. The Microsoft Excel Solver program was used to minimize the sum of the squared errors (SSE) of the measured and the predicted rutting or cracking by varying the coefficient parameters of the transfer function. Table 2.8 lists local calibration factors of rutting and alligator cracking transfer functions obtained in this study. This study concluded that the standard error for the rutting model and the alligator cracking model is significantly less after the calibration.

Table 2.8: North Carolina Local Calibration Factors of Rutting and Alligator Cracking Transfer Functions (*Muthadi and Kim 2008*)

Recalibration	Calibration Coefficient	National Calibration	National Recalibration	Local Calibration
Rutting				
AC	k_1	-3.4488	-3.35412	-3.41273
	k_2	1.5606	1.5606	1.5606
	k_3	0.479244	0.479244	0.479244
GB	β_{GB}	1.673	2.03	1.5803
SG	β_{SG}	1.35	1.67	1.10491
Fatigue				
AC	k_1	0.00432	0.007566	0.007566
	k_2	3.9492	0.9492	0.9492
	k_3	1.281	1.281	1.281
	C_1	1	1	0.437199
	C_2	1	1	0.150494

The Washington State DOT (*Li et al. 2009*) developed procedures to calibrate the MEPDG (version 1.0) HMA pavement performance models using data obtained from the Washington State Pavement Management System (WSPMS). Calibration efforts were concentrated on the asphalt mixture fatigue damage, longitudinal cracking, alligator cracking, and rutting models. There were 13 calibration factors to be considered in the four related models. An elasticity analysis was conducted to describe the effects of those calibration factors on the pavement distress models, i.e., the higher the absolute value of elasticity, the greater impact the factor has on the model. The calibration results of typical Washington State HMA pavement systems determined from this study presents in Table 2.9. This study also reported that a version 1.0 of the MEPDG software bug does not allow calibration of the roughness model.

Table 2.9: Local Calibrated Coefficient Results of Typical Washington State Flexible Pavement Systems (*Li et al. 2009*)

Calibration Factor		Default	Calibrated Factors
AC Fatigue	B_{f1}	1	0.96
	B_{f2}	1	0.97
	B_{f3}	1	1.03
Longitudinal cracking	C1	7	6.42
	C2	3.5	3.596
	C3	0	0
	C4	1000	1000
Alligator cracking	C1	1	1.071
	C2	1	1
	C3	6000	6000
AC Rutting	B_{r1}	1	1.05
	B_{r2}	1	1.109
	B_{r2}	1	1.1
Subgrade Rutting	B_{s1}	1	0
IRI	C1	40	----
	C2	0.4	----
	C3	0.008	----
	C4	0.015	----

Similar to the study conducted in NC (*Muthadi and Kim 2008*), Banaerjee (*Banaerjee et al. 2009*) minimized the SSE between the observed and the predicted surface permanent deformation to determine the coefficient parameters of HMA permanent deformation performance model after values based on expert knowledge assumed for the subgrade permanent deformation calibration factors (β_{s1}) and the HMA mixture temperature dependency calibration factors (β_{r2}). Pavement data from the Texas SPS-1 and SPS-3 experiments of the LTPP database were used to run the MEPDG and calibrate the guide to Texas conditions. The set of state-default calibration coefficients for Texas was determined from joint minimization of the SSE for all the sections after the determination of the Level 2 input calibration coefficients for each section. The results of calibration factors as obtained from this study are given in Figure 2.9. Souliman (*Souliman et al. 2010*) also presented the calibration of the MEPDG (Version 1.0) predictive models for flexible pavement design in Arizona conditions. This calibration was performed using 39 Arizona pavement sections included in the LTPP database. The results of calibration factors as obtained from this study are given in Table 2.10.

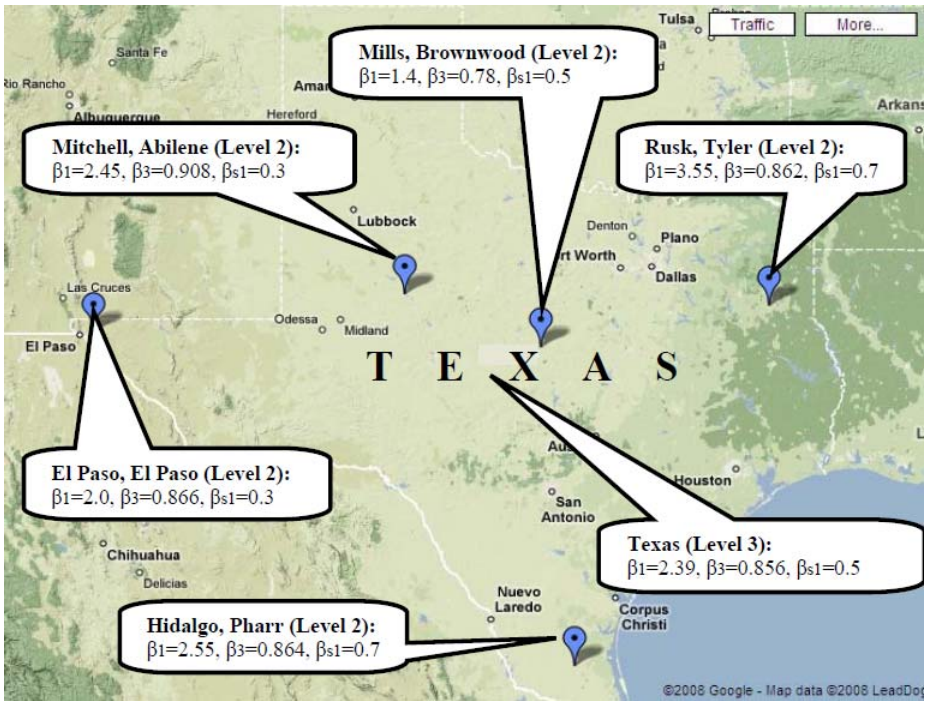

Figure 2.9: Regional and State Level Calibration Coefficients of HMA Rutting Depth Transfer Function for Texas (*Banerjee et al. 2009*)

Table 2.10: Calibration Coefficients of the MEPDG HMA Pavement Distress Models in Arizona Conditions (*Souliman et al. 2010*)

MEPDG Model	Coefficients before Calibration	Coefficients after Calibration	Net Effect of Calibration
Alligator Fatigue Transfer Function	β_{f1} =1	β_{f1} = 0.729	Increased prediction
	β_{f2} =1	β_{f2} = 0.8	
	β_{f3} =1	β_{f3} = 0.8	
	C_1 =1.0	C_1 = 0.732	
	C_2 =1.0	C_2 = 0.732	
Longitudinal Fatigue Transfer Function	β_{f1} =1	β_{f1} =0.729	Decreased prediction
	β_{f2} =1	β_{f2} =0.8	
	β_{f3} =1	β_{f3} =0.8	
	C_1 =7.5	C_1 =1.607	
	C_2 =3.5	C_2 = 0.803	
AC Rutting Model	β_{r1} =1	β_{r1} = 3.63	Increased prediction
	β_{r2} =1	β_{r2} = 1.1	
	β_{r3} =1	β_{r3} = 0.7	
Granular Base Rutting Model	β_{gb} =1	β_{gb} = 0.111	Decreased prediction
Subgrade Rutting Model	β_{sg} =1	β_{sg} = 1.38	Increased prediction
Roughness Model	C_1 = 40	C_1 = 5.455	Decreased prediction
	C_2 = 0.4	C_2 = 0.354	
	C_3 = 0.008	C_3 = 0.008	
	C_4 = 0.015	C_4 = 0.015	

Hoegh (*Hoegh et al. 2010*) utilized time history rutting performance data for pavement sections at the Minnesota Department of Transportation (Mn DOT) full-scale pavement research facility (MnROAD) for an evaluation and local calibration of the MEPDG rutting model. Instead of an adjustment of the calibration parameters in the current MEPDG rutting model, a modified rutting model was suggested to account for the forensic and predictive evaluations on the local conditions. This study demonstrated that the current MEPDG subgrade and base rutting models grossly overestimate rutting for the MnROAD test sections.

Some type of maintenance or rehabilitation activity can make actual distress measurements decrease in distress time-history plots (*Kim et al. 2010*). Banerjee (*Banerjee et al. 2010*) found that the calculation factors of the MEPDG permanent deformation performance models are influenced by maintenance strategies. Liu (Liu et al. 2010) suggested historical pavement performance model to account for rehabilitation or maintenance activity using piecewise approximation. The whole pavement serviceable life was divided into three zones: Zone 1 for the early age pavement distress, Zone 2 in rehabilitation stage, and Zone 3 for over-distressed situations. The historical pavement performance data were regressed independently in each time zone. This approach is able to accurately predict the pavement distress progression trends in each individual zone by eliminating the possible impacts from the biased data in the other zones. It is also possible to compare the pavement distress progression trends in each individual zone with the MEPDG incremental damage approach predictions.

Mamlouk and Zapata (*Mamlouk and Zapata 2010*) discussed differences between the Arizona Department of Transportation (ADOT) PMS data and the LTPP database used in the original development and national calibration of the MEPDG distress models. Differences were found between the following: rut measurements, asphalt cracking, IRI, and all layer backcalculated moduli found from NDT measurements done by ADOT and those of the LTPP. Differences in distress data include types of data measured, types of measuring equipment, data processing methods, units of measurements, sampling methods, unit length of pavement section, number of runs of measuring devices, and survey manuals used. Similar findings were reported in NC DOT PMS by Corley-Lay (*Corley-Lay et al. 2010*).

Table 2.11 summarizes the findings of agency's efforts on calibration of performance prediction models for HMA pavements.

Table 2.11: Summary of Calibration Effort Conducted by Agencies

Model/ Agency	*Rutting*	*Alligator (Bottom-up)*	*Longitudinal (Top-down)*	*Transverse (Thermal)*	*Roughness*
Arkansas DOT	Good	Good	Poor	Poor	-
Arizona DOT	Good	Good	Poor	N/A	Poor
Minnesota DOT	Good	-	-	-	-
North Carolina DOT	Good	Good	-	-	-
Montana DOT	Good	Average	Poor	Average	Good
Nebraska DOT	-	-	-	-	Good
Washington DOT	Good	Average	Average	Average	Poor

Portland Cement Concrete Pavements

The Washington State DOT (*Li et al. 2006*) developed procedures to calibrate the MEPDG (Version 0.9) PCC pavement performance models using data obtained from the WS PMS. Some significant conclusions from this study are as follows: (a) WSDOT PCC pavement performance prediction models require calibration factors significantly different from default values; (b) the MEPDG software does not model longitudinal cracking of PCC pavement, which is significant in WSDOT pavements; (c) WS PMS does not separate longitudinal and thermal cracking in PCC pavements, a deficiency that makes calibration of the software's thermal cracking model difficult; and (d) the software does not model studded tire wear, which is significant in WS DOT pavements. This study also reported that: (a) the calibrated software can be used to predict future deterioration caused by faulting, but it cannot be used to predict cracking caused by the thermal or longitudinal cracking issues in PCC pavement, and (b) with a few improvements and resolving software bugs, the MEPDG software can be used as an advanced tool to design PCC pavements and predict future pavement performance. The local calibration results of typical Washington State PCC pavement systems determined from this study are presented in Table 2.12.

Table 2.12: Calibration Coefficients of the MEPDG (Version 0.9) PCC Pavement Distress Models in the State of Washington (*Li et al. 2006*)

Calibration Factor		Default for New Pavements	Undoweled	Undoweled-MP[a]	DBR[b,c]
Cracking	C_1	2	2.4	2.4	2.4
	C_2	1.22	1.45	1.45	1.45
	C_4	1	0.13855	0.13855	0.13855
	C_5	-1.68	-2.115	-2.115	-2.115
Faulting	C_1	1.29	0.4	0.4	0.934
	C_2	1.1	0.341	0.341	0.6
	C_3	0.001725	0.000535	0.000535	0.001725
	C_4	0.0008	0.000248	0.000248	0.0004
	C_5	250	77.5	77.5	250
	C_6	0.4	0.0064	0.064	0.4
	C_7	1.2	2.04	9.67	0.65
	C_8	400	400	400	400
Roughness[d]	C_1	0.8203	0.8203	0.8203	0.8203
	C_2	0.4417	0.4417	0.4417	0.4417
	C_3	1.4929	1.4929	1.4929	1.4929
	C_4	25.24	25.24	25.24	25.24

Khazanovich (*Khazanovich et al. 2008*) evaluated the MEPDG PCC pavement performance prediction models for the design of low-volume concrete pavements in Minnesota. It was found that the faulting model in versions 0.8 and 0.9 of the MEPDG produced acceptable predictions, whereas the cracking model had to be adjusted. The cracking model was recalibrated using the design and performance data for 65 pavement sections located in Minnesota, Iowa, Wisconsin, and Illinois. The recalibrated coefficients of the 0.8 and 0.9 versions of the MEPDG for cracking model predictions in this study are (1) $C_1 = 1.9875$, (2) $C_2 = -2.145$. Since the MEPDG software evaluated in this study was not a final product, the authors recommended that these values should be updated for the final version of the MEPDG software.

Bustos (*Bustos et al. 2009*) attempted to adjust and calibrate the MEPDG PCC pavement distress models to Argentina conditions. A sensitivity analysis of distress model transfer functions was conducted to identify the most important calibration coefficient. The C_6 of joint faulting model transfer function and the C_1 or C_2 of cracking model transfer function were the most sensitive coefficients.

3.0 RESEARCH PLAN

3.1 INTRODUCTION

The research plan developed for calibrating the MEPDG generally followed the flow chart recommended by Von Quintus et al. (*2009*) with some modifications as outlined in Figures 3.1 and 3.2 summarized below.

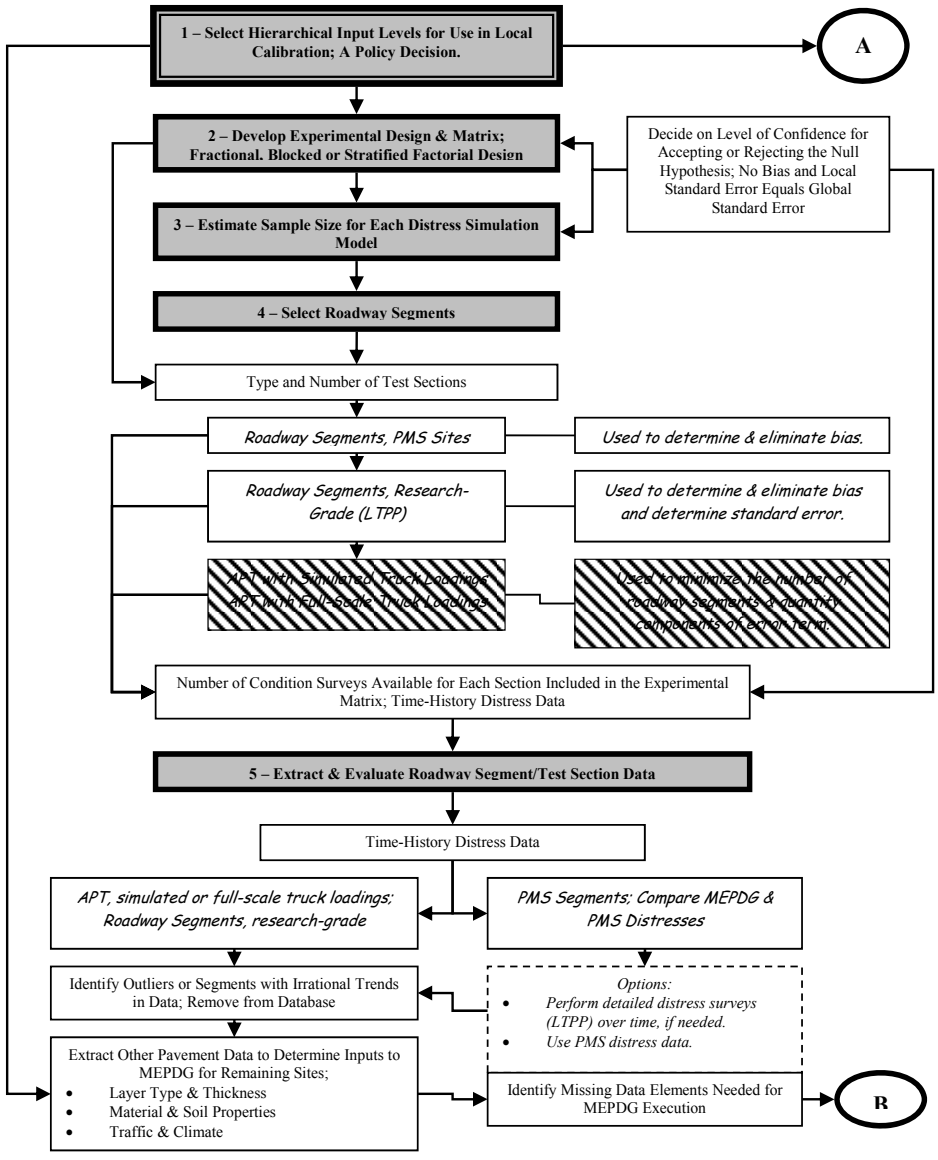

Figure 3.1: Flow Chart for the Procedure and Steps
Suggested for Local Calibration: Steps 1-5 (*Von Quintus et al. 2009*)

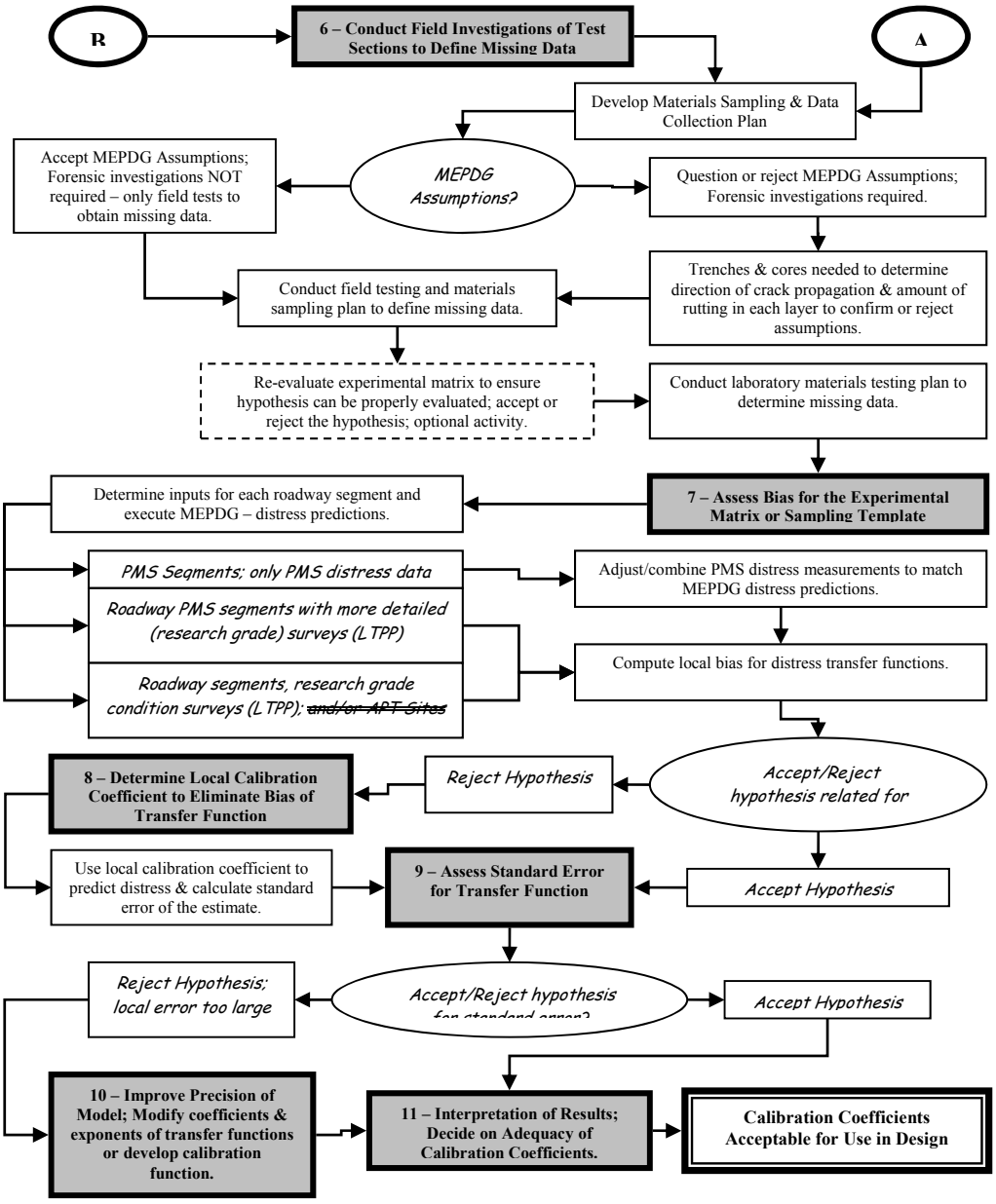

Figure 3.2: Flow Chart for the Procedure and Steps
Suggested for Local Calibration: Steps 6-11 (*Von Quintus et al. 2009*)

It is important to point out that since Accelerated Pavement Testing (APT) does not exist in Oregon, this has been struck out in Figures 3.1 (step 4) and 3.2 (step 7). Further, the research team did forensic investigation only in so far as to determine the type of load related cracking, e.g. top-down as compared to bottom-up cracking, via coring at the end of cracks.

The data mining of Oregon DOT databases included identifying pavement types with varying levels of distresses, as well as historical mix design, structural design, and traffic information for rehabilitated pavements. The research team pursued obtaining pavement sections with a range of distress levels for the types of pavement types for cracking and rutting. Further challenging the research team in this endeavor is understanding the differences between materials used

historically as compared to those being used today (e.g. pre-Superpave mixes as compared to Superpave). It was necessary to plan for conducting distress surveys in accordance with the FHWA Long Term Pavement Performance (LTPP) publication *Data Collection Guide For Long Term Pavement Performance* for calibrating the simulated outcomes of the MEPDG. The pavement test sections needed to cover a range of climatic conditions from coastal areas (western Oregon) to central and eastern Oregon, a range of trafficking levels, and typically used materials. The research team segmented the trafficking levels into two categories: low volume (less than 10 million Equivalent Single Axle Load (ESALs)), and high volume (greater than 10 million ESALs). This was based upon the changes in the mix design criteria which includes the materials specified in the various design levels.

3.2 DEVELOPMENT OF CALIBRATION PLAN

The calibration of the MEPDG needed to consider a number of different factors including the following:

- Pavement type/structure,
- Pavement age,
- Pavement performance,
- Trafficking level, and
- Region (climatic variation).

A brief discussion of the identified factors ensues to illustrate the importance of these factors in the experimental plan.

3.2.1 Pavement Type

There are five primary pavement types in Oregon consisting of hot mix asphalt over aggregate base (HMA/Agg), HMA inlay or overlay over aggregate base (HMA/HMA/Agg), HMA inlay or overlay over cement treated base (HMA/HMA/CTB), continuously reinforced concrete pavement (CRCP), and HMA overlay of CRCP (HMA/CRCP). Open-graded friction coarse mixes are often used as surface mixes in lieu of dense-graded ones and they needed to be considered. Also, polymer modified asphalt binders have only been used for the past five years and the longer term performance aspects may not exist in older pavement sections. The primary pavement types included in the calibration were HMA over aggregate base, HMA inlay or overlay over aggregate base, HMA inlay or overlay over cement treated base, HMA overlay of CRCP, and CRCP.

3.2.2 Pavement Age and Performance

The pavement performance at various ages is critical to calibrating the MEPDG. The three primary distresses targeted for HMA pavement types were HMA rutting, fatigue cracking, and thermal cracking. The MEPDG considers two types of fatigue cracking: the classical bottom-up (alligator) and top-down (longitudinal). Most pavement management systems do not delineate between the two types of fatigue cracking, thus the research team attempted to identify whether

the cracking was bottom- up or top-down. It was important for rutting to be delineated between material shear flow as compared to wear rutting of open-graded friction coarse mixes. Based upon discussion with the Technical Advisory Committee (TAC), subgrade rutting is not a problem in Oregon and thus it was not reasonable to identify pavements with a range in performance for this distress. The performance characteristics for CRCP are cracking and surface defects. Cracking in CRCP includes durability (D), longitudinal cracking, thermal cracking, punch-outs (with crack width for calibration), and determine the international roughness index. Whereas surface defects are map cracking/scaling, polishing, and pop-outs.

3.2.3 Trafficking Level

The trafficking levels are important to identify as varying materials are used depending upon a pavements design level. As an example, varying amounts of RAP are allowable depending upon the ESAL design level as the number of design gyrations. The research team's initial thinking was that two trafficking levels be considered: 1. less than 10million ESALs, and 2. more than 10million ESALs. This would delineate the higher quality aggregates and the use of polymer modified binder in high volume roads, and have the HMA overlays of cold mixes in low volume roads. Also, CRCP only occurs in high volume roads.

3.2.4 Region (Climatic Variation)

Oregon has vastly different climatic conditions that occur on the Coast as compared to in the Valley and on the Eastern portion of the state. As a result, the research team considered three different regions, however, not all pavement types necessarily occur in each region. The locations of the pavement sections surveyed are shown in Figure A.1, Appendix-A.

3.2.5 Initial Field Experimental Plan

The developed initial field experimental plan that considered the factors addressed above was developed and pursued is represented in Table 3.1. The plan included the three aforementioned regions (Coastal, Valley, and Eastern), the five primary types of pavements (HMA over aggregate base = HMA/Agg, HMA inlay or overlay over aggregate base= HMA/HMA/Agg, HMA inlay or overlay over cement treated base=HMA/HMA/CTB, HMA overlay of CRCP=HMA/CRCP, and CRCP), low and high trafficked roads, and three different levels of pavement performance (very good-excellent, as expected, and inadequate). Each experimental block has three replicate locations for condition surveys to be conducted within a selected roadway section. As an example, X_{011} represent section 01, location 1. The three locations were randomly selected within the segment length using a random number generator and then normalized. To simplify the coordination of the condition surveys, only one traffic direction underwent condition surveys and again the direction was randomly selected. The draft experimental plan called for identifying 36 pavement sections for conducting condition surveys for a total of 108 pavement condition surveys.

Table 3.1: Draft Field Experimental Plan

		Region								
		Coastal			Valley			Eastern		
Traffic	Pavement Performance	HMA/Agg, HMA/HMA /CTB	HMA/HM A/Agg	HMA/CRCP , CRCP	HMA/Agg, HMA/ HMA/CTB	HMA/HM A/Agg	CRCP	HMA/Agg, HMA/HM A/CTB	HMA/HM A/Agg	HMA/ CRCP, CRCP
Low Volume	Very Good-Excellent	X_{011}, X_{012}, X_{013}	X_{021}, X_{022}, X_{023}		X_{031}, X_{032}, X_{033}	X_{041}, X_{042}, X_{043}		X_{051}, X_{052}, X_{053}	X_{061}, X_{062}, X_{063}	
	As Expected	X_{071}, X_{072}, X_{073}	X_{081}, X_{082}, X_{083}		X_{091}, X_{092}, X_{093}	X_{101}, X_{102}, X_{103}		X_{111}, X_{112}, X_{113}	X_{121}, X_{122}, X_{123}	
	Inadequate	X_{131}, X_{132}, X_{133}	X_{141}, X_{142}, X_{143}		X_{151}, X_{152}, X_{153}	X_{161}, X_{162}, X_{163}		X_{171}, X_{172}, X_{173}	X_{181}, X_{182}, X_{183}	
High Volume	Very Good-Excellent	X_{191}, X_{192}, X_{193}		X_{201}, X_{202}, X_{203}	X_{211}, X_{212}, X_{213}		X_{221}, X_{222}, X_{223}	X_{231}, X_{232}, X_{233}		X_{241}, X_{242}, X_{243}
	As Expected	X_{251}, X_{252}, X_{253}		X_{261}, X_{262}, X_{263}	X_{271}, X_{272}, X_{273}		X_{281}, X_{282}, X_{283}	X_{291}, X_{292}, X_{293}		X_{301}, X_{302}, X_{303}
	Inadequate	X_{311}, X_{312}, X_{313}		X_{321}, X_{322}, X_{323}	X_{331}, X_{332}, X_{333}		X_{341}, X_{342}, X_{343}	X_{351}, X_{352}, X_{353}		X_{361}, X_{362}, X_{363}

3.3 FIELD EXPERIMENTAL PLAN

The research team in coordination with the Oregon DOT updated the experimental plan to reflect the needs to best calibrate the MEPDG. This updated field plan is reflected in Table 3.2 on the ensuing page. It is important to point out that all of these pavements had at least three pavement condition surveys conducted on three randomly selected 500 foot sections. In some instances, the initial random sections needed to be adjusted for safety reasons, e.g. avoiding intersections and on or off ramps for divided roadways as well as bridge structures. In a couple of instances, it was necessary to shorten the survey section length from 500 to 300 feet, because the overall pavement section was less than one mile, yet the surveyed sections did represent a substantial percentage of the overall pavement. Where the pavement being surveyed was less than 0.5 mile, the entire pavement was surveyed.

Table 3.2: Pavement Sections Surveyed

		Region								
		Coastal		Valley				Eastern		
Traffic	Pavement Performance	HMA/HMA/Agg	HMA/HMA/CTB	HMA/HMA/Agg	HMA/Agg	CRCP/stab or unstab	HMA/CRCP	HMA/HMA/Agg	HMA/Agg	CRCP/stab or unstab
Low Volume	Very good-Excellent	US 101: Neptune Dr-Camp Rilea	US 101: NCL Bandon-June Ave, US 101: Sutton Creek-Munsel Lake Rd	US 20: Sweet Home-18th Ave, OR 34: Wcl Lebanon-RXR X-ing,				US 730: I-84 Canal Rd, OR 201: Washington Ave-Airport Way, OR 140: Jct Hwy 019-Bowers Bridges Creek		
	As expected	US 101:Tillamook Couplet (SB), US 101: Wilson R.-Tillamook Couplet	US 101:Elk Hill Rd-Port Orford	OR 99 E:Albany Ave-Calapooia St				US 97: Weighb St-Crawford Rd, US 20: MP 10.3-MP 12.5	US 26: Prairie City-Dixie Summit, US 26: Prairie City Section, US 395: Jct Hwy 2-Hwy 33	
	Inadequate	US 101: Dooley Br-Jct Hwy 047, US 101: Florida Ave-Washington Ave			OR 221: N. Salem-Orchard Heights Rd			US730: Canal Rd-Umatilla Bridge		
High Volume	Very good-Excellent			US 30: Cornelius Pass Rd-Begin JCP, OR 120: End Jcp-Beg Hwy 081			I-5:Wilsonville Intch-Tualatin R	US 97: S. Century Dr-MP 161		
	As expected			OR 569: Hwy 091-Willametter R. (EB)	OR 99W: Marys R-Kiger Island Dr, OR 99W: N. Sherwood-SW 12th St.	I-5:Corvallis/Leanon Interchange-N. Albany	I-5: Haysville Intch to Woodburn	US 97: Madras Couplet-Hwy 360		I-84:N. Powder-Baldock Slough, I-84: N. FK Jocobsen Gulch-Malheur River (WB)
	Inadequate			I-5: Azalea-Canyonville, OR 99W: Brustschr St. - Jct Hwy 151,	OR 22: End Hwy 072-I-5 NB Ramps		I-84: NE Union Ave-S. Banfield Intch	I-84: N.FK Jocobsen Gulch-Malheur River (EB), US 97: N. Chiloquin Intch-Williamson Dr		I-84: Stanfield Int-Pendleton,

4.0 DARWIN M-E INPUT DATA AND FIELD SURVEY RESULTS

4.1 INTRODUCTION

The research team coordinated with the Oregon DOT on obtaining the pavement characteristic data. This data includes pavement structural data such as pavement layer type, layer thickness, volumetric characteristics of the asphalt layers, gradation and binder characteristics. The primary effort for calibrating the Darwin M-E was on the Level 3 analysis, however some Level 2 calibration is done with the realization that the binder properties based on the performance grade was based upon those provided by Lundy (*Lundy et al. 2005*). Level 1 analysis was done to illustrate the effects of having the dynamic modulus data rather than using default values developed by Lundy (*Lundy et al. 2005*). For certain input data, the Darwin M-E default values were used as default, since the specific information for Oregon has not been developed.

4.2 SECTION GENERAL CHARACTERISTIC INFORMATION

The first step to Darwin M-E is to enter general information at the *General Information* area located in the top left corner of the Project Tab. General information includes design type, pavement type, design life, month and year of existing and new pavement, and month and year to opening to traffic. A screen-shot of *General Information* area is provided in Figure B.1 in Appendix B.

4.3 TRAFFIC

Traffic data for Darwin M-E design consists of the following lists:

- Base year traffic volume and speed,
- Traffic capacity,
- Axle configuration,
- Lateral wander,
- Wheelbase,
- Vehicle class distribution and growth,
- Hourly adjustment,
- Axles per truck,
- Monthly adjustment, and
- Axle load distribution factors.

Darwin M-E uses a hierarchical approach (Level 1 through Level 3) to define traffic inputs based on the source of traffic data available. Level 3 default values (nationwide average) were selected for all the aforementioned lists except for traffic volume and speed. Traffic growth rate for each of the vehicle class was assumed to be same. A screen shot of *Traffic Tab* is shown in Figure B.2 in Appendix B.

4.4 CLIMATE

Darwin M-E requires longitude, latitude, and elevation of the project for the creation of virtual weather station to simulate the environmental conditions encountered. The depth to water table measured in feet is also required.

4.5 HMA LAYER PROPERTIES

Information regarding HMA surface shortwave absorptivity and rehabilitation (condition of existing pavement) are required for HMA layer properties. Default value of 0.85 for HMA surface shortwave absorptivity and rehabilitation Level 3 was used for HMA layer properties. For rehabilitation Level 3 shown in Figure B.4 in Appendix B, information related to milled thickness, pavement rating, and total rutting are required by Darwin M-E. A pavement rating of fair (3) and total rut depth of 0 inches- were used as there was no information available related to rehabilitation.

4.6 PAVEMENT STRUCTURE

The following subsections summarize the input values for the HMA, non-stabilized base, and subgrade layers.

4.6.1 Flexible Pavement Layer

HMA layer properties related to thickness, volumetric properties, mechanical properties, and thermal properties as shown in Figure B.5 in Appendix B are required. For dynamic modulus input Level 1, values from dynamic modulus testing are required. Aggregate gradation is required for dynamic modulus characterization for Level 2 and 3. For input Level 1 for asphalt binder, asphalt binder dynamic shear modulus (G*) and phase angle at different temperatures are required. Asphalt binder grade is required for Level 3 analysis. Input level for asphalt binder is dependent on the input level for dynamic modulus, shown in Table 4-1.

Table 4.1: Input Level for Dynamic Modulus and Asphalt Binder

Parameter	Input Level		
Dynamic Modulus	1	2	3
Asphalt Binder	1	1	3

Input Level 3 for indirect tensile strength and creep compliance were chosen as no information related to indirect tensile strength and creep compliance was provided. Darwin M-E automatically calculates these values once dynamic modulus and asphalt binder values are entered. Other default values provided by Darwin M-E were selected for HMA layer properties.

4.6.2 Non-Stabilized Base Layer

Properties related to non-stabilized base layer includes thickness, Poisson's ratio, co-efficient of lateral earth pressure, resilient modulus, type of base layer, gradation and other engineering properties are required. These values are required for Darwin M-E. Default values for the aforementioned properties except type and thickness of the base layer were selected for the calibration.

4.6.3 Subgrade

For subgrade layer characterization, Poisson's ratio, co-efficient of lateral earth pressure, resilient modulus, type of base layer, gradation and other engineering properties are required. Web Soil Survey was employed to determine the type of soil and resilient modulus values provided by Oregon DOT. At several sites, historic subgrade modulus values derived from falling weight deflectometer testing was used. Other default values provided by Darwin M-E were used.

4.7 ASPHALT MIXTURE DYNAMIC MODULUS VALUES

The dynamic modulus values, E*, used for calibrating Darwin M-E were those developed for the Oregon DOT by Lundy and Sandoval-Gil (*2005*). The specific E* values used were interpolated between the 4% and 7% reported in Table 4-2 below for the specific air void value based upon the actual voids of each specific project. Further, the values used corresponded to the binder grade used in the specific project.

Table 4.2: E* Values used for Calibrating Darwin M-E (*Lundy & Sandoval-Gil 2005*)

				Frequency, HZ					
			Test Temp., C	0.1	0.5	1	5	10	25
5.8% Binder, 4.0% Air, 100 Gyrations	PG 64-22	Series 1-1	-10	2623	3097	3260	3554	3649	3750
			4.4	945	1533	1807	2424	2662	2943
			21.1	143	308	423	818	1042	1377
			37.8	27	47	63	130	180	279
			54.4	13	17	19	29	36	51
	PG 70-22	Series 1-2	-10	2696	3236	3442	3849	3994	4159
			4.4	1118	1664	1921	2527	2778	3091
			21.1	272	483	611	1008	1219	1530
			37.8	67	109	137	243	312	433
			54.4	30	40	46	70	86	114
	PG 70-28	Series 1-3	-10	2681	3207	3398	3754	3873	4004
			4.4	958	1522	1793	2427	2685	2998
			21.1	183	351	463	836	1048	1367
			37.8	46	74	93	171	225	327
			54.4	24	30	34	48	58	77
	PG 76-22	Series 1-4	-10	2612	2967	3093	3313	3386	3466
			4.4	1208	1722	1946	2428	2611	2825
			21.1	294	527	667	1081	1291	1585
			37.8	73	118	150	269	347	483
			54.4	35	44	51	75	92	123
5.8% Binder, 7.0% Air, Gyrations, as required	PG 64-22	Series 2-1	-10	1891	2349	2527	2886	3016	3165
			4.4	657	1052	1248	1730	1938	2203
			21.1	119	235	311	563	708	930
			37.8	24	43	56	109	146	215
			54.4	9	13	16	26	33	46
	PG 70-22	Series 2-2	-10	2246	2659	2806	3078	3168	3267
			4.4	853	1337	1563	2077	2281	2524
			21.1	153	306	408	742	928	1203
			37.8	32	54	70	135	183	272
			54.4	15	19	22	33	41	56
	PG 70-28	Series 2-3	-10	1897	2349	2525	2878	3005	3151
			4.4	652	1032	1222	1696	1902	2165
			21.1	138	251	324	566	704	918
			37.8	37	59	73	128	166	233
			54.4	18	23	27	38	46	61
	PG 76-22	Series 2-4	-10	2647	3056	3200	3464	3552	3647
			4.4	1100	1637	1879	2417	2626	2875
			21.1	237	442	571	972	1184	1489
			37.8	56	91	117	215	283	404
			54.4	26	34	39	57	70	95

4.8 FIELD CONDITION SURVEY RESULTS

The field condition distress surveys were conducted according to the FHWA Long Term Pavement Performance (LTPP) publication Data Collection Guide For Long Term Pavement Performance (*2003*). The summary of the field condition surveys are provided in Table 4.3 and 4.4. It is important to point out that the vast majority of the pavements had condition surveys conducted on three 500 foot sections and the data represented in the table is the average of the three condition surveys. Longitudinal (top-down) cracking and thermal cracking were reported linear feet per mile while for alligator (bottom-up) cracking, the linear feet of cracking recorded in the field distress surveys were converted a percentage of the surveyed section for calibrating with Darwin M-E as the software estimates the percentage of a sections' cracked area.

Table 4.3: Summary of Field Condition Distress Surveys for AC Sections

Region	Name	Highway Number	Traffic Level, ESALs	Begin MP	End MP	Rut, inch	Thermal Cracking, ft/mi	Top Down Cracking, ft/mi	Bottom Up Cracking, %
Coast	US 101	9	8.4	6.83	10.16	0.044	0	0	0
	US 101	9	4.5	65.64	66.43	0.161	0	1144	1.05
	US 101	9	6.8	22.48	24.93	0.260	0	1467.8	11.2425
	US 101	9	5.5	261.2	273.56	0.060	0	0	0
	US 101	9	10.2	64.23	65.64	0.094	0	833.07	0.33
	US 101	9	3.4	235.09	235.51	0.109	0	0	0.33
	US 101	9	4.3	184.72	187.76	0.071	0	1510	1.55
	US 101	9	4.1	298.26	299.94	0.154	0	133.76	0.46
Valley	US 20	16	3.9	26.64	27.72	0.114	0	1510.1	0.011
	OR 99	58	9.3	0.42	2.93	0.128	0	2875.8	4.73
	OR 34	210	5.2	16.92	17.89	0.072	0	1766.2	0.00833
	OR 221	150	7.5	17.3	20.15	0.196	0	8930.2	1.79
	OR 22	162	25.3	1.17	1.68	0.167	0	10629	4.38
	I-5	1	49.9	89.54	97.9	0.168	0	4620	0.061
	I-5	1	-	169.7	170	0.140	0	0	0.0125
	I-5	1	100.8	259.1	272.29	0.119	0	0	0
	I-5	1	39	283.92	289.82	0.114	0	0	0
	I-84	2	-	0.4	5.56	0.337	0	35.2	0.003
	OR569	69	39.8	6.56	9.59	0.413	0	0	0
	OR 99W	91	12.1	84.24	86.5	0.200	0	9504	3.36
	OR 99W	91	14.9	21.8	23.76	0.219	0	5244.8	0.042
	OR 99W	91	11.3	14.67	15.67	0.349	0	0	0
	US 30	92	18.2	13.12	17.9	0.382	0	0	0
	OR 120	120	23	2.49	2.71	0.225	0	1804.7	0.163
	US 97	4	13.04	247.80	252.02	0.313	0	2646	12.53
	OR 140	431	0.75	0.00	9.33	0.052	0	16.67	0
East	US 730	2	5.5	168.23	174.3	0.135	61.8	0	0
	US 730	2	10.1	174.3	182.6	0.119	317.2	2277.4	1.43
	US 97	4	16.5	96.04	97.29	0.309	22.3	0	0.4296
	US 97	4	12.4	153.67	161	0.246	248.8	0	4.71
	US 97 (SB)	4	10.8	146.48	149.48	0.082	0	0	0
	US 97 (NB)	4	10.8	146.48	149.48	0.681	1.2	0	1.27
	US 26	5	2.3	175.65	183.21	0.078	0	0	0

	US 26	5	2.9	174.89	175.65	0.051	0	48	0
	I-84	6	30.1	368.16	374.08	0.499	70.4	0	0.19
	US 20	17	6.7	10.3	12.5	0.621	0	0	0
	US 395	54	7.2	0.04	4.83	0.320	2.3	4202.9	2.22
	OR 201	455	3.3	25.75	29.6	0.065	138.45	0	7

Table 4.4: Summary of Field Condition Distress Surveys for CRCP

Region	Project ID	Highway Number	Oregon Route Number	Begin MP	End MP	No. of Punchouts per Mile		
						Low	Medium	High
Valley	I-5 Corvallis/Lebanon Interchange	001	I-5	227.68	234.65	156.5	42	7.5
East	I-84:Stanfield Int-Pendleton	006	I-84	188.04	203.65	160.5	138.6	7
East	I-84:N.Powder-Baldock Slough	006	I-84	285.33	297.08	54.5	12.3	0
East	I-84:N.FK Jocobsen Gulch-Malheur River	006	I-84	368.16	374.08	394	215.1	21.1

Similar to the national calibration, low, medium, and high severity cracking were summed up without adjustment for both alligator cracking and longitudinal cracking. For thermal (transverse) cracking, low, medium, and high severity cracking were summed up using the same weighting function in the national calibration that is shown in the following equation (*ARA 2004*).

$$\text{Thermal Cracking (TC)} = \frac{LowSeverityTC + 3 * MediumSeverityTC + 5 * HighSeverityTC}{9} \quad \textbf{(4.1)}$$

5.0 UNCALIBRATED DARWIN M-E SIMULATION RESULTS AND SENSITIVITY ANALYSIS

5.1 INTRODUCTION

The research team coordinated with the Oregon DOT on obtaining the pavement characteristic data. This data includes pavement structural data such as pavement layer type, layer thickness, volumetric characteristics of the asphalt layers, gradation and binder characteristics. The primary effort for calibrating the Darwin M-E was on the Level 3 analysis, however, some Level 2 calibration is done with the realization that the binder properties based on the performance grade was based upon those provided by Lundy et al (*2005*). Level 1 analysis was done to illustrate the effects of having the dynamic modulus data rather than using default values developed by Lundy et al (*2005*). For certain input data, the Darwin M-E default values were used as the specific information for Oregon has not been developed.

5.2 SUMMARY OF DARWIN M-E SIMULATION RESULTS

The results of the Darwin M-E simulation results and the corresponding actual measured field performance are presented in this section in Figures 5.1 through 5.4. The simulation results are shown at the 90% and 50% (Mean) levels of reliability to illustrate the effect of reliability on the Darwin M-E simulation results. Figures 5.1 through 5.4 summarize the Darwin M-E simulation results from rutting, thermal cracking, longitudinal (top-down) cracking, and alligator (bottom-up) cracking as compared to the actual field measured values at the same corresponding age. The rutting reflected in Figure 5.1 is the total amount of rutting including all pavements, e.g. asphalt paving lifts as well as base and subbase layers. Generally, one should be concerned in the instances where Darwin M-E is estimating pavement distress levels greater than failure, e.g. more than 0.4 inches for rutting are estimated by Darwin M-E when in fact all but two pavement section had less than 0.4. It is important to point out that the two sections that had higher levels of rutting were likely the result of studded tires and use of chains. It is thus important that the calibration be focused on being accurate at actual high levels of distress where failure may occur. Examination of Figures 5.2 through 5.4 illustrates that Darwin M-E will need a substantial amount of effort in calibration for the thermal, longitudinal (top-down), and alligator (bottom-up) cracking, respectively.

From Figure 5.1, it is evident that Darwin M-E over predicted total rutting compared to the measured total rutting. The subgrade rutting predicted by Darwin M-E ranged from 31% to 100% of total rutting, with an average value of 68%. Base rutting predicted ranged from 0% to 16% of total rutting, with an average of 8%. So, most of the rutting predicted by Darwin M-E came from the subgrade, which supports the study findings conducted by the Montana DOT. The Montana DOT conducted the local calibration study of MEPDG for flexible pavements. They concluded that the rutting prediction model in the MEPDG over-predicted total rut depth because significant rutting was predicted in unbound layers and embankment soils. A study by Hoegh

(*Hoegh et al. 2010*) demonstrated that current MEPDG subgrade and base rutting models grossly overestimated rutting for the MnROAD test sections.

The Coastal and Valley regions of Oregon do not experience low-temperature thermal cracking (transverse cracking). But, the Eastern region displays a considerable amount of thermal cracking. It is shown in Figure 5.2 (b) that Darwin M-E predicted no thermal cracking even in the Eastern region. A constant thermal cracking of 27 ft/mile was predicted for all the pavement sections, as evident by Figure 5.2 (a). While Darwin M-E predicted no alligator cracking (Figure 5.4 (b)) for all the sections considered, a high variability between predicted and measured longitudinal cracking was observed, as shown in Figure 5.3.

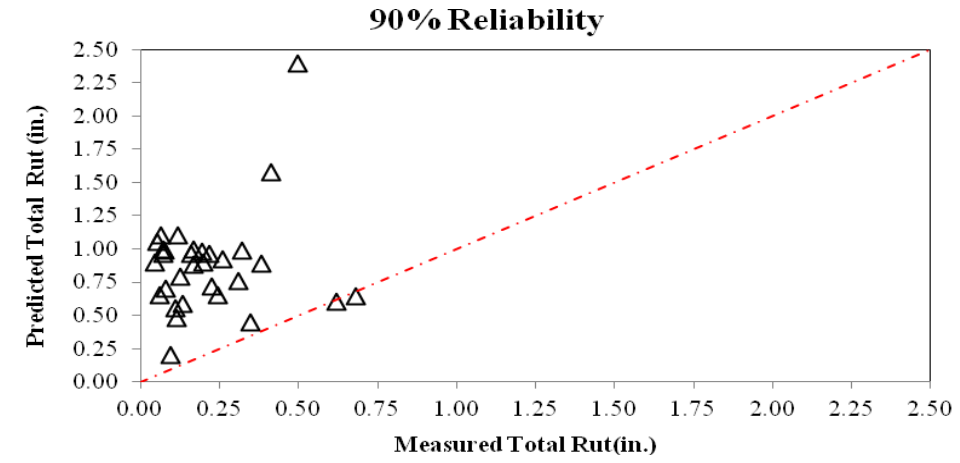

(a)

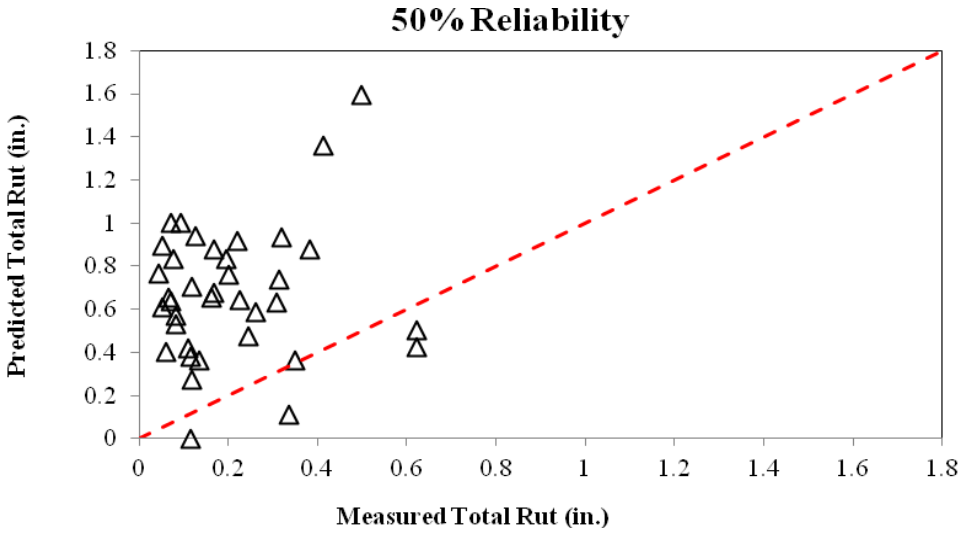

(b)

Figure 5.1: Predicted Total Rut versus Measured Total Rut
for (a) 90% Reliability and (b) 50% Reliability

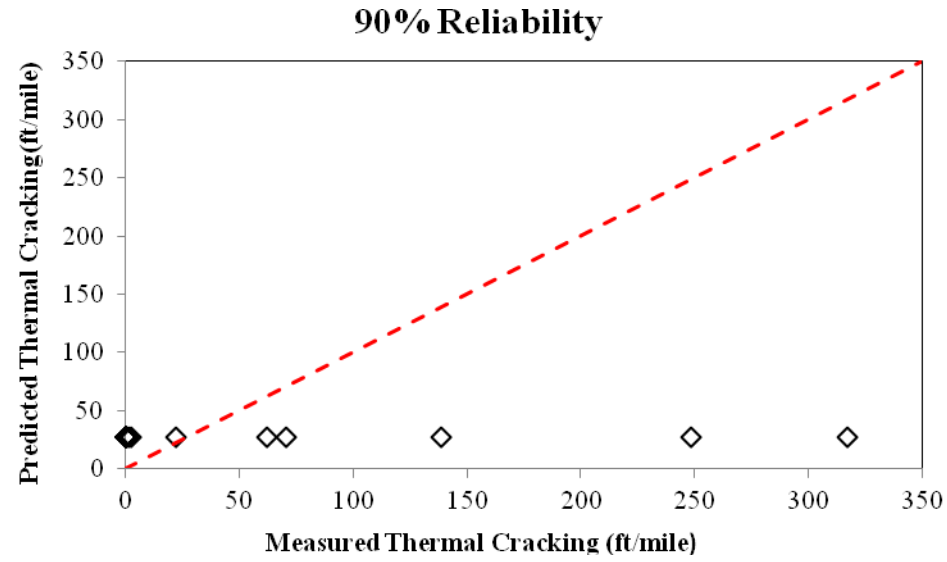

(a)

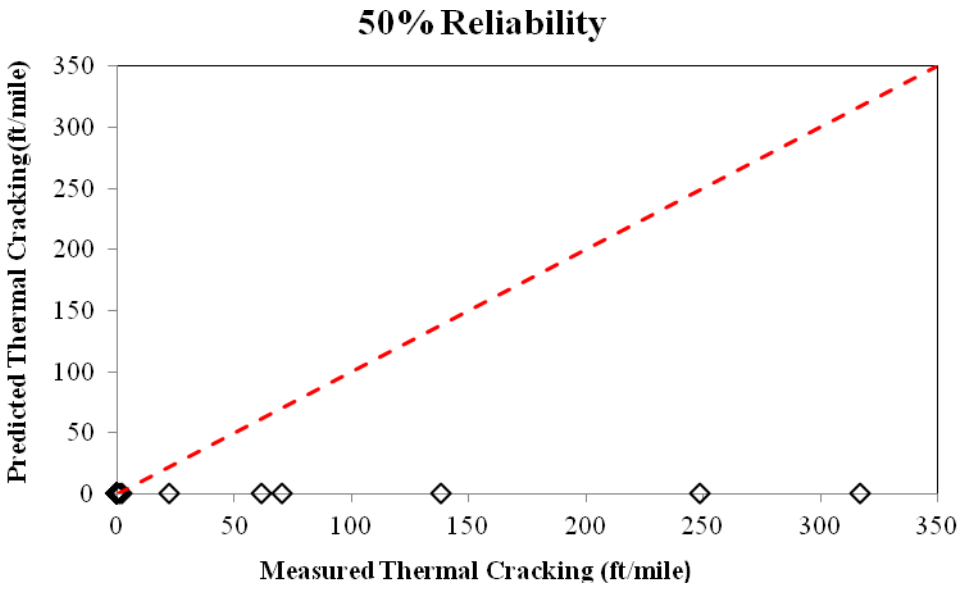

(b)

Figure 5.2: Predicted Thermal Cracking versus Measured Thermal Cracking for (a) 90% Reliability and (b) 50% Reliability

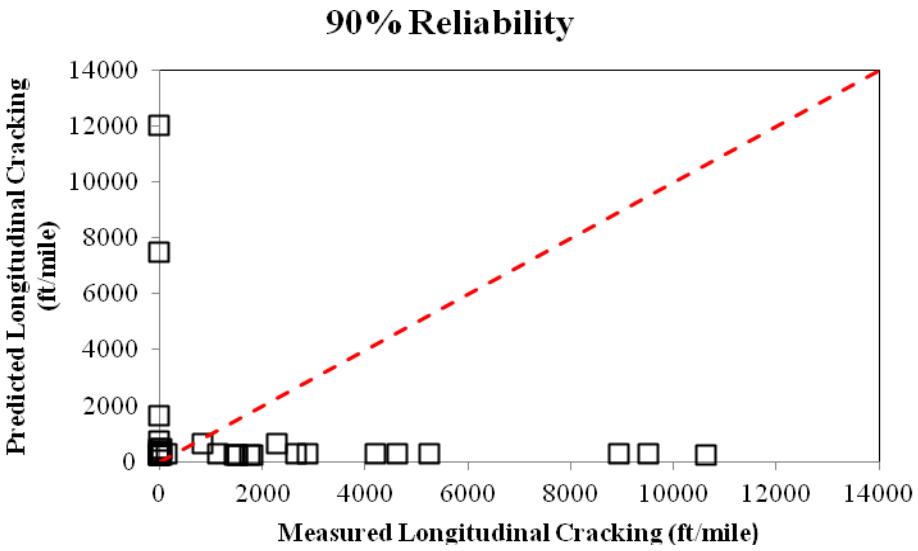

(a)

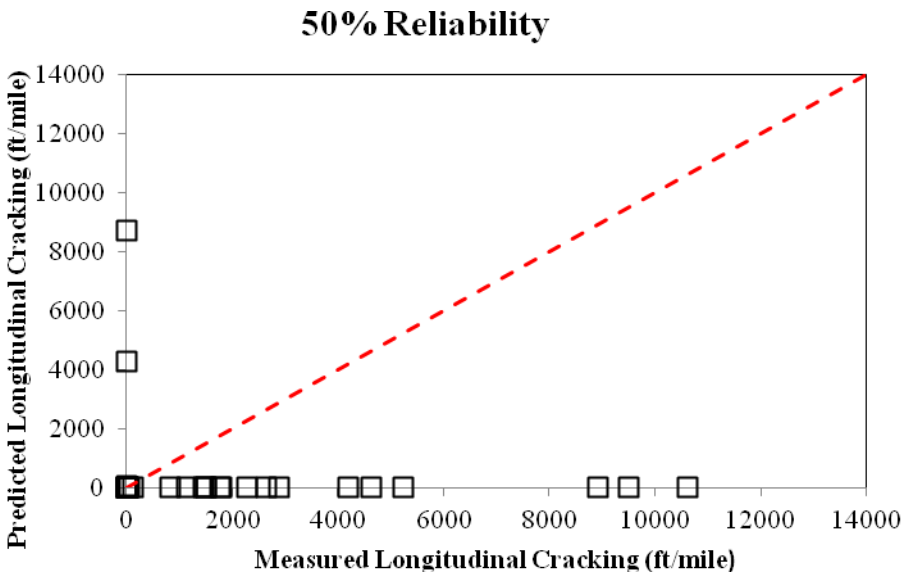

(b)

Figure 5.3: Predicted Longitudinal Cracking versus Measured Longitudinal Cracking for (a) 90% Reliability and (b) 50% Reliability

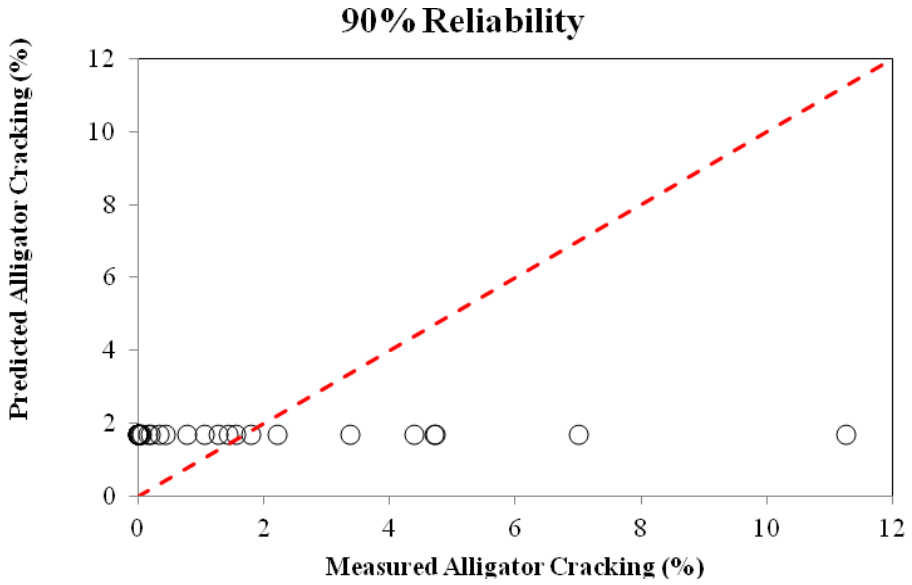

(a)

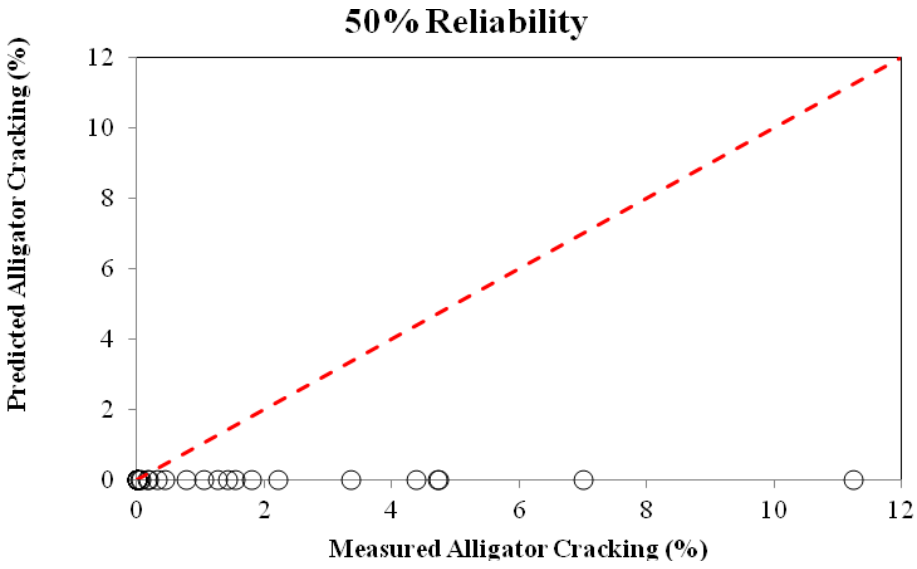

(b)

Figure 5.4: Predicted Alligator Cracking versus Measured Alligator Cracking for (a) 90% Reliability and (b) 50% Reliability

5.3 SUMMARY OF DARWIN M-E RESULTS WITH CLIMATE SEGMENTATION

Figures 5.5 through 5.8 summarizes the distresses for the three different climatic zones in Oregon; Coastal, Valley and Eastern. Specifically, Figure 5.5 illustrates that the Darwin M-E program over estimates the amount of rutting in all three climatic zones as the data lies above the line of equality for all three regions. However, in Figure 5.6 the reverse is true- Darwin M-E underestimates the amount of thermal cracking. Similarly the results for longitudinal (top-down) cracking in Figure 5.7 show that Darwin M-E underestimates the amount of cracking as compared to what is measured with the exception of the Eastern region. Darwin M-E provides reasonably accurate results for the pavement sections in the Eastern Oregon region. Figure 5.8 highlights the results of the alligator (bottom-up) cracking. Generally, Darwin M-E underestimates alligator (bottom-up) cracking as compared to measured cracking for all the three regions.

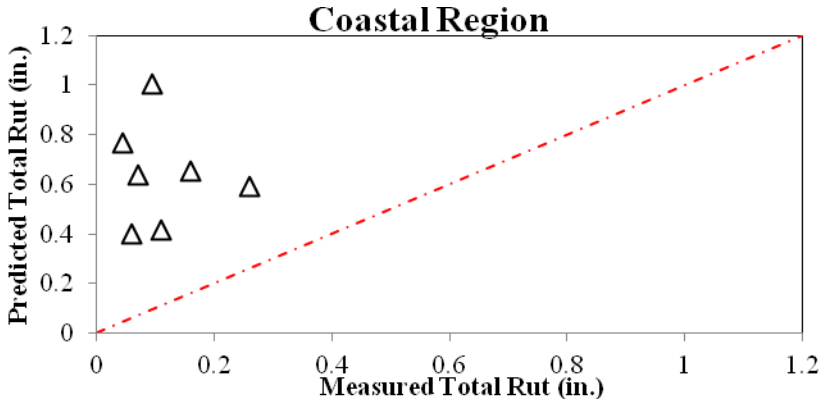

(a)

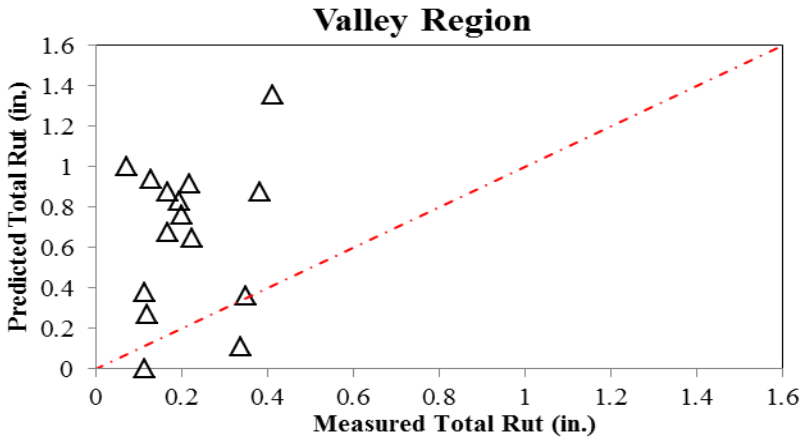

(b)

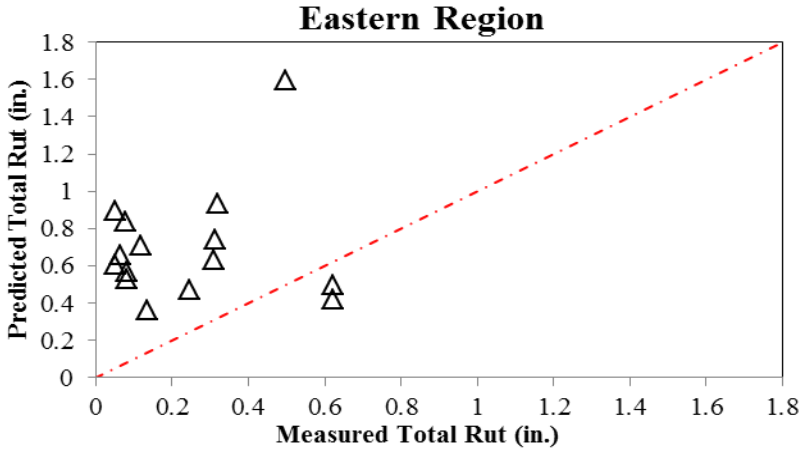

(c)

Figure 5.5: Predicted Mean Total Rut (50% Reliability) versus Measured Total Rut for (a) Coastal, (b) Valley and (c) Eastern Regions

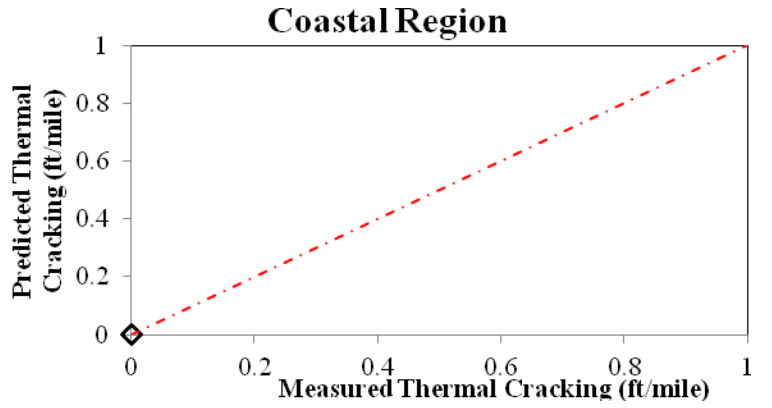

(a)

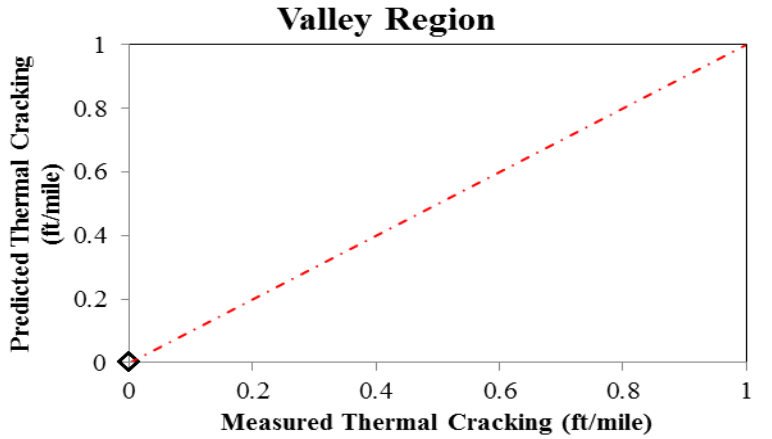

(b)

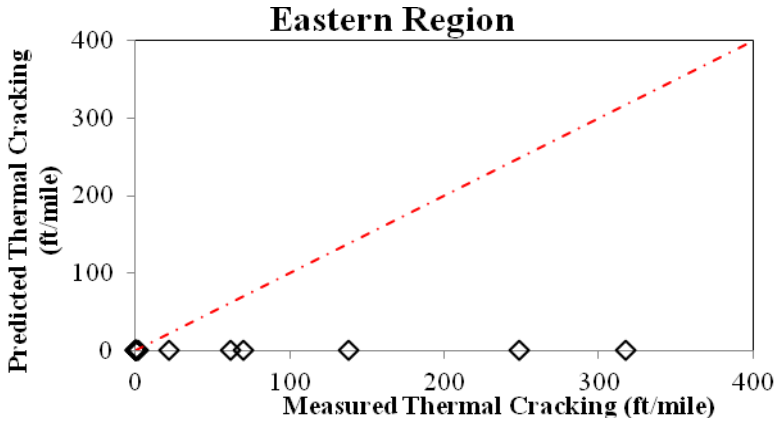

(c)

Figure 5.6: Predicted Mean Thermal Cracking (50% Reliability) versus Measured Thermal Cracking for (a) Coastal, (b) Valley and (c) Eastern Regions

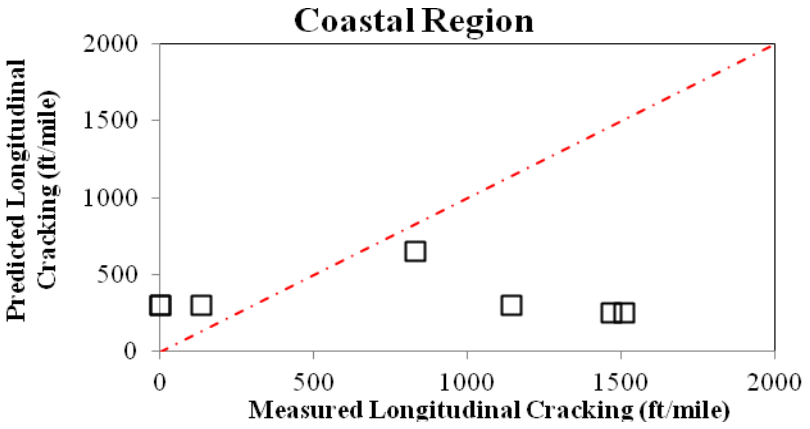

(a)

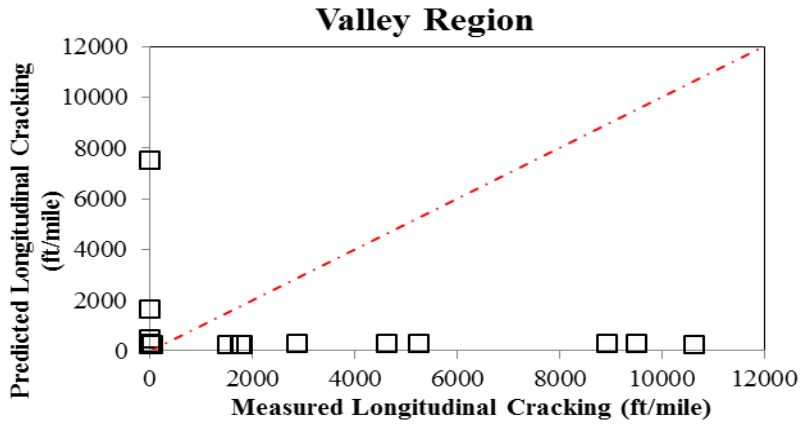

(b)

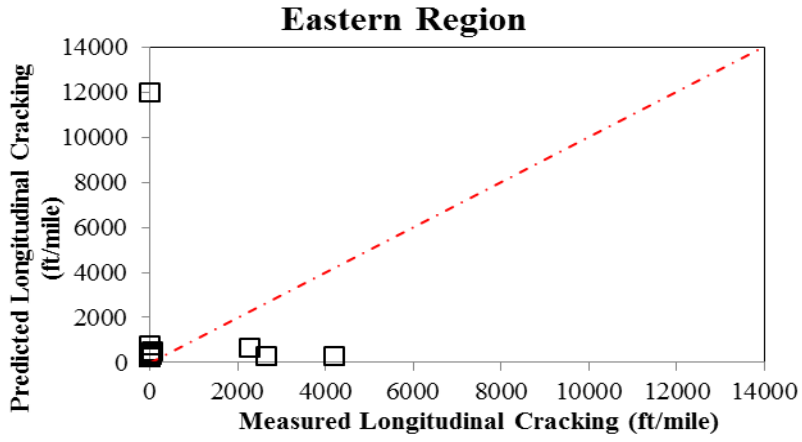

(c)

Figure 5.7 Predicted Longitudinal Cracking (90% Reliability) versus Measured Longitudinal Cracking for (a) Coastal, (b) Valley and (c) Eastern Regions

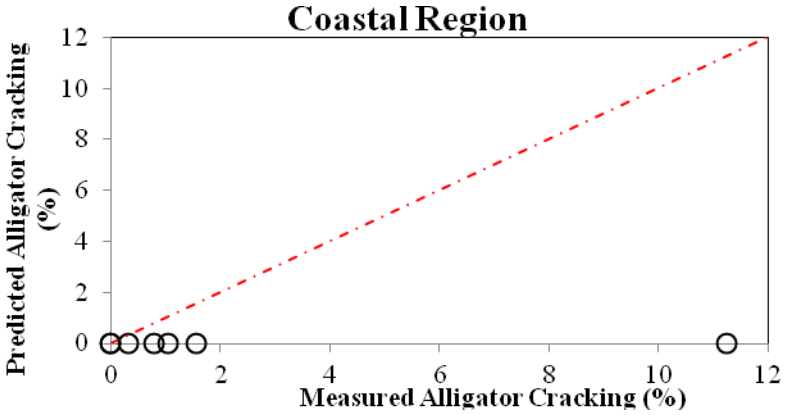

(a)

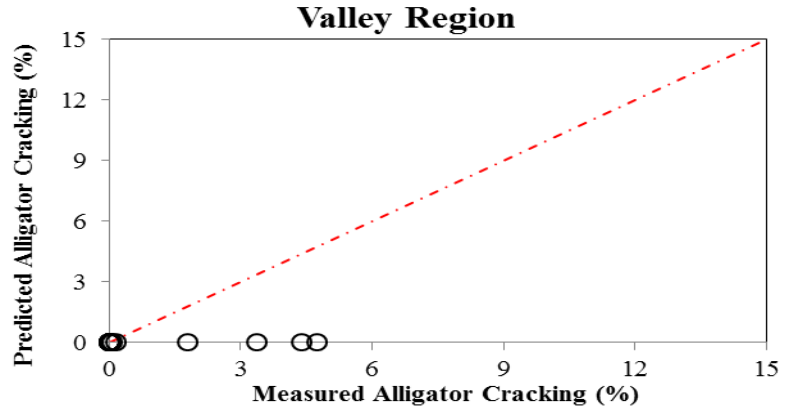

(b)

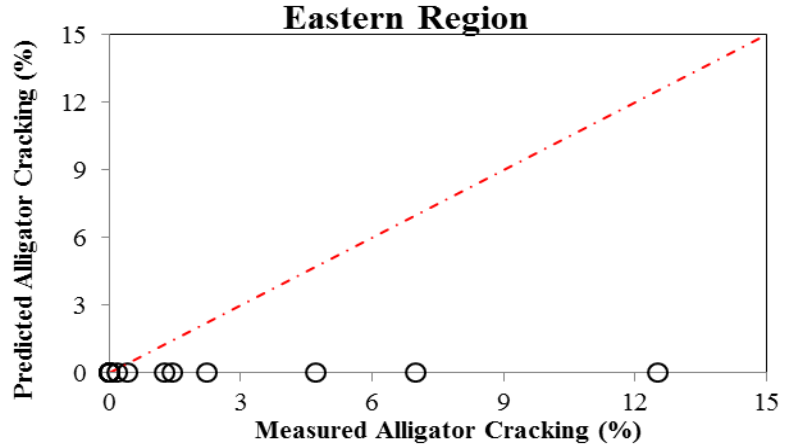

(c)

Figure 5.8: Predicted Mean Alligator Cracking (50% Reliability) versus Measured Alligator Cracking for (a) Coastal, (b) Valley and (c) Eastern Regions

5.4 SUMMARY OF DARWIN M-E RESULTS WITH TRAFFIC LEVEL SEGMENTATION

The outcomes of the Darwin M-E simulations were next segmented based upon trafficking level to determine if the national level models were affected by load level. These results are contained in Figures 5.9 through 5.12. As can be seen in Figure 5.9, Darwin M-E over estimates the amount of rutting considerably regardless of trafficking level. In Figure 5.10, the reverse of rutting is true for the thermal cracking as the Darwin M-E software underestimates the amount of thermal cracking as compared to the actual amount observed in the field for all levels of trafficking...For the longitudinal (top-down) cracking, the Darwin M-E is reasonable for the low trafficking level, but underestimates the amount of cracking for the medium and high levels of trafficking as can be seen in Figure 5.11. Figure 5.12 summarizes the results for the alligator (bottom-up) cracking and illustrates that the Darwin M-E underestimates the amount of alligator cracking for all three levels of trafficking.

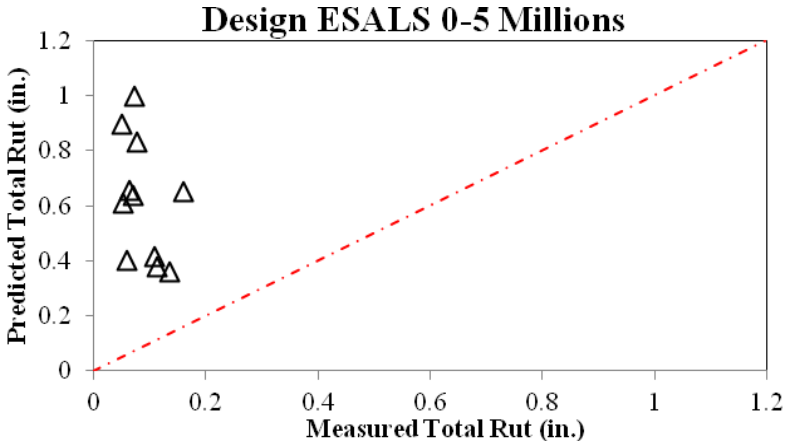

(a)

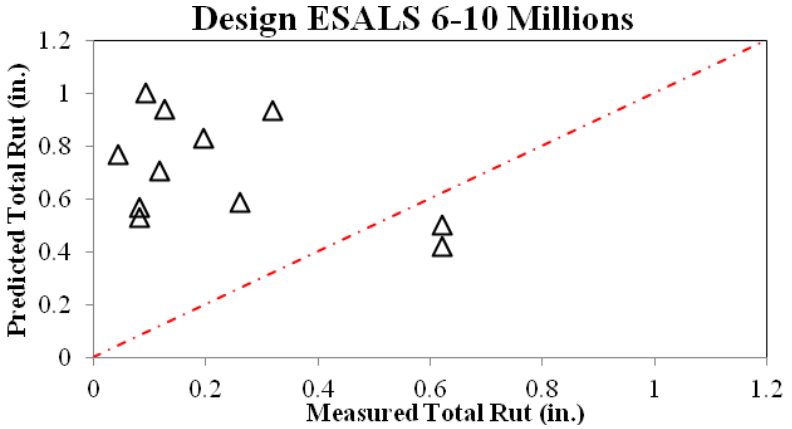

(b)

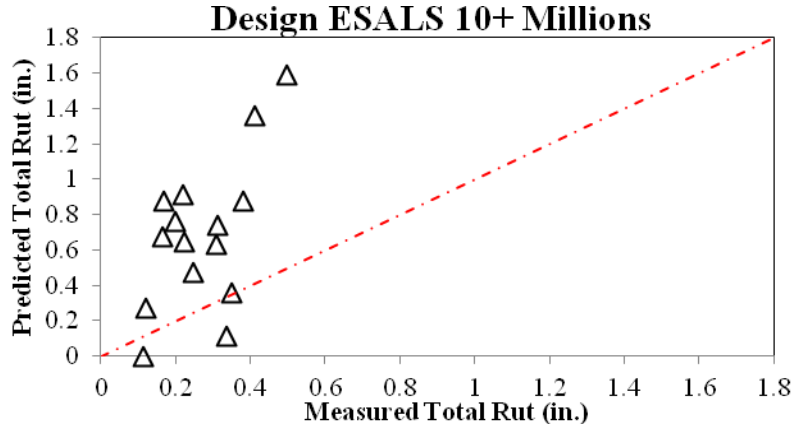

(c)

Figure 5.9: Predicted Mean Total Rut (50% Reliability) versus Measured Total Rut for (a) Low, (b) Medium, and (c) High Volume Roads

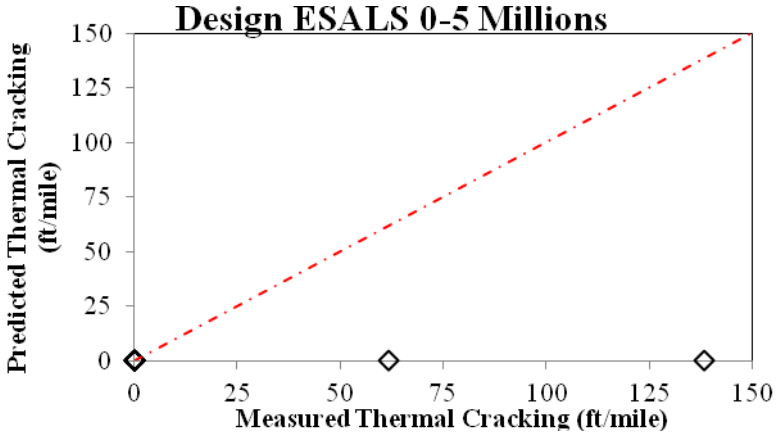

(a)

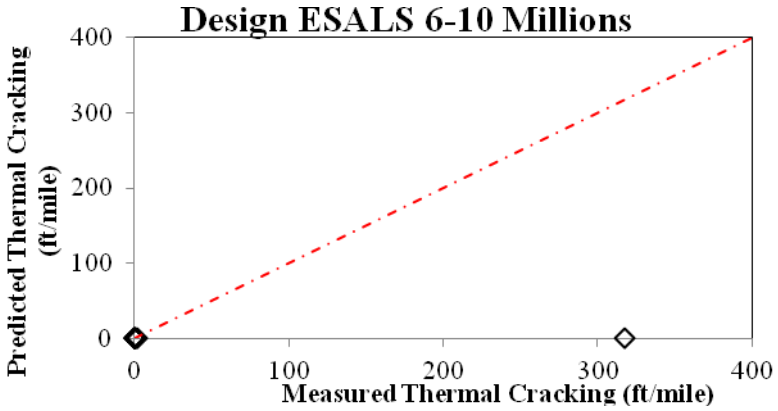

(b)

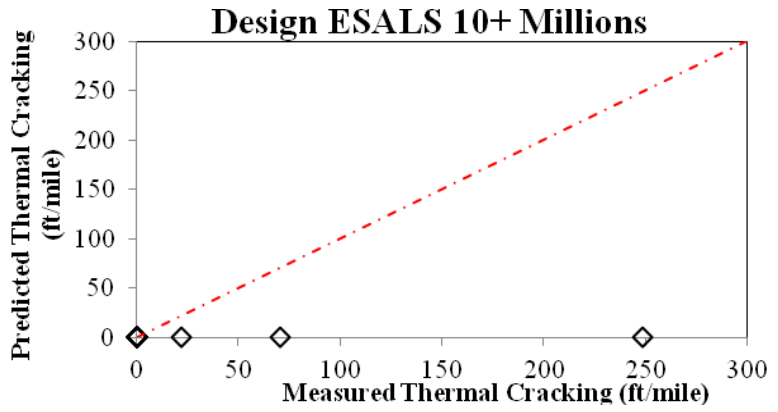

(c)

Figure 5.10: Predicted Mean Thermal Cracking (50% Reliability) versus Measured Thermal Cracking for (a) Low, (b) Medium, and (c) High Volume Roads

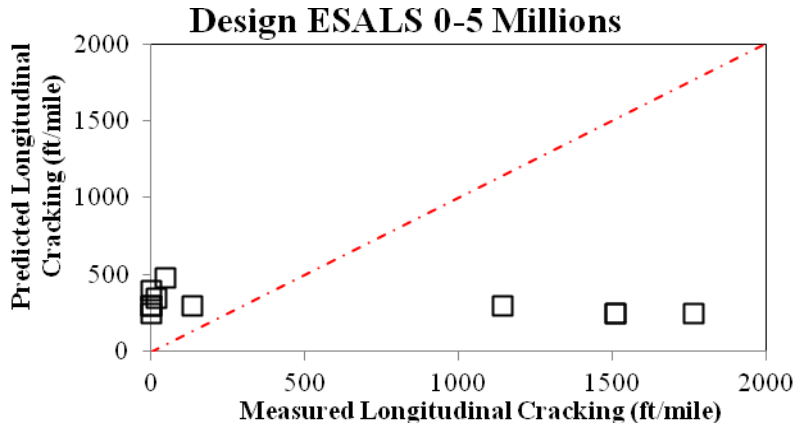

(a)

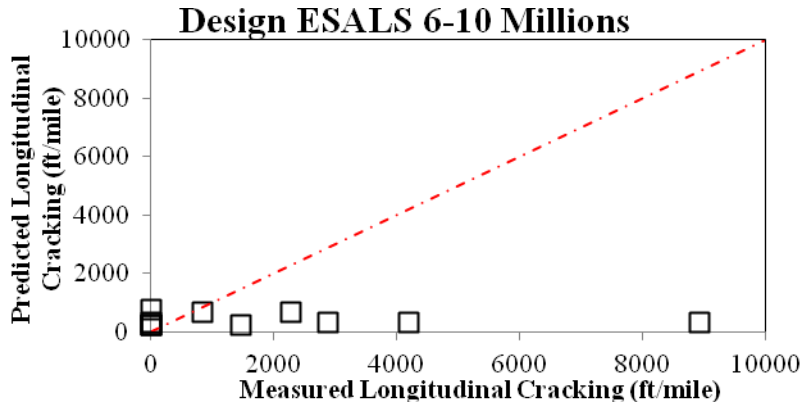

(b)

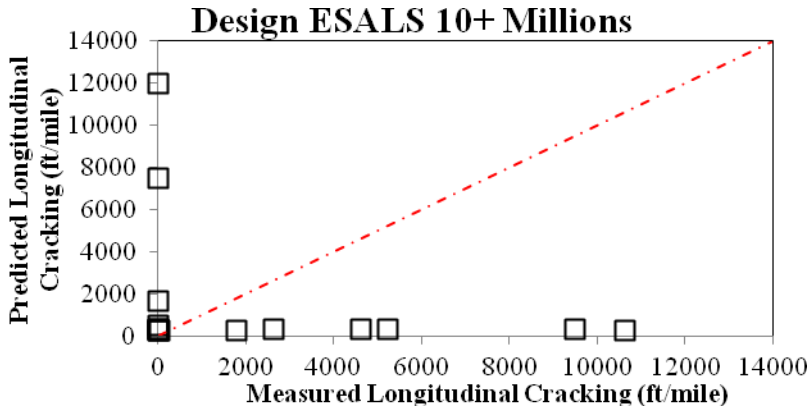

(c)

Figure 5.11: Predicted Longitudinal Cracking (90% Reliability) versus Measured Longitudinal Cracking for (a) Low, (b) Medium, and (c) High Volume Roads

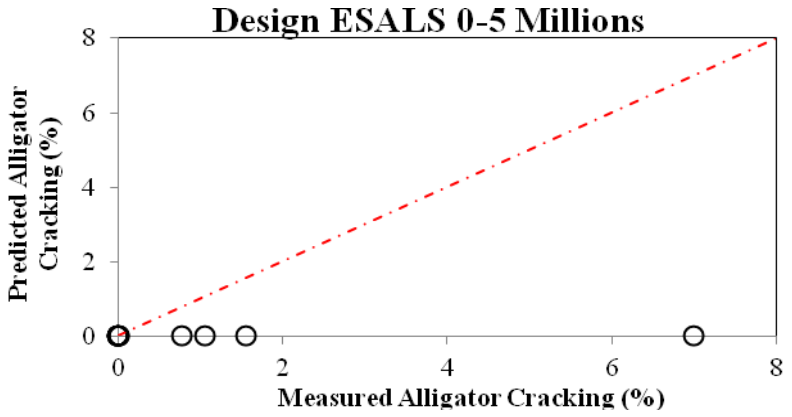

(a)

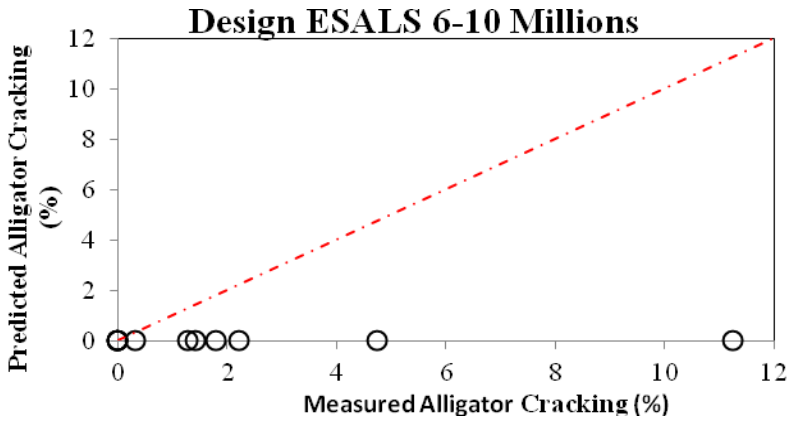

(b)

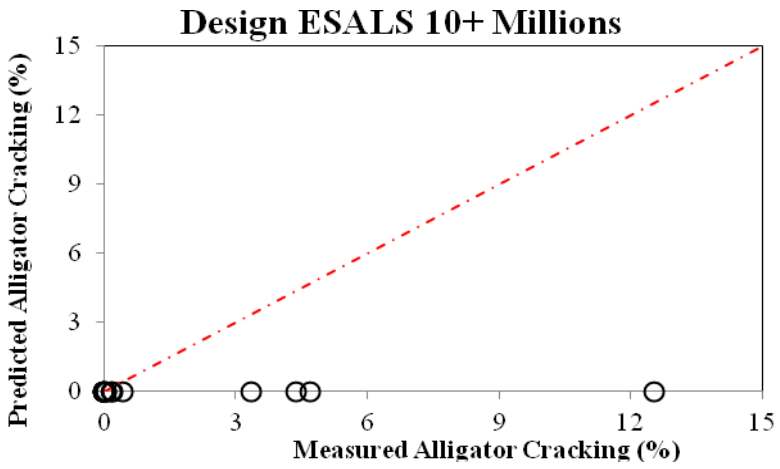

(c)

Figure 5.12: Predicted Mean Alligator Cracking (50% Reliability) versus Measured Alligator Cracking for (a) Low, (b) Medium, and (c) High Volume Roads

5.5 SUMMARY OF DARWIN M-E RESULTS WITH AGE SEGMENTATION

The last type of segmentation was done on age at two levels: 0-10 years and 11-25 years. The summary of the results are shown in Figures 5.13 through 5.16. As has been the case with the other segmentations, the Darwin M-E software overestimates the amount of rutting considerably and is illustrated in Figure 5.13. Like the other segmentations, the Darwin M-E software underestimates the amount of thermal cracking and alligator (bottom-up) cracking regardless of age as illustrated in Figure 5.14 and 5.16, respectively. Figure 5.15 summarizes the outcomes of the longitudinal (top-down) cracking and shows that either the distress is considerably overestimated or considerably underestimated by the Darwin M-E software.

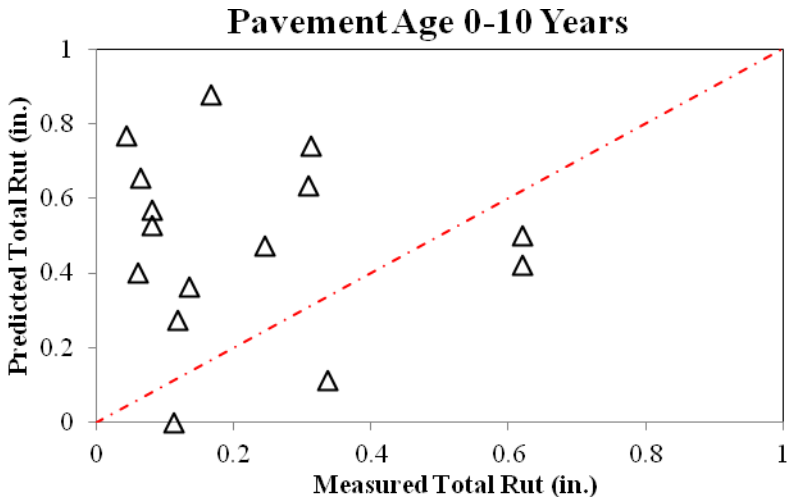

(a)

(b)

Figure 5.13: Predicted Mean Total Rut (50% Reliability) versus Measured Total Rut for Pavement Ages (a) 0-10 Years and (b) 11-25 Years

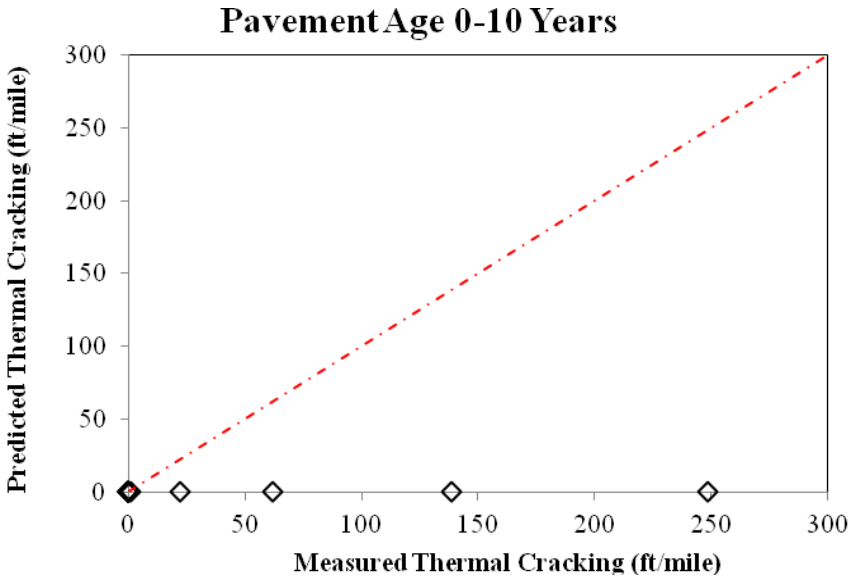

(a)

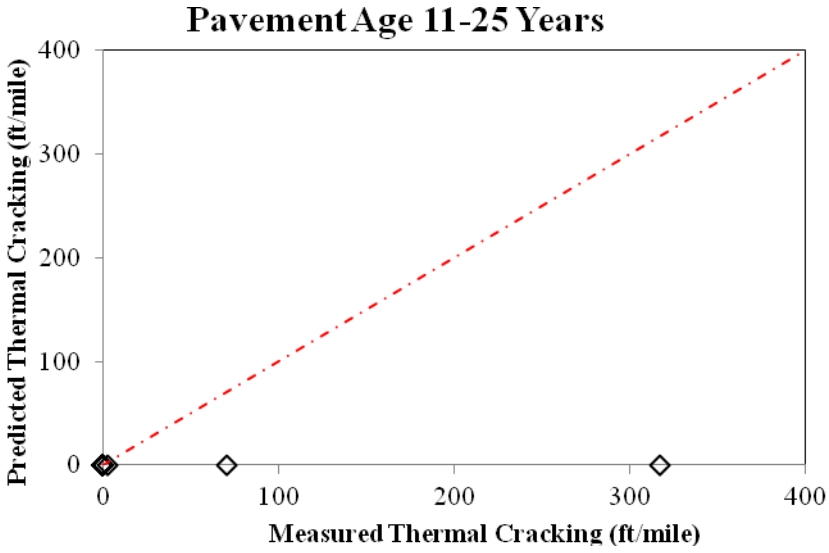

(b)

Figure 5.14: Predicted Mean Thermal Cracking (50% Reliability) versus Measured Thermal Cracking for Pavement Ages (a) 0-10 Years and (b) 11-25 Years

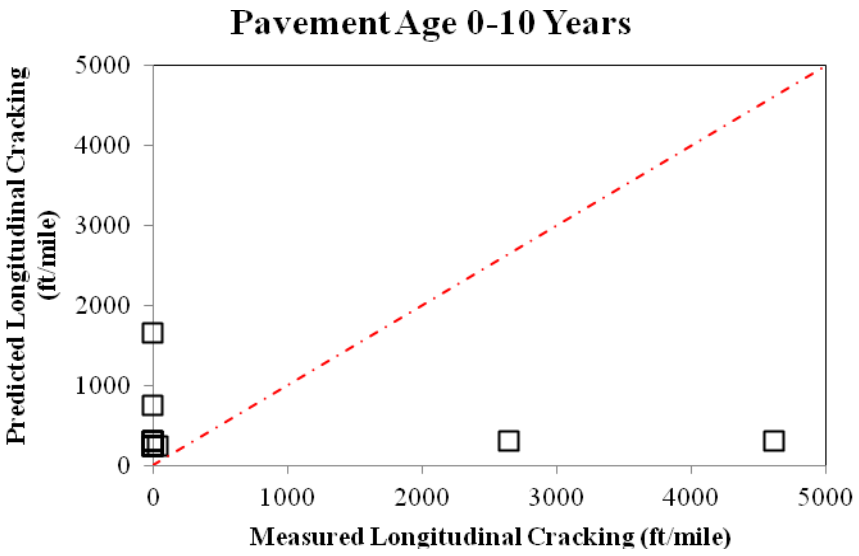

(a)

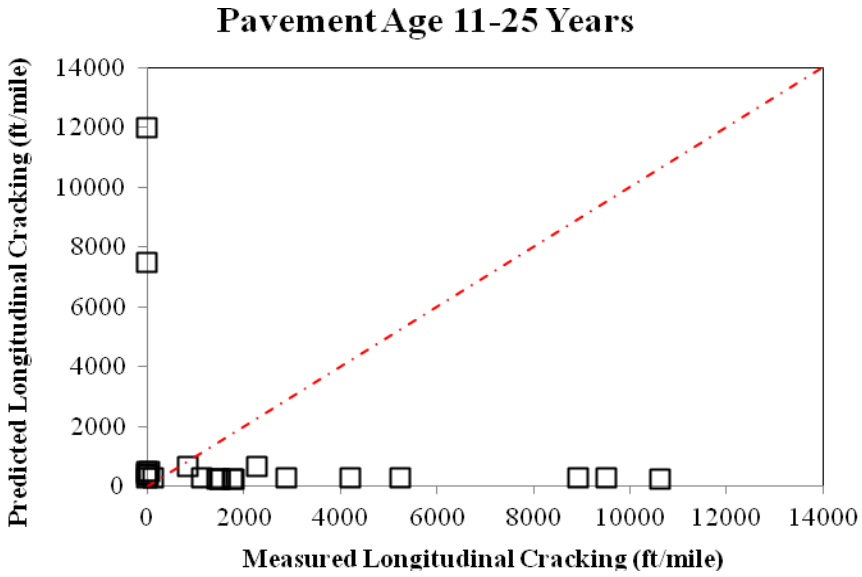

(b)

Figure 5.15: Predicted Longitudinal Cracking (90% Reliability) versus
Measured Longitudinal Cracking for Pavement Ages (a) 0-10 Years and (b) 11-25 Years

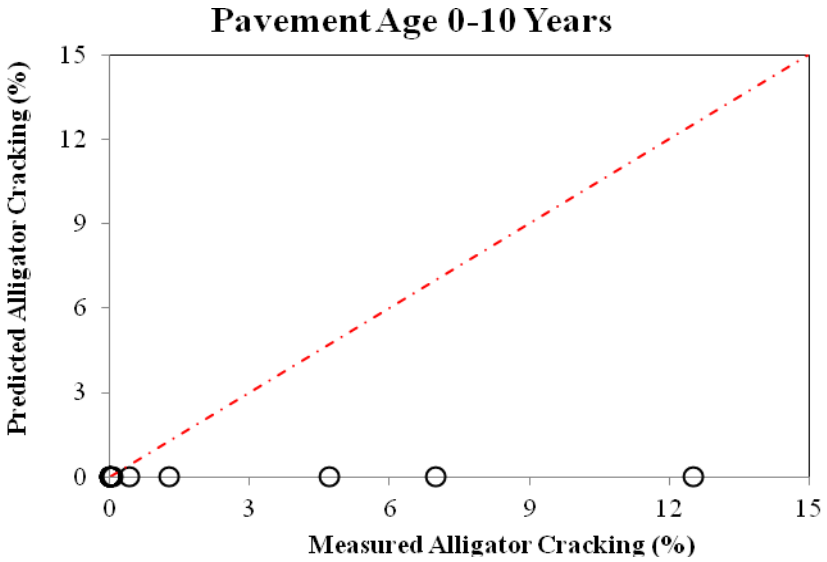

(a)

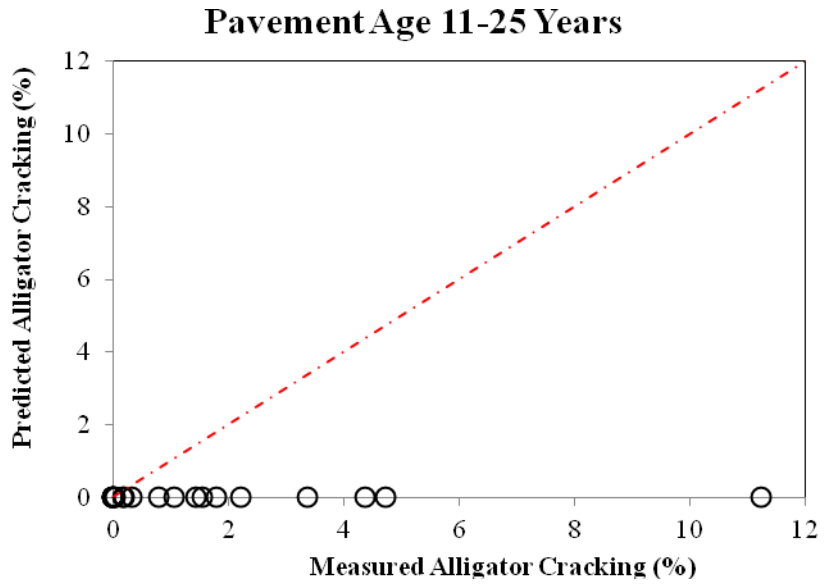

(b)

Figure 5.16: Predicted Mean.Alligator Cracking (50% Reliability) versus Measured Alligator Cracking for Pavement Ages (a) 0-10 Years and (b) 11-25 Years

5.6 SENSITIVITY ANALYSIS

A sensitivity analysis was performed to evaluate the effect of HMA overlay properties on the pavement distresses. Two pavement sections from each region were selected for the sensitivity analysis by Darwin M-E. Among the two pavement sections, one was low volume and the other one was high volume. It is important to point out that two pavement sections from coastal regions were low volume roads as high volume roads from coastal region were not included in the study. In the sensitivity analysis, overlay properties such as overlay thickness, effective binder content and air voids, were varied and pavement distresses (rutting, thermal cracking, top-down cracking and bottom-up cracking) were evaluated. The sensitivity analysis reveals that both thermal cracking and bottom-up cracking are insensitive to overlay properties while the other distresses, top-down cracking in particular, are significantly dependent of overlay properties. Table 5.1 shows the pavement sections and parameters used in the sensitivity analysis. Figure 5.17 shows the structural layer thicknesses of the pavement sections used in the sensitivity study.

Table 5.1: Parameters Used in Sensitivity Analysis

Region	Pavement Section	Traffic (20-year ESALS)	HMA Overlay Thickness (in) Varied	Effective Binder Content (%) Varied	Air Voids (%) Varied	Unbound Layer Thickness (in) Varied	Distresses Viewed @ Year
Coast	US 101:Neptune Dr-Camp Rilea	8.4	2-12	6-18	4-14	8-18	20
	US 101:Dooley Br-Jct Hwy 047	6.8	2-12	6-18	4-14	8-18	20
Valley	US 20: Sweet Home-18th Ave	3.9	2-12	6-18	4-14	8-18	20
	US 30: Cornelius Pass Rd	18.2	2-12	6-18	4-14	8-18	20
Eastern	US 26: Prairie City-Dixie Summit	2.3	2-12	6-18	4-14	8-18	20
	US 730: Canal Rd-Umatilla Bridge	10.1	2-12	6-18	4-14	8-18	20

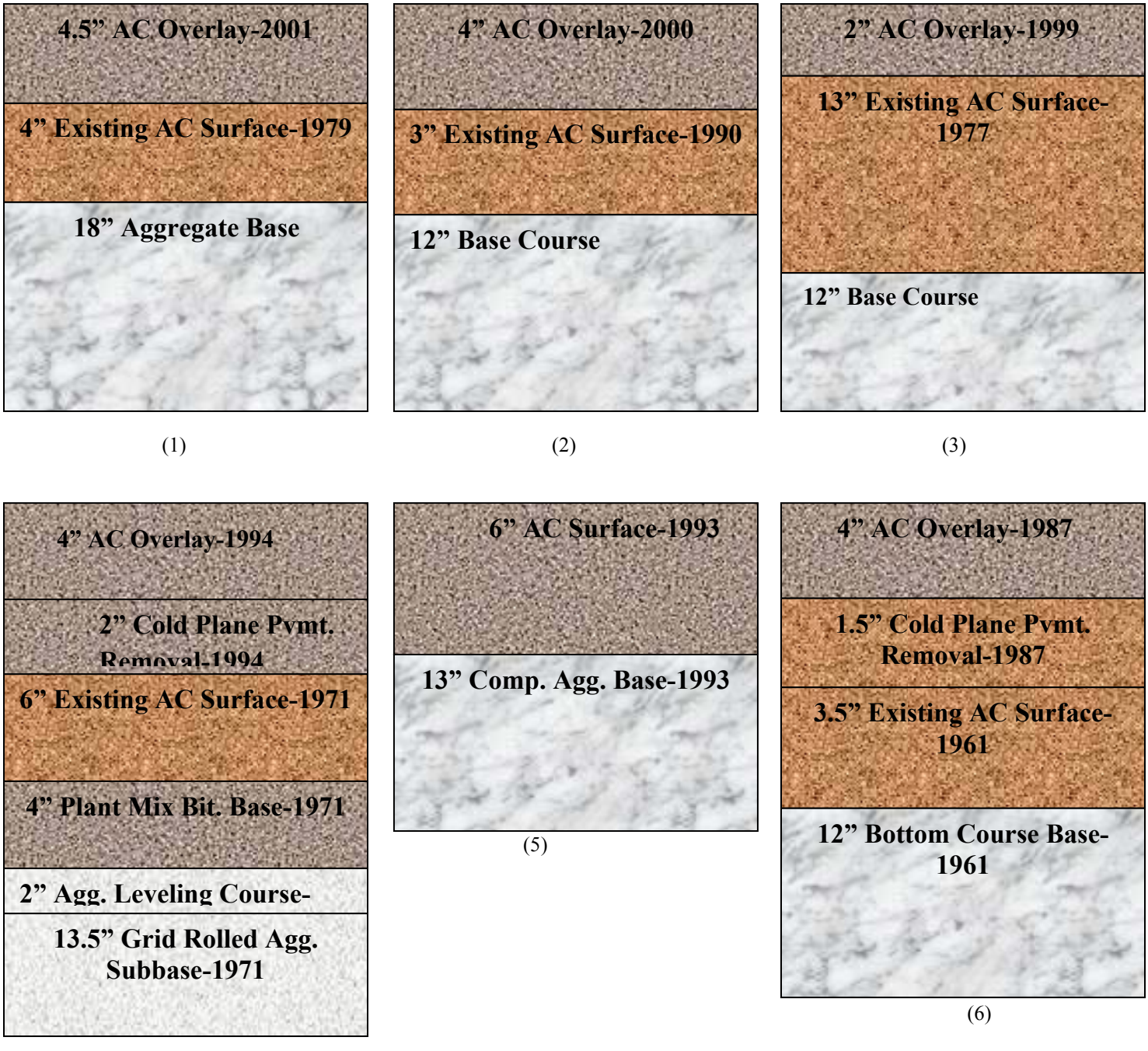

Figure 5.17: Pavement Structural Layer Thicknesses for (1) US 101: Neptune Dr-Camp Rilea, (2) US 101: Dooley Br-Jct Hwy 047, (3) US 20: Sweet Home-18th Ave, (4) US 30: Cornelius Pass Rd, (5) US 26: Prairie City-Dixie Summit and (6) US 730: Canal Rd-Umatilla Bridge

5.6.1 Coastal Region

The pavement sections from the Coastal region were identified as US101 (Neptune Dr.-Camp Rilea) and US101 (Dooley Br-Jct Hwy 047). Figures 5.18 and 5.19 summarize the outcomes of the sensitivity analysis for US101 (Neptune Dr.-Camp Rilea) and Figures 5.20 and 5.21 summarize the outcomes for US101 (Dooley Br-Jct Hwy 047). As would be expected, both pavement sections illustrated reasonable level of sensitivity for rutting to air voids, effective binder content, overlay thickness and thickness of the unbound layer that are shown in Figure 5.18 and 5.20. As the air voids increase, the amount of rutting increases and similarly as the effective binder content increases, the amount of rutting increases too. As the HMA and unbound layer thicknesses increase, the amount of total rutting decreases and this would be expected. It is important to point out that as the effective binder content of a mix is being placed, likely the air voids would be lower. So there is some interrelationship between the parameters in the sensitivity analysis.

Figures 5.19 and 5.21 summarize the sensitivity analysis for the top-down (longitudinal) cracking. Clearly the top-down cracking is more sensitive to the change in air voids and effective binder content than the total amount of rutting. Again, one would expect the amount of top-down cracking to increase with an increase in air voids and decrease with an increase in effective binder content. Top-down cracking is sensitive to the thickness of the HMA overlay from 2 to 4 inches, but is otherwise not very sensitive. This illustrates that for structural purposes, an HMA overlay should be at least 4 inches thick. For the unbound layer thickness, the sensitivity analysis illustrates that having more than 12 inches of an unbound layer has limited additional performance benefit.

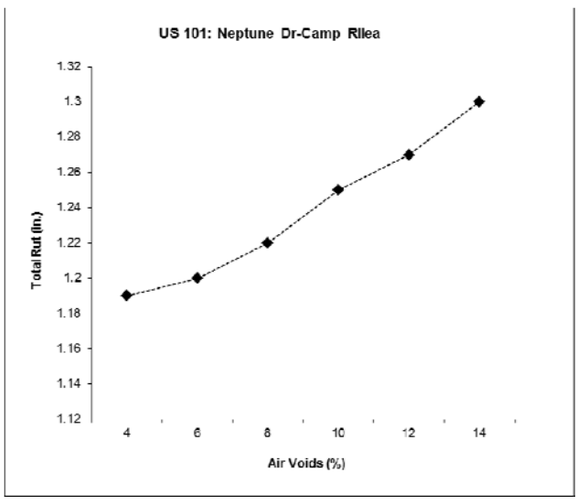

(a)

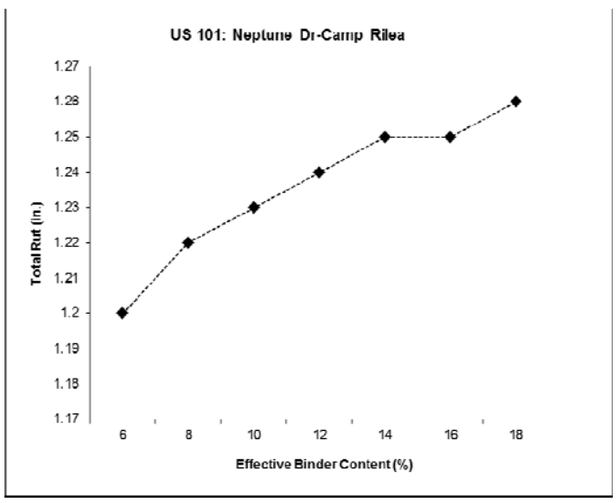

(b)

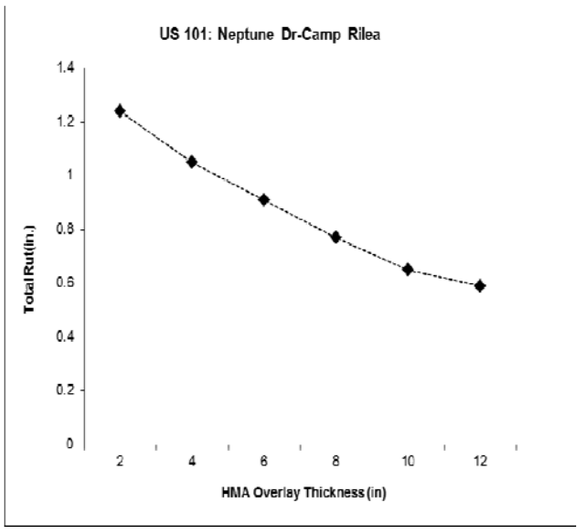

(c)

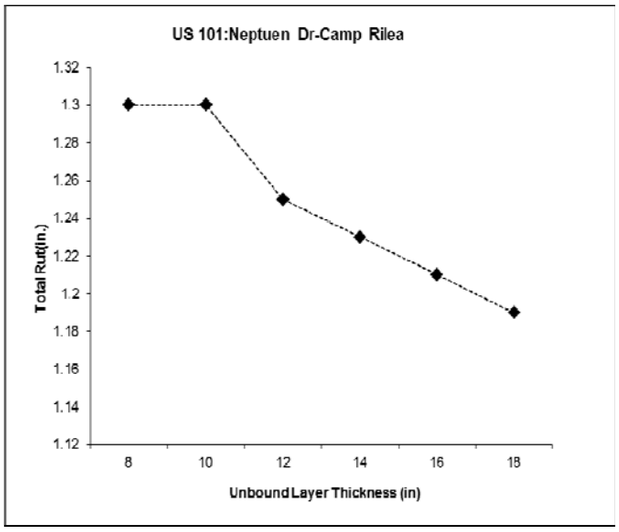

(d)

Figure 5.18: Sensitivity of Rutting on (a) Air Voids, (b) Effective Binder Content, (c) HMA Overlay Thickness, and (d) Unbound Layer Thickness

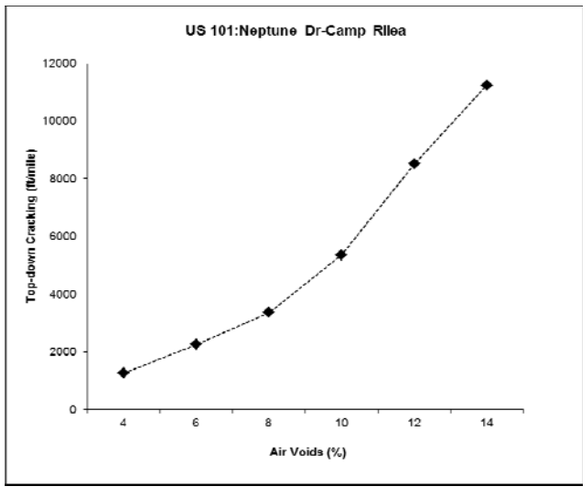

(a)

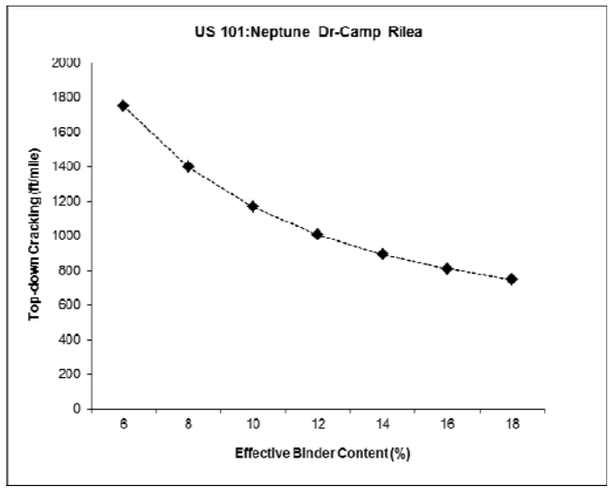

(b)

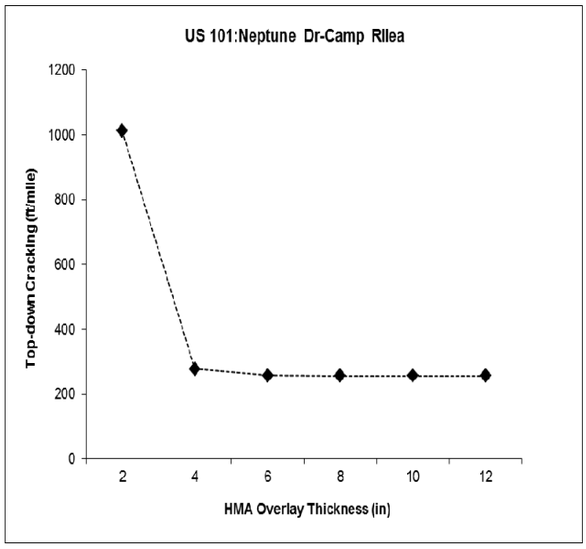

(c)

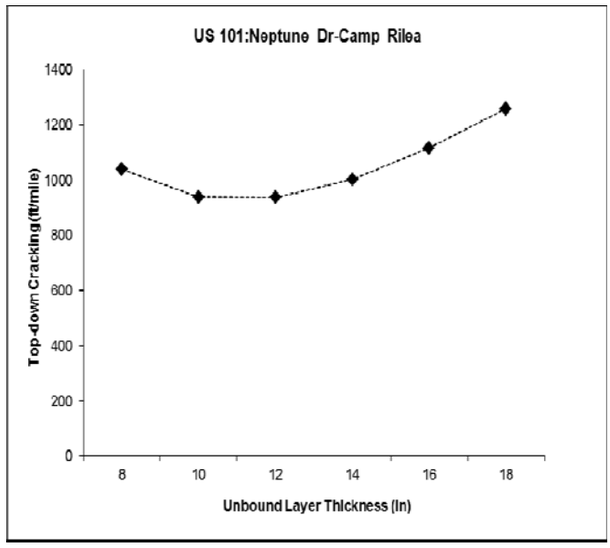

(d)

Figure 5.19: Sensitivity of Top-down Cracking on (a) Air Voids, (b) Effective Binder Content, (c) HMA Overlay Thickness, and (d) Unbound Layer Thickness

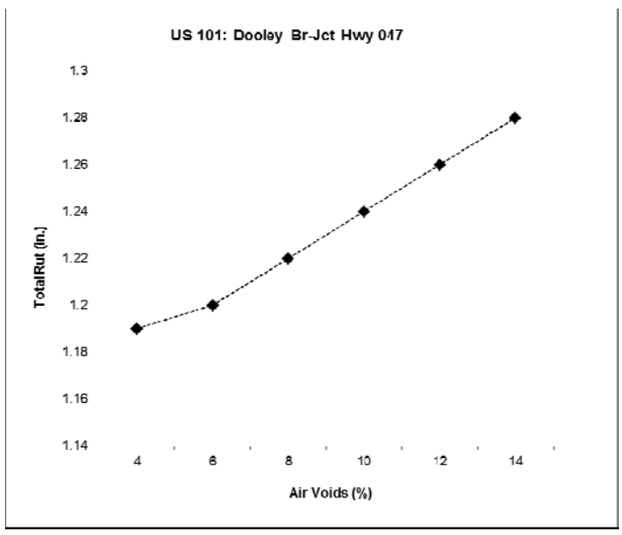

(a)

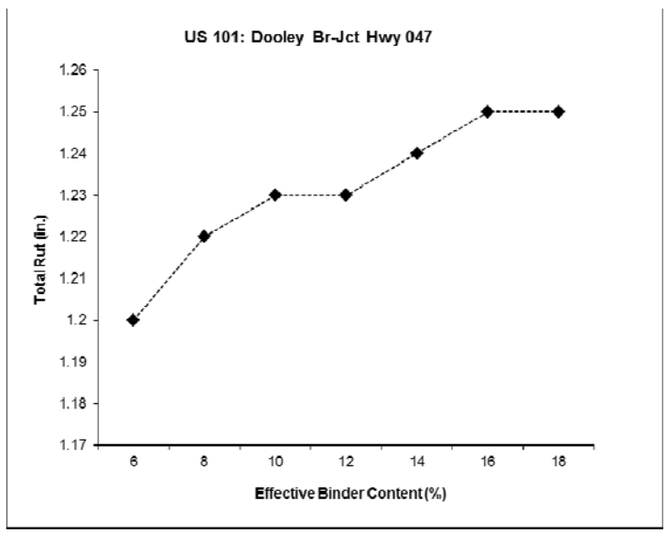

(b)

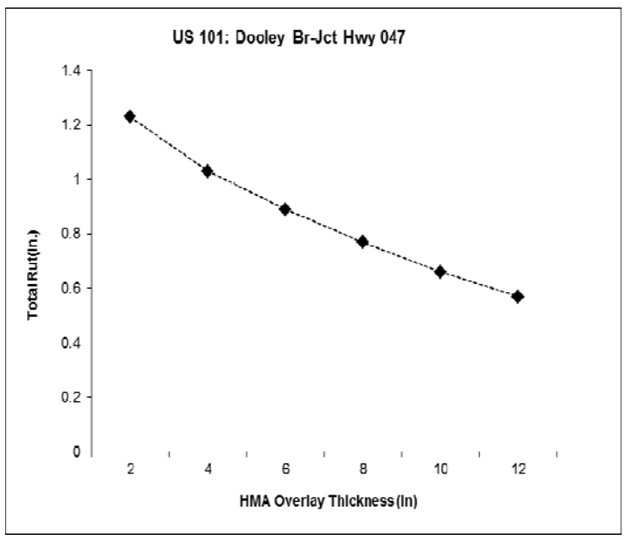

(c)

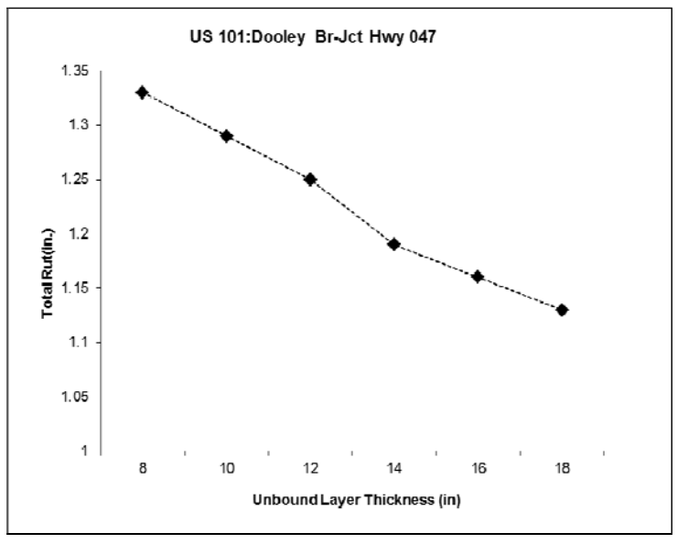

(d)

Figure 5.20: Sensitivity of Rutting on (a) Air Voids, (b) Effective Binder Content, (c) HMA Overlay Thickness, and (d) Unbound Layer Thickness

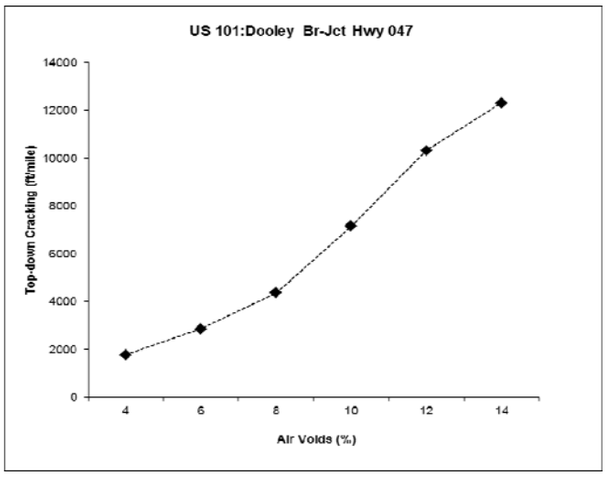

(a)

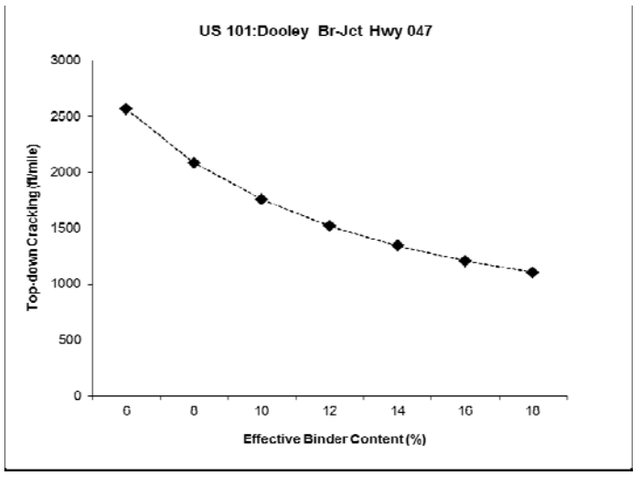

(b)

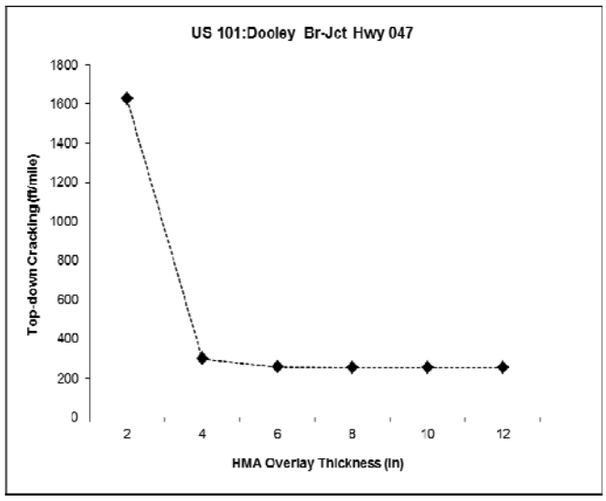

(c)

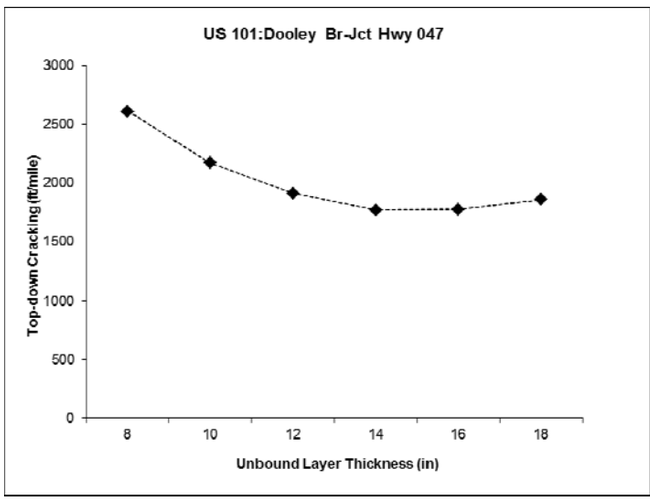

(d)

Figure 5.21: Sensitivity of Top-down Cracking on (a) Air Voids, (b) Effective Binder Content, (c) HMA Overlay Thickness, and (d) Unbound Layer Thickness

5.6.2 Valley Region

Figures 5.22 through 5.25 summarize the sensitivity analysis of the two pavement sections in the Valley region. US20 (Sweet Home- 18th Avenue) and US30 (Cornelius Pass Rd) were the two pavement sections used in the Valley Region. Figures 5.22 and 5.24 summarize the sensitivity analysis for total rutting whereas Figures 5.23 and 5.25 summarize the sensitivity analysis for the to-down cracking for the two pavement sections. Similar to the Coastal Region, the trend for the air voids and effective binder content is identical as would be expected. However, overall both sections are showing relatively low amount of sensitivity to air voids and effective binder content contributing to total rutting. The contribution to total rutting from the HMA and unbound layer thicknesses are trending correctly, but are not that sensitive. Both sections show that increasing the HMA overlay thickness or the unbound layer thickness leads to a reduction in total rutting. These sections do not illustrate the same level of sensitivity of the 2 inch vs. 4 inch overlay thickness that was shown in the Coastal Region.

For the top-down cracking distress shown in Figures 5.23 and 5.25, the sensitivity analysis shows that an increase in air voids and a decrease in the effective binder content leads to more distress as would be expected. Overall, the US20 section is far less sensitive to the variation in the four parameters in the sensitivity analysis than the US30 section and could be due to the lower speed limit for the US20 section and/or the lower design ESAL level.

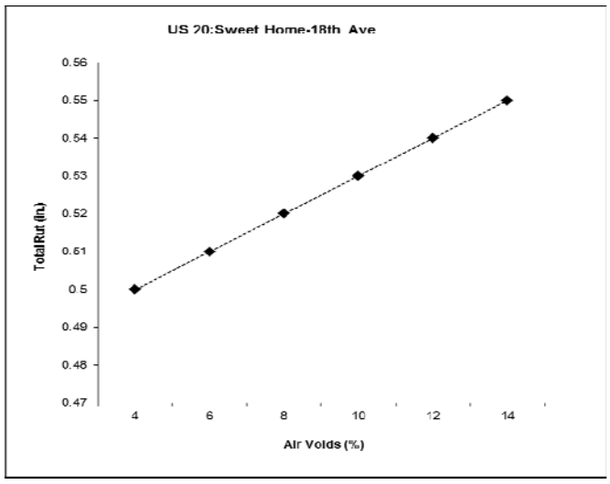

(a)

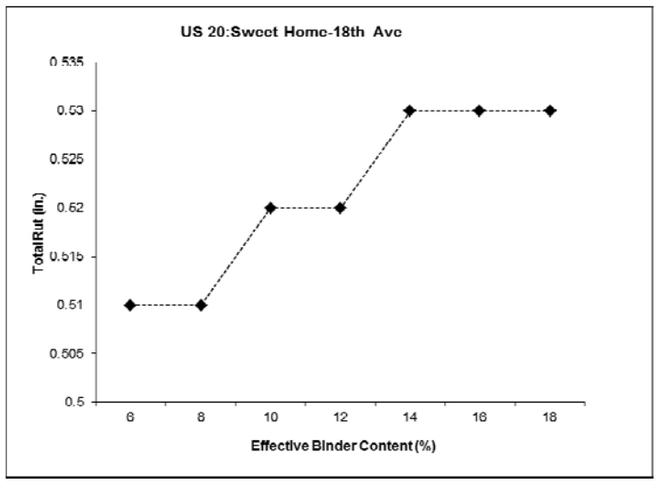

(b)

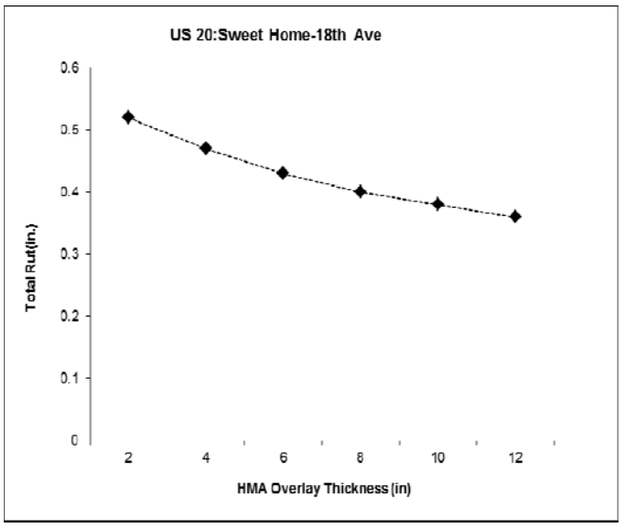

(c)

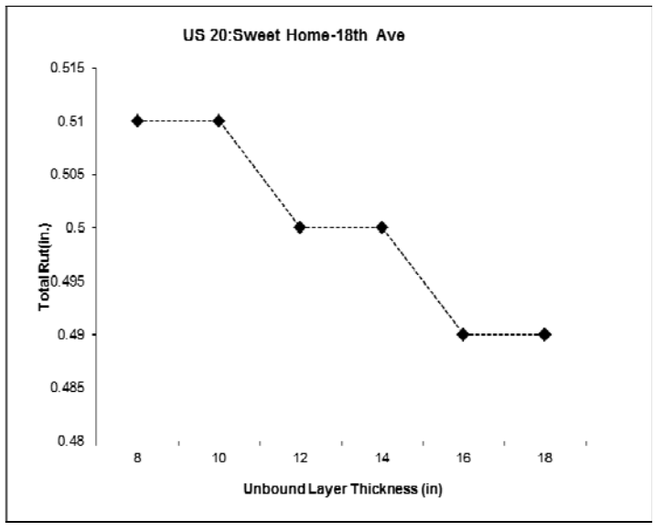

(d)

Figure 5.22: Sensitivity of Rutting on (a) Air Voids, (b) Effective Binder Content, (c) HMA Overlay Thickness, and (d) Unbound Layer Thickness

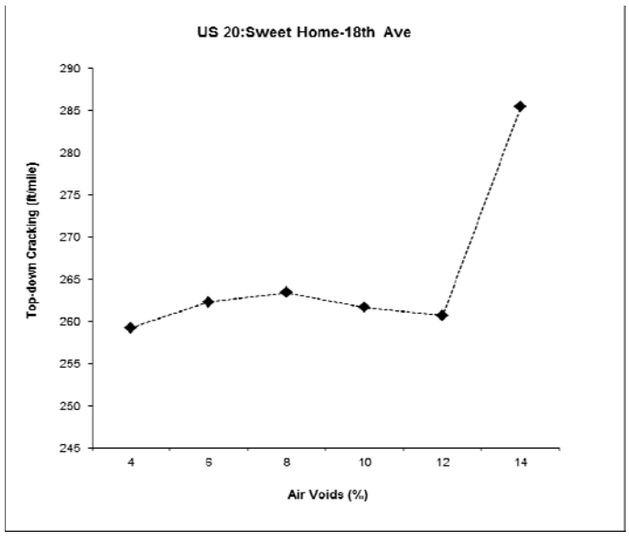

(a)

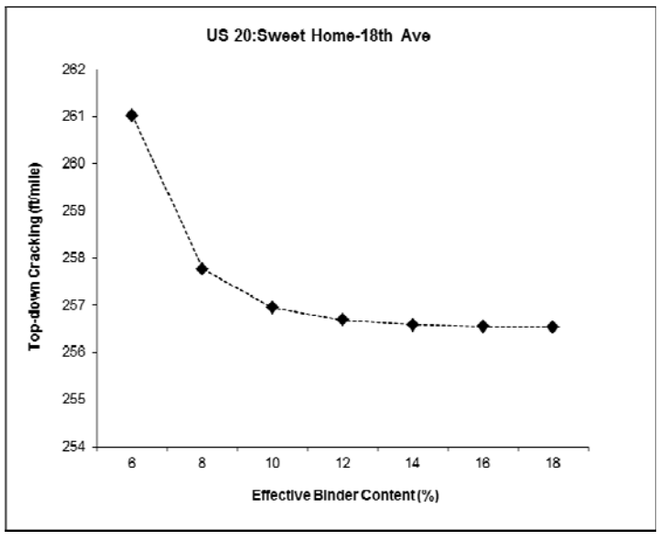

(b)

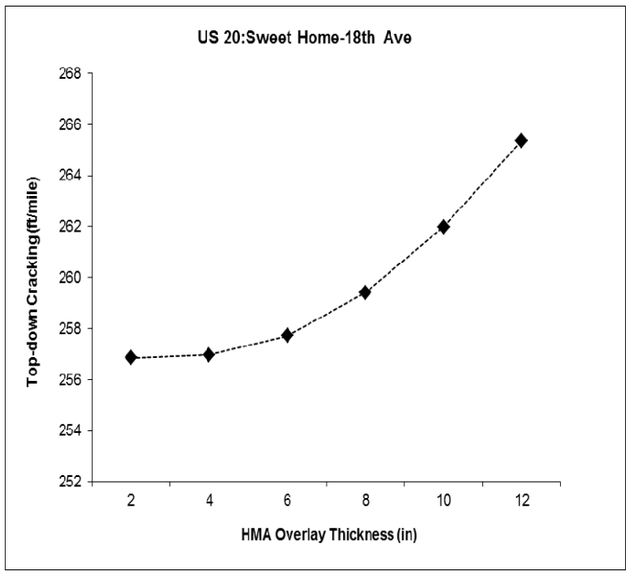

(c)

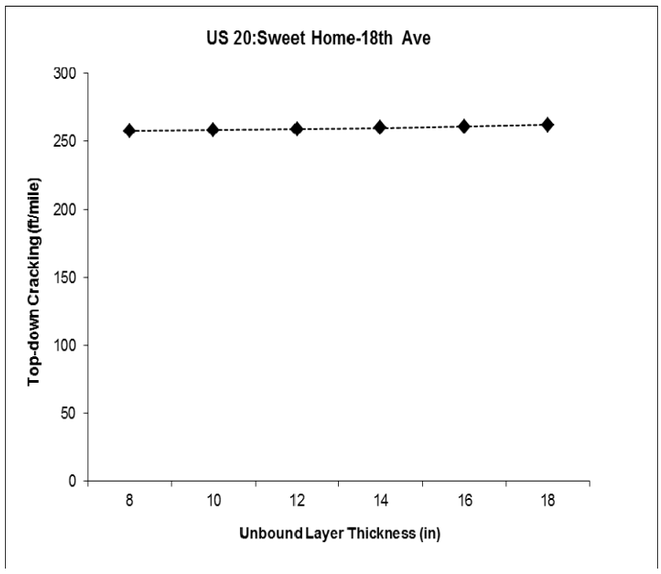

(d)

Figure 5.23: Sensitivity of Top-down Cracking on (a) Air Voids, (b) Effective Binder Content, (c) HMA Overlay Thickness, and (d) Unbound Layer Thickness

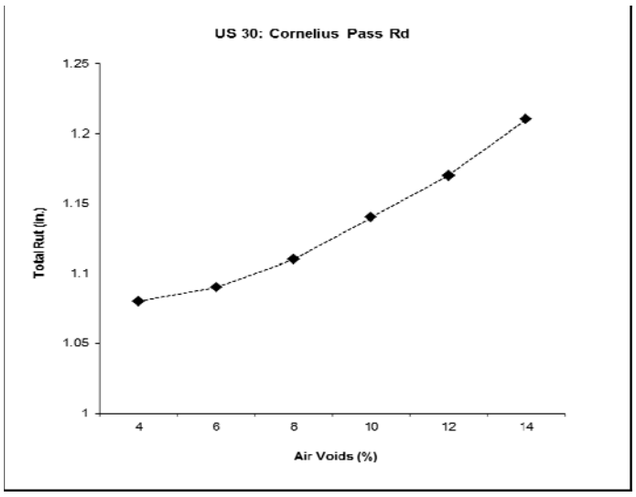

(a)

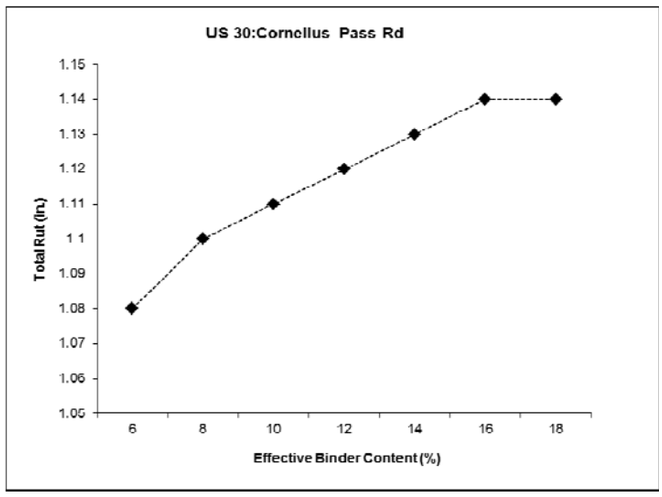

(b)

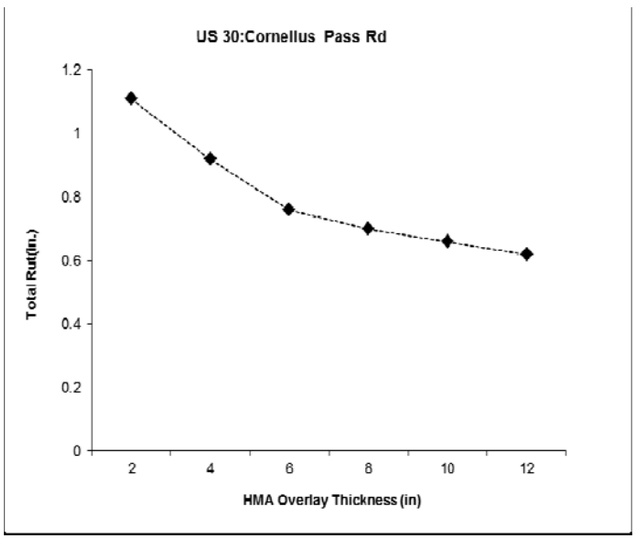

(c)

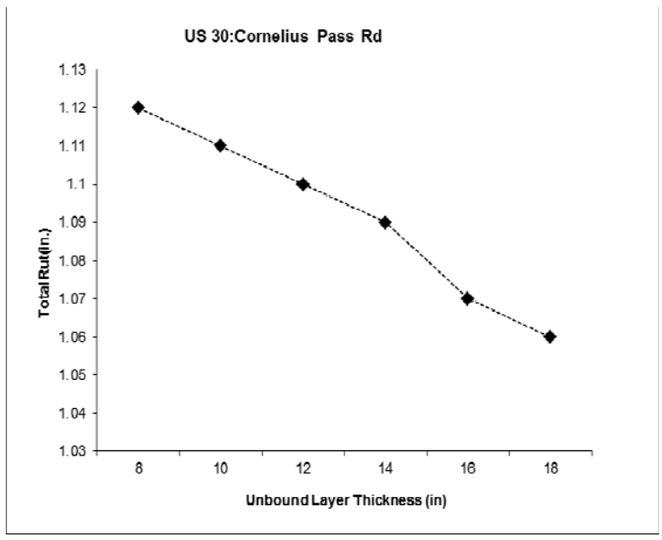

(d)

Figure 5.24: Sensitivity of Rutting on (a) Air Voids, (b) Effective Binder Content, (c) HMA Overlay Thickness, and (d) Unbound Layer Thickness

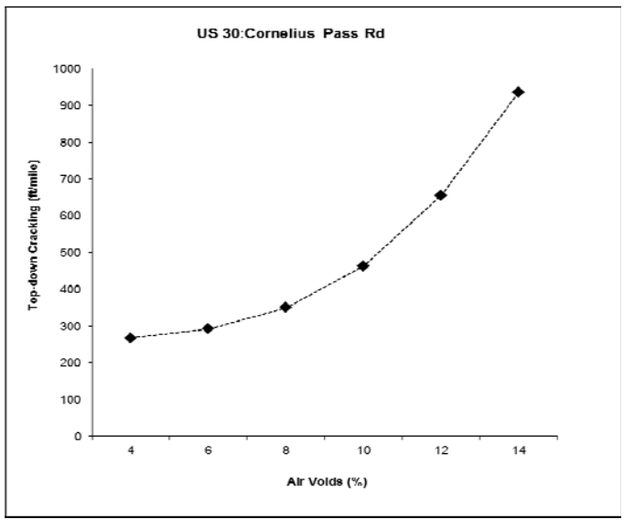

(a)

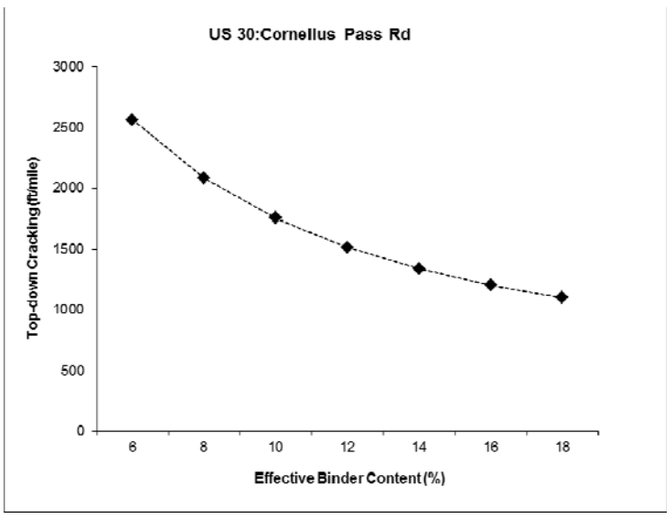

(b)

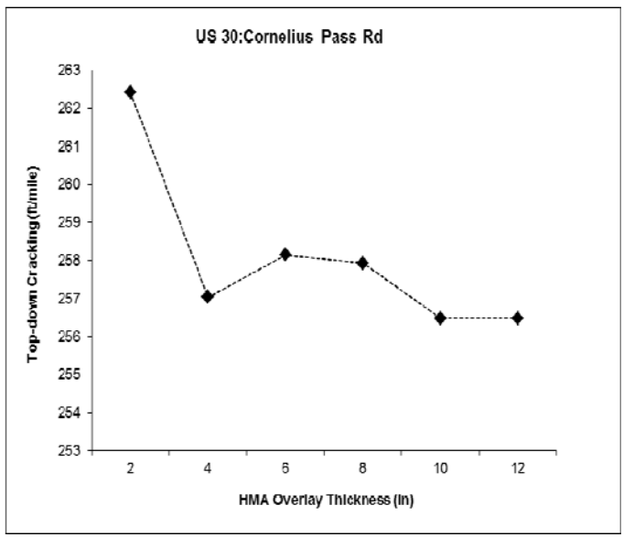

(c)

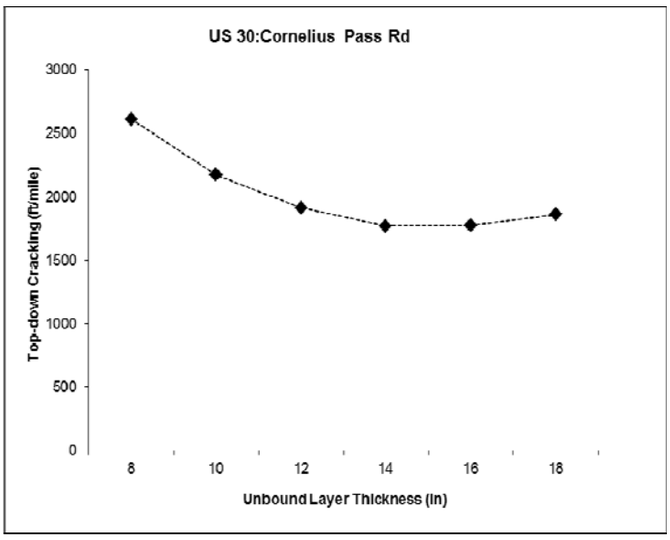

(d)

Figure 5.25: Sensitivity of Top-down Cracking on (a) Air Voids, (b) Effective Binder Content, (c) HMA Overlay Thickness, and (d) Unbound Layer Thickness

5.6.3 Eastern Region

The two sections from the Eastern Region used in the sensitivity were US26 (Prairie City-Dixie Summit) and US730 (Canal Rd-Umatilla Bridge) with the results summarized in Figures 5.26 through 5.29. Figures 5.26 and 5.28 summarize the sensitivity analysis for the total rutting for the two pavement sections. Like the other two regions, the sensitivity analysis shows the effect that higher air voids and higher effective binder content increases the amount of the total rutting. Whereas the increased thickness in the HMA and unbound layers decreases the amount of total rutting. Of the four parameters, the HMA layer thickness has the greatest influence on the total amount of rutting.

All four parameters used in the sensitivity analysis have a greater effect on top-down cracking than on total rutting as shown in Figures 5.27 and 5.29. Interestingly, the HMA layer thickness becomes less sensitive at 6 inches of thickness or greater for the US730 project and greater than 4 inches for the US26 project. It is important to point out that the US730 project has more than 10 million ESALs in its 20 year design life and thus is more sensitive to the HMA overlay thickness than a lower volume roadway like the US26 project.

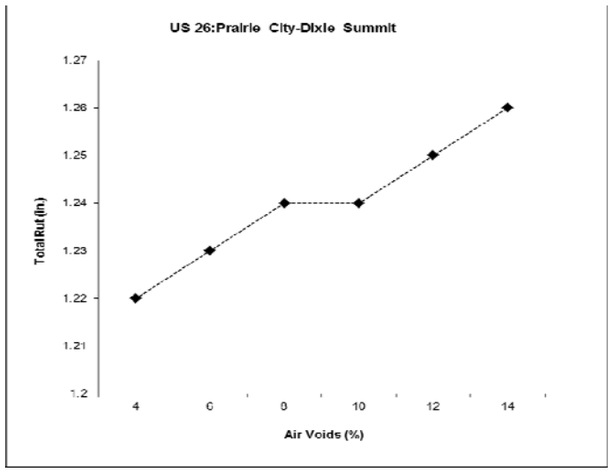

(a)

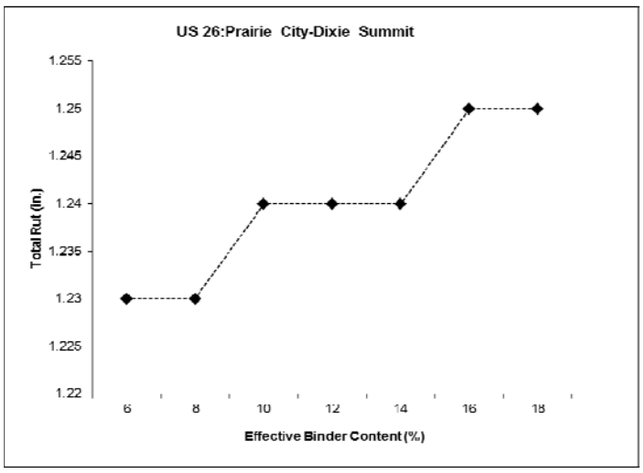

(b)

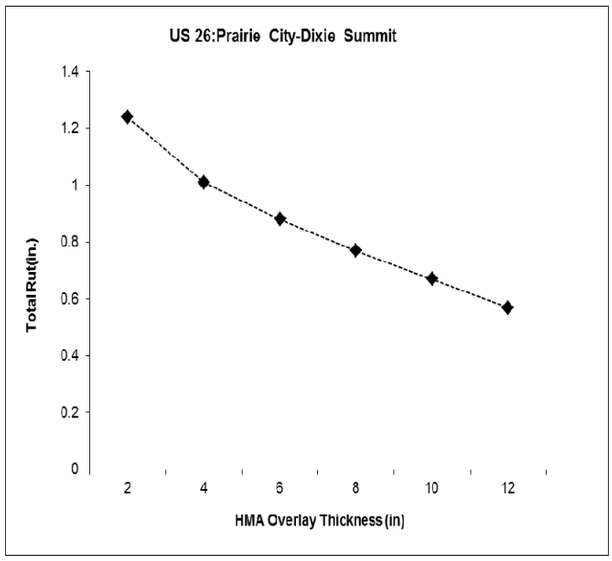

(c)

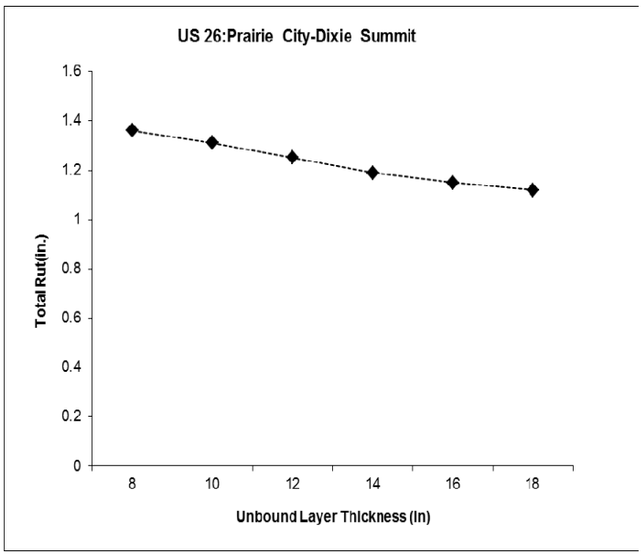

(d)

Figure 5.26: Sensitivity of Rutting on (a) Air Voids, (b) Effective Binder Content, (c) HMA Overlay Thickness, and (d) Unbound Layer Thickness

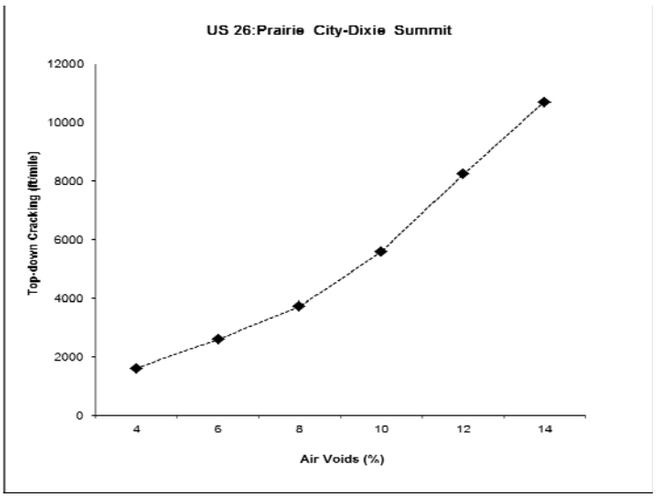

(a)

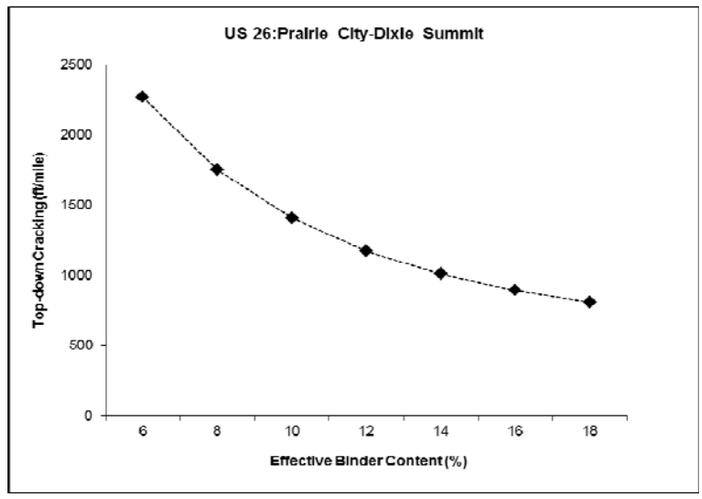

(b)

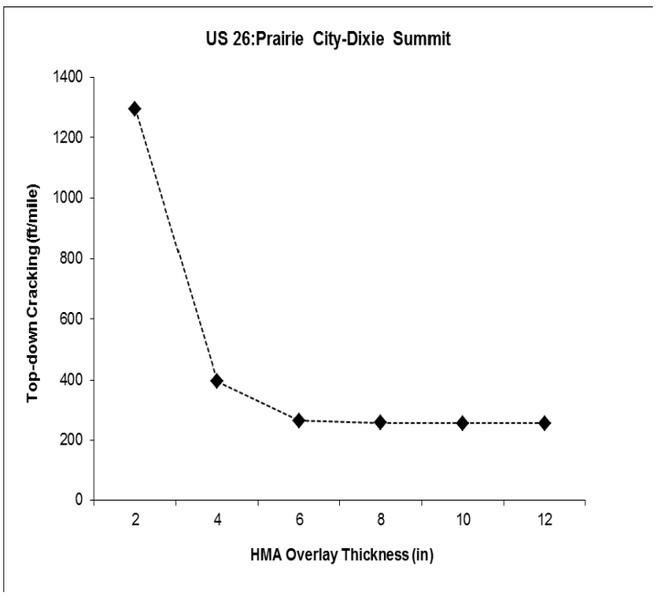

(c)

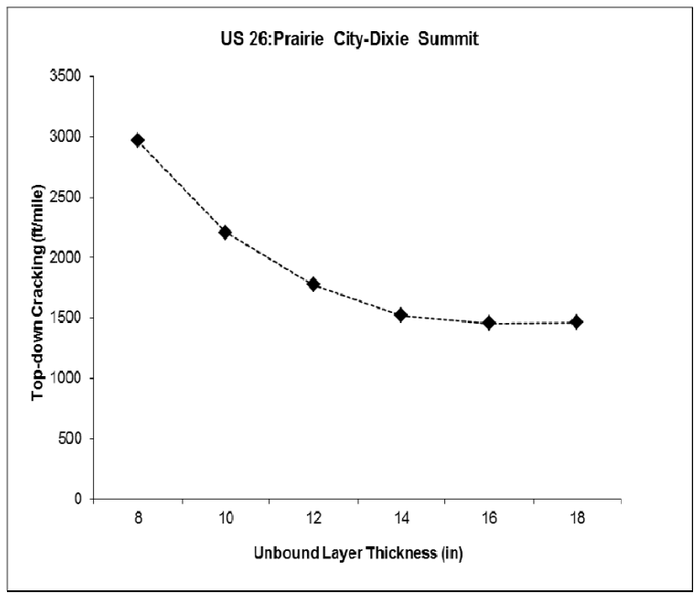

(d)

Figure 5.27: Sensitivity of Top-down Cracking on (a) Air Voids, (b) Effective Binder Content, (c) HMA Overlay Thickness, and (d) Unbound Layer Thickness

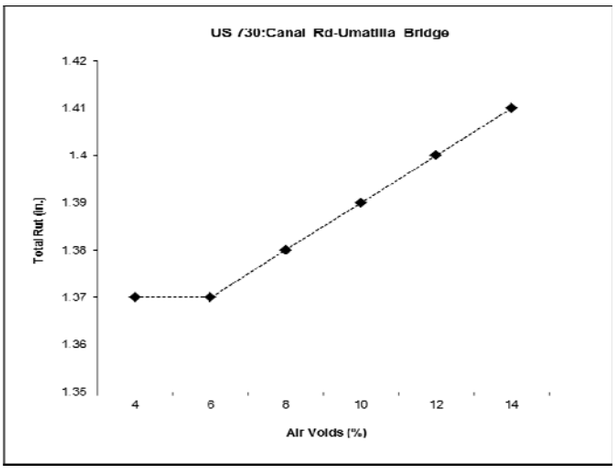

(a)

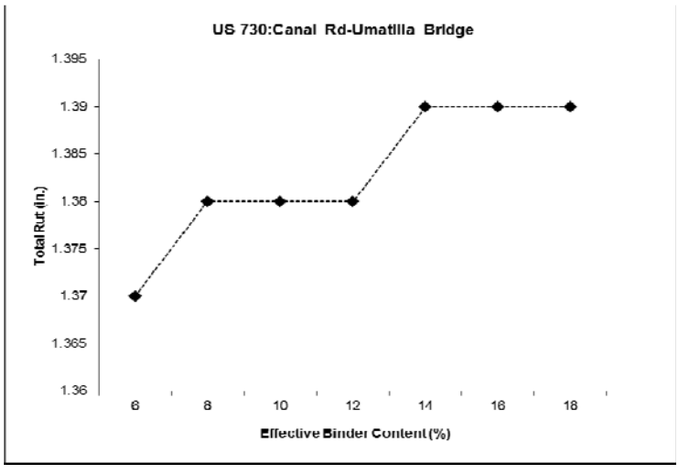

(b)

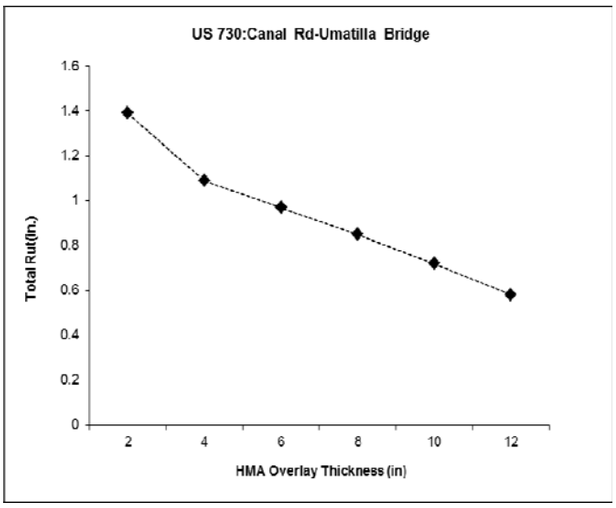

(c)

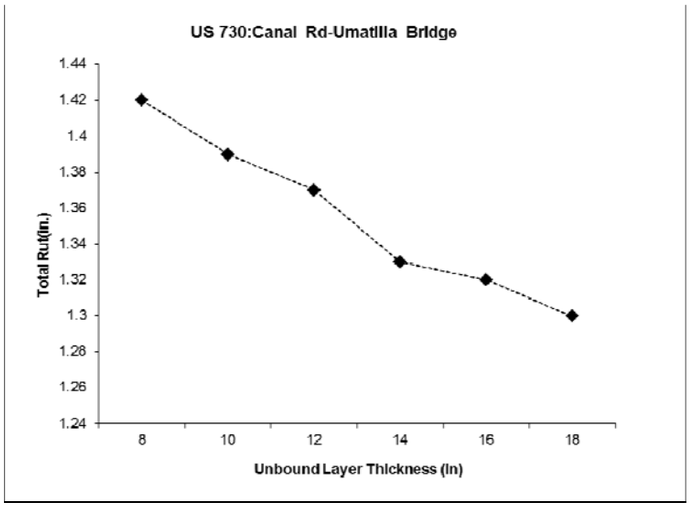

(d)

Figure 5.28: Sensitivity of Rutting on (a) Air Voids, (b) Effective Binder Content, (c) HMA Overlay Thickness, and (d) Unbound Layer Thickness

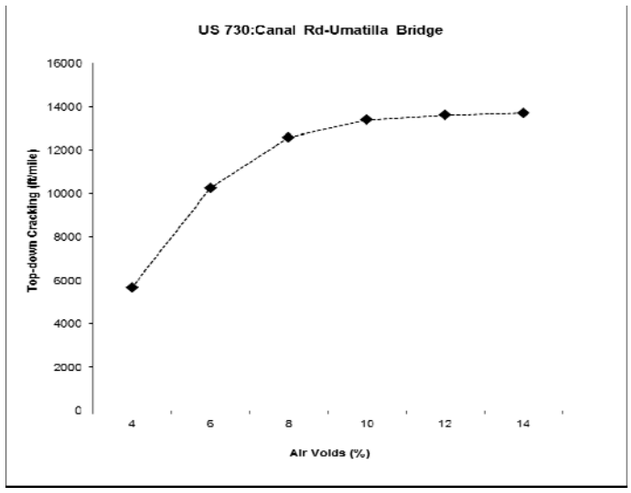

(a)

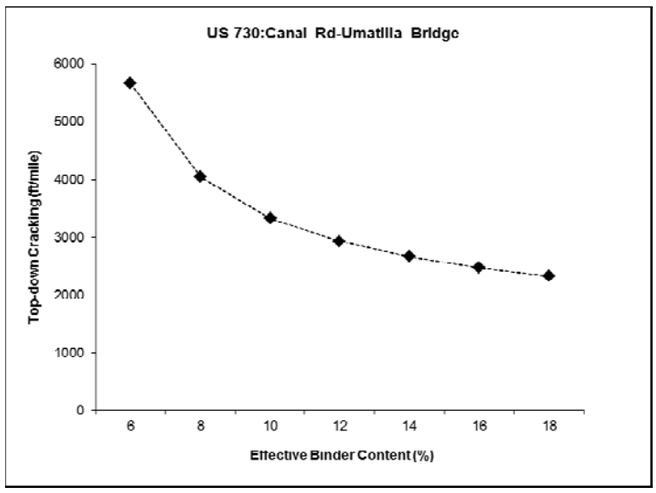

(b)

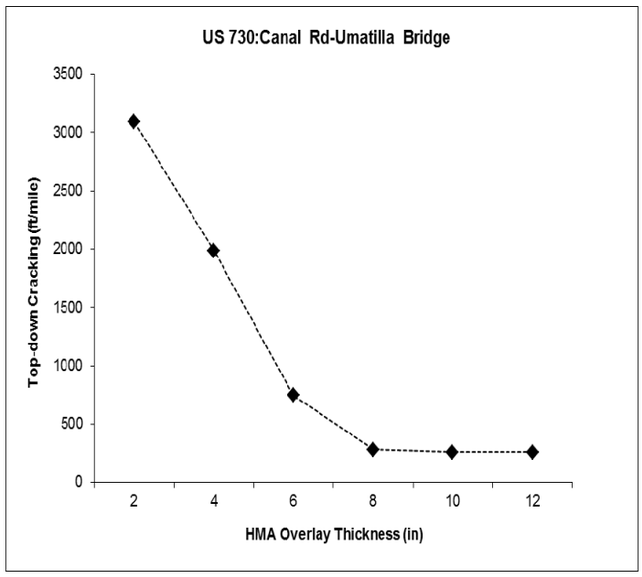

(c)

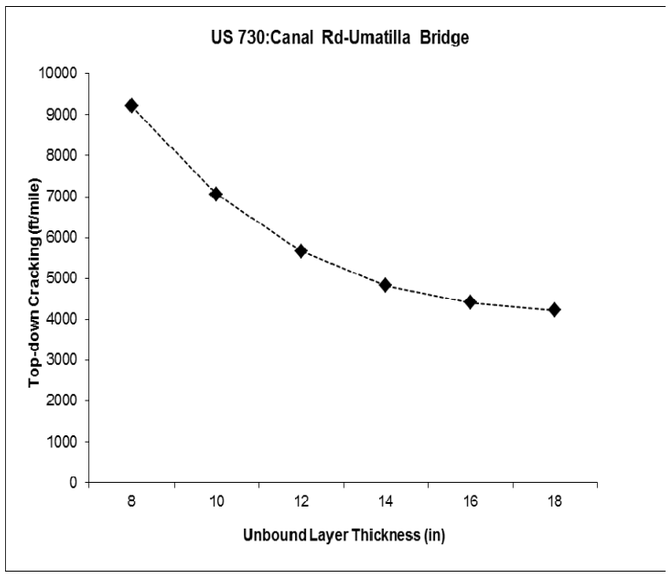

(d)

Figure 5.29: Sensitivity of Top-down Cracking on (a) Air Voids, (b) Effective Binder Content, (c) HMA Overlay Thickness, and (d) Unbound Layer Thickness

Table 5.2: Summary of Sensitivity Analysis

Rutting Sensitivity	Coastal		Valley		East	
	US101:ND-CR	US101:DB-JH	US 20	US 30	US 26	US 730
Air voids	High	Medium	Low	Low	Low	Low
Effective binder content	Medium	Medium	Low	Low	Low	Low
HMA overlay thickness	High	High	Low	High	High	High
Unbound layer thickness	Medium	Medium	Low	Low	Low	Low
Top-down Cracking Sensitivity	Coastal		Valley		East	
	US101:ND-CR	US101:DB-JH	US 20	US 30	US 26	US 730
Air voids	High	High	Low	High	High	High
Effective binder content	High	High	Low	High	High	High
HMA overlay thickness	High	High	Low	Low	High	High
Unbound layer thickness	Low	Low	Low	Low	Medium	Medium

5.7 SUMMARY OF DARWIN M-E SIMULATION RESULTS OF THE CRCP SECTIONS

Figure 5.30 summarizes the Darwin M-E simulation results from punchout on the four CRCP pavement sections as compared to the actual field measured values at the same corresponding age. The simulation results are shown at the 90% and 50% levels of reliability to illustrate the effect of reliability on the Darwin M-E simulation results. As shown in Figure 5.30, the Darwin M-E under predicts the number of punchouts per mile on the three CRCP sections while the remaining CRCP section's punchouts per mile are over predicted as compared to what was actually measured in the field. It is difficult to comment on the accuracy of the nationally calibrated punchout model based on only four pavement sections, however, it seems the nationally calibrated Darwin M-E model provides a reasonable estimate of the punchouts.

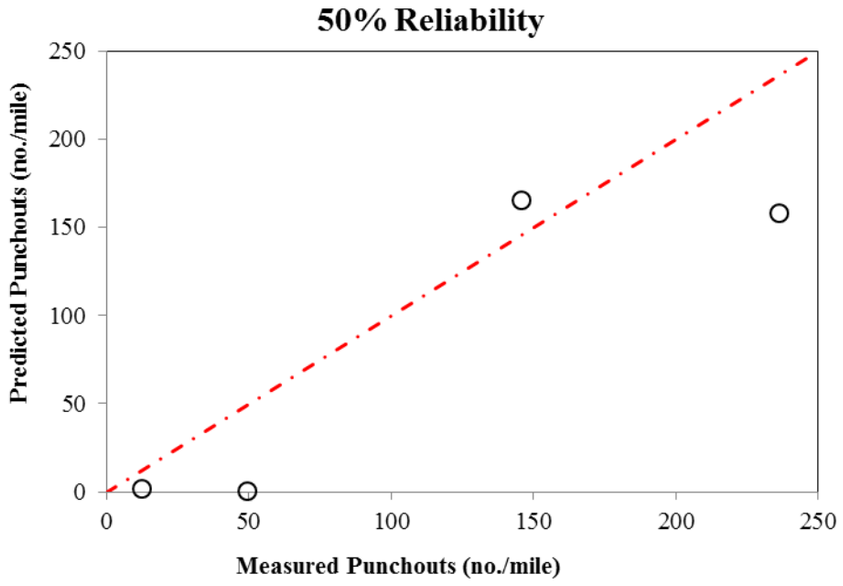

(a)

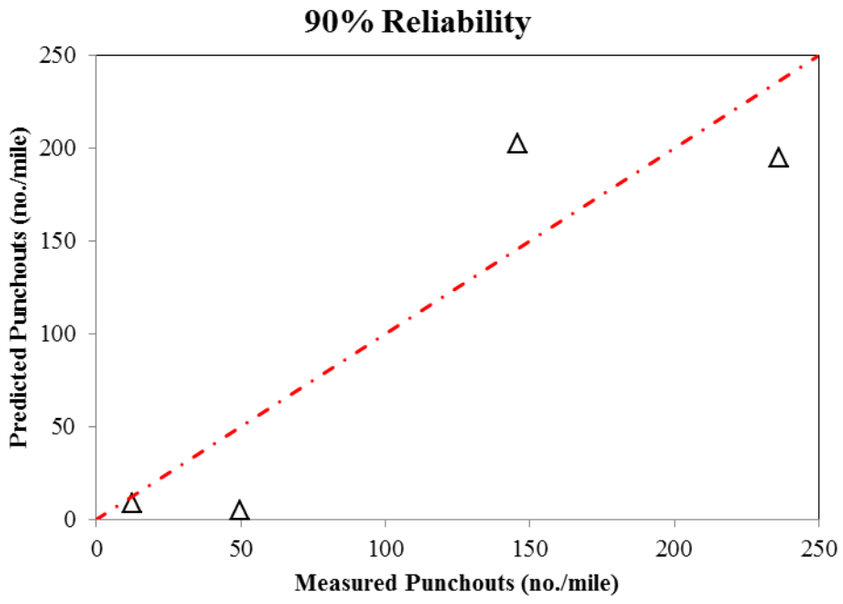

(b)

Figure 5.30: Predicted Punchouts versus Measured Punchouts for (a) 50% Reliability and (b) 90% Reliability

6.0 CALIBRATION OF THE DARWIN M-E PREDICTIVE DISTRESS MODELS

6.1 INTRODUCTION

The importance of local calibration of performance prediction models contained in Darwin M-E is well-documented by different transportation agencies throughout the United States. The verification runs discussed earlier in Chapter 5 were done using the national-defualt calibration coefficients. From the verification runs, it was observed that the predicted distresses did not match well with the measured distresses, suggesting an extensive local calibration was required. The following section discusses about the calibration process of the performance prediction models.

6.2 RUTTING MODEL CALIBRATION

Rutting (permanent deformation) is one of the most important load associated pavement distresses in hot mix asphalt (HMA) pavement systems. A rut is a depression in the wheel path of a HMA pavement, caused by the accumulation of permanent strains in all or some of the layers in the pavement structure. The Darwin M-E predicts rutting in HMA layer, base, and subgrade individually. Then the total rut is calculated by summing the rutting in the HMA layer, base, and subgrade as shown in equation 6.1:

$$Total\ Rutting = AC\ Rutting + Base\ Rutting + Subrage\ Rutting \quad \textbf{(6.1)}$$

where *Total Rutting* is the predicted total rutting due to the subgrade, base, and HMA layer, *AC Rutting* is the predicted rutting in the HMA layer only, *Base Rutting* is the predicted rutting in the base layer only, and *Subgrade Rutting* is the predicted rutting in the subgrade only.

The Darwin M-E field-calibrated mathematical equation that is used to predict rutting in the HMA layer is of the form:

$$\Delta_{p(HMA)} = \varepsilon_{p(HMA)} h_{HMA} = \beta_{r_1} k_z \varepsilon_{r(HMA)} 10^{k_1} n^{k_2 \beta r 2} T^{k_2 \beta r 2} \quad \textbf{(6.2)}$$

where,

$\Delta_{p(HMA)}$ = Accumulated permanent or plastic vertical deformation in the HMA layer/sublayer, inches

$\varepsilon_{p(HMA)}$ = Accumulated permanent or plastic axial strain in the HMA layer/sublayer, inches/inches

h_{HMA} = Thickness of the HMA layer/sublayer, inches

n = Number of axle load repetitions

T = Mix or pavement temperature, °F

k_z = Depth confinement factor, inches

$k_{1,2,3}$ = Global field calibration parameters (from the NCHRP 1-40D recalibration; *k1* = -3.35412, *k2* =1.5606, *k3* = 0.4791)

$\beta_{r_{1,2,3}}$ = Local or mixture field calibration constants; for the global calibration, these constants were all set to 1.0

$$k_z = (C_1 + C_2 D) * 0.328196^{D} \quad \textbf{(6.3)}$$

$$C_1 = -0.1039 * (H_{HMA})^2 + 2.4868 H_{HMA} - 17.324 \quad \textbf{(6.4)}$$

$$C_2 = 0.0172 * (H_{HMA})^2 - 1.7331 H_{HMA} + 27.428 \quad \textbf{(6.5)}$$

where,

D = Depth below the surface, inches

$H_{(HMA)}$ = Total HMA thickness, inches

Equation 6.6 shows the field-calibrated mathematical equation used to calculate plastic vertical deformation within all unbound pavement sublayers and the foundation or embankment soil.

$$\delta_a(N) = \beta_{s1} k_1 \varepsilon_v h_{soil} \left(\frac{\varepsilon_o}{\varepsilon_r} \right) e^{-\left(\frac{\rho}{n} \right)^{\beta}} \quad \textbf{(6.6)}$$

where,

$\delta_a(N)$ = Permanent or plastic deformation for the layer/sublayer, inches

n = Number of axle load applications

ε_o = Intercept determined from laboratory repeated load permanent deformation tests, inches/inches

ε_r = Resilient strain imposed in laboratory test to obtain material properties ε_o, β, and ρ, inches/inches

ε_v = Average vertical resilient or elastic strain in the layer/sublayer and calculated by the structural response model, inches/inches

h_{soil} = Thickness of the unbound layer/sublayer, inches

k_1 = Global calibration coefficients; k_1=2.03 for granular materials and 1.35 for fine-grained materials

β_{s1} = Local calibration constant for the rutting in the unbound layers (base or subgrade); the local calibration constant was set to 1.0 for the global calibration effort. Note that β_{s1} represents subgrade layer while β_{B1} represents base layer.

$$\log \beta = -0.61119 - 0.017638(W_e) \quad \textbf{(6.7)}$$

$$\rho = 10^9 \left(\frac{C_o}{\left(1 - \left(10^9\right)^{\beta}\right)} \right)^{\frac{1}{\beta}} \quad \textbf{(6.8)}$$

$$C_o = Ln\left(\frac{a_1 M_r^{b1}}{a_9 M_r^{b9}} \right) = 0.0075 \quad \textbf{(6.9)}$$

W_e = Water content, percent

M_r = Resilient modulus of the unbound layer or sublayer, psi

$a_{1,9}$ = Regression constants; *a1*=0.15 and *a9*=20.0

$b_{1,9}$ = Regression constants; *b1*=0.0 and *b9*=0.0

As discussed earlier, there are five calibration factors (three for HMA layers, one for the unbound granular base, and one for the subgrade layers) in the rutting (permanent deformation) model calibration. It is important to point out that in Oregon, rutting in base and subgrade layers is not a problem, most of the rutting coming from the HMA layers only. Therefore, calibration factors for base and subgrade layers are set to 0.

Iterative runs of the Darwin M-E using discrete calibration coefficients were employed to optimize the HMA rutting model. The first step involved the simulation runs using the Darwin M-E software for a combination of βr2 and βr3 on the asphalt model only. Table 6-1 lists the possible combinations of βr2 and βr3 calibration values. And Figure 6-1 shows the sum of squared error between predicted and measured rutting variation compared to combination values for βr2 and βr3. As seen from Figure 6-1, a combination values for βr2 and βr3 was found to be 1 and 0.9 with minimum sum of standard error (SSE). After βr2 and βr3 calibration values were chosen, value for βr1 was estimated using the Solver function within Microsoft Excel to further reduce the SSE. Table 6-2 shows the adjusted calibration coefficients. Figure 6-2 illustrates a comparison of the predicted and measured rutting before and after calibration. Before calibration, the standard error of the estimate (SEE) of the rutting model was found to be 0.568. SEE was reduced to 0.180 after calibration, indicating almost 70% increase in accuracy of the prediction was observed after calibration.

Table 6.1: All Combinations of Calibration Values for Rutting Model

Trial Number	βr2	βr3
1	0.8	0.8
2		0.9
3		1
4		1.2
5	1	0.8
6		0.9
7		1
8		1.2
9	1.2	0.8
10		0.9
11		1
12		1.2

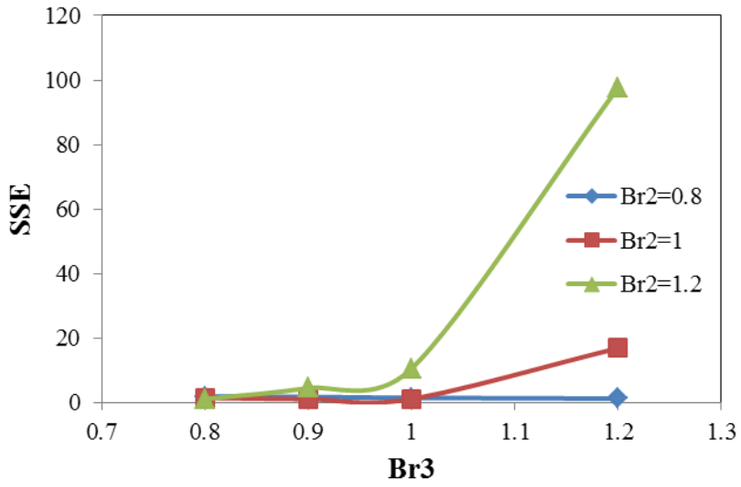

Figure 6.1: Sum of Standard Error (SSE) Variation with βr2 and βr3

Table 6.2: Summary of Calibration Factors

Calibration Factor	Default Value	Calibrated Valued
AC Rutting		
βr1	1	1.48
βr2	1	1
βr3	1	0.9
Base Rutting		
βs1	1	0
Subrage Rutting		
βs1	1	0

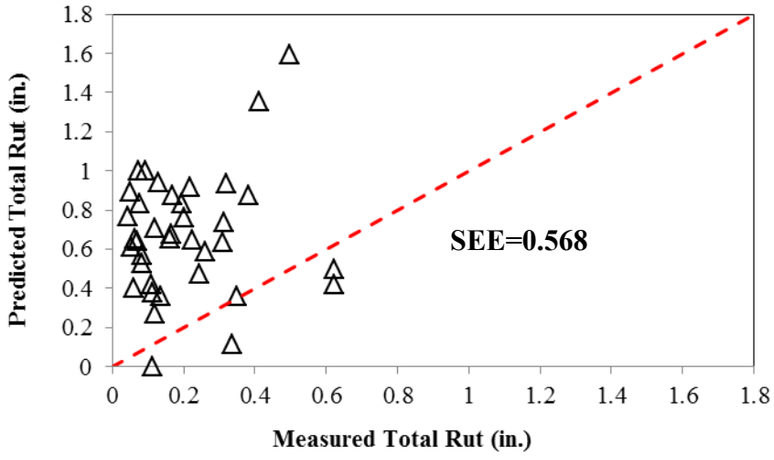

(a)

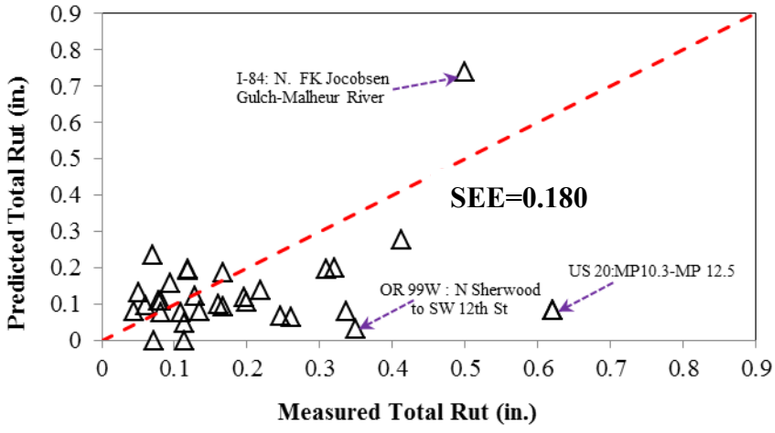

(b)

Figure 6.2: Comparison of Predicted and Measured Rutting (a) Before Calibration and (b) After Calibration

Figure 6.2 also highlights two sections, OR99W (N. Sherwood to SW 12th St) and US20 (MP 10.3 to MP 12.5), that experienced a high amount of rutting due to studded tires. Of the calibrated sections that adjusted for calibration, the I-84 (N. FK Jocobsen Gulch – Malheur River) is well beyond the failure criteria of 0.4 inches and is the section leading to the highest amount of error in the SSE. However, this section also had already failed, about 0.5 inch of rutting as compared to the predicted amount of about 0.75 inch and thus from a practical perspective, the level of failure is great enough from the design limit that a new design would be done to ensure the predicted rutting would be less than 0.4 inches.

6.3 FATIGUE CRACKING MODEL CALIBRATION

Both alligator (bottom-up) and longitudinal (top-down) cracking prediction models were calibrated. The Darwin M-E predicts both bottom- and surface-initiated fatigue cracks using an incremental damage index approach. Alligator cracks are assumed to initiate at the bottom of HMA layers, while longitudinal cracks are assumed to initiate at the surface of the pavement. The damage is calculated as the ratio of the cumulative load repetitions from traffic to the allowable number of load repetitions as shown in Equation 6.10.

$$DI = \sum (\Delta DI)_{j,m,l,p,T} = \sum \left(\frac{n}{N_{f-HMA}} \right)_{j,m,l,p,T} \quad \textbf{(6.10)}$$

where,

n = Actual number of axle load applications within a specific time period,

N_{f-HMA} = Allowable number of axle load applications for a flexible pavement and HMA overlays to fatigue cracking,

j = Axle-load interval,

m = Axle-load type (single, tandem, tridem, quad, or special axle configuration),

l = Truck type using the truck classification groups included in the MEPDG,

p = Month, and

T = Median temperature for the five temperature intervals used to subdivide each month.

The Darwin M-E calculates the amount of alligator area cracking and the length of longitudinal cracking based on the incremental damage index. The damage transfer functions used in the Darwin M-E for alligator cracking and longitudinal cracking are shown in Equations 6.11 and 6.12, respectively.

$$FC_{Bottom} = \left(\frac{6000}{1 + e^{\left(C_1 * C_1^{\delta} + C_2 * C_2^{\delta} * Log\left(DI_{Bottom}\right)\right)}} \right) * \left(\frac{1}{60} \right) \quad \textbf{(6.11)}$$

where,

FC_{Bottom} = Alligator cracking, percent of total lane area,

C_1 = Calibration coefficient,

C_2 = Calibration coefficient,

C_1^{δ} = $-2 * C_2^{\delta}$,

C_2^{δ} = $-2.40874 - 39.748\left(1 + H_{HMA}\right)^{-2.856}$

H_{HMA} = Total HMAC thickness, inches;, and

DI_{Bottom} = Bottom incremental damage, percent.

$$FC_{TOP} = \left(\frac{C_4}{1 + e^{\left(C_1 - C_2 * Log\left(DI_{Top}\right)\right)}} \right) * 10.56 \quad \textbf{(6.12)}$$

where,

FC_{Top} = Longitudinal cracking, ft/mile,

C_1 = Calibration coefficient,

C_2 = Calibration coefficient, and

DI_{Top} = Surface incremental damage, percent.

Both alligator cracking and longitudinal cracking transfer functions have two calibration coefficients; C1 and C2. Both the transfer functions used in Darwin M-E for alligator cracking and longitudinal cracking were calibrated by minimizing the sum of standard error between predicted and measured values using Equation 6.13:

$$Sum \cdot of \cdot S\tan dard \cdot Error\left(SSR\right) = \sum_{i=1}^{N} \left(\Pr edicted \cdot Distress - Measured \cdot Distress\right)^2 \quad \textbf{(6.13)}$$

The Solver function within Microsoft Excel was employed to optimize the calibration coefficients in the alligator cracking and longitudinal cracking models. The calibrated coefficients for both alligator and longitudinal cracking models are shown in Table 6.1.

Table 6.1 Calibration Factors for Fatigue Prediction Models in the Darwin M-E

Calibration Factor	Darwin M-E Default Value	Calibrated Value
Alligator cracking		
C1	1	0.560
C2	1	0.225
C3	6000	6000
Longitudinal cracking		
C1	7	1.453
C2	3.5	0.097
C3	0	0
C4	1000	1000

Figures 6.3 and 6.4 illustrate a comparison of the predicted and measured alligator cracking and longitudinal cracking, respectively, before and after calibration. Both alligator cracking and longitudinal cracking models were improved by calibration. However, there was a high degree of variability between the predicted and measured distresses, especially for longitudinal cracking, even after the calibration. For alligator cracking, SEE values were found to be 3.384 (before calibration) and 2.644 (after calibration) while SEE values of 3601 (before calibration) and 2569 (after calibration) were found for longitudinal cracking. There is a continuing concern regarding the accuracy of prediction of longitudinal cracking model. Based on the findings from the NCHRP 9-30 study, it was noted that longitudinal cracking be dropped from the local calibration guide development in NCHRP 1-40B study due to lack of accuracy in the predictions (*Von Quintus et al. 2009*). The Montana DOT conducted the local calibration study of MEPDG for flexible pavements. Regarding the longitudinal cracking prediction model they concluded that no consistent trend in the predictions could be identified to reduce the bias and standard error, and improve the accuracy of this prediction model. It is believed that there is a significant lack-of-fit modeling error for the occurrence of longitudinal cracks (*Von Quintus and Moulthrop 2007*). A study by Galal and Chehab (*2005*) in Indiana indicated that MEPDG provided good estimation to the distress measure except longitudinal cracking.

It is important to point out that only one year of distress data for each pavement section considered in this study were available in this verification and calibration process. Moreover, many default values recommended by the Darwin M-E were used in this study due to the unavailability of data. It is recommended that additional sites be established to include in the future calibration efforts and thus, improve the accuracy of the predictive models.

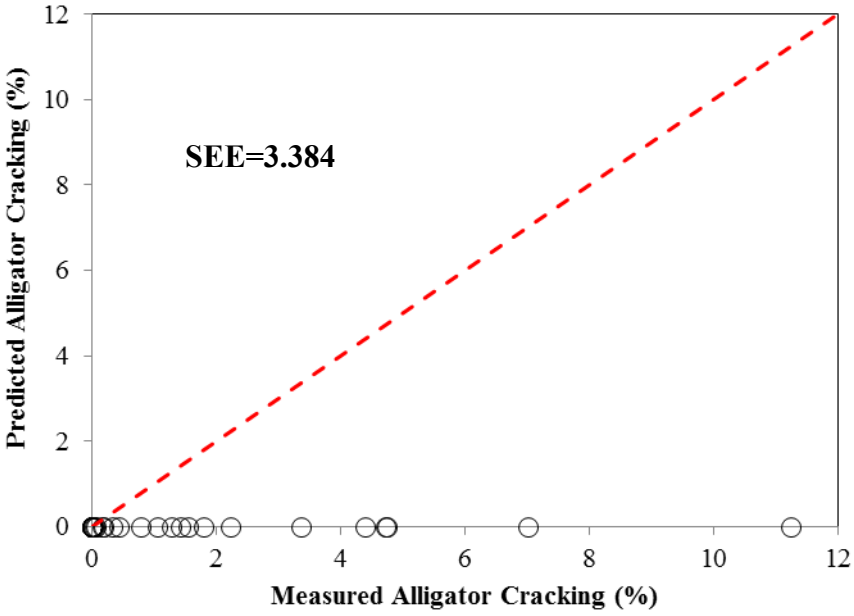

(a)

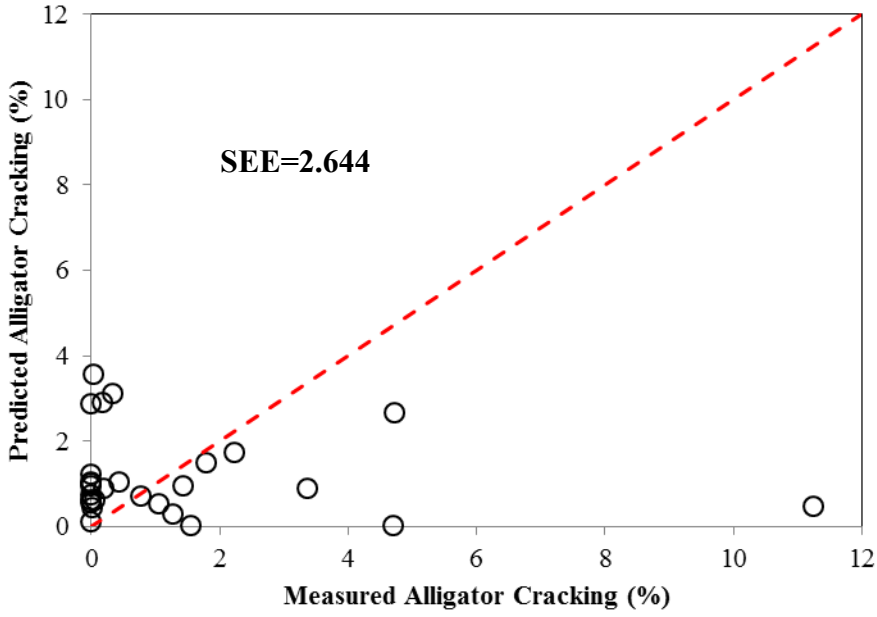

(b)

Figure 6.3: Comparisons of Predicted and Measured Alligator Cracking
(a) Before Calibration and (b) After Calibration

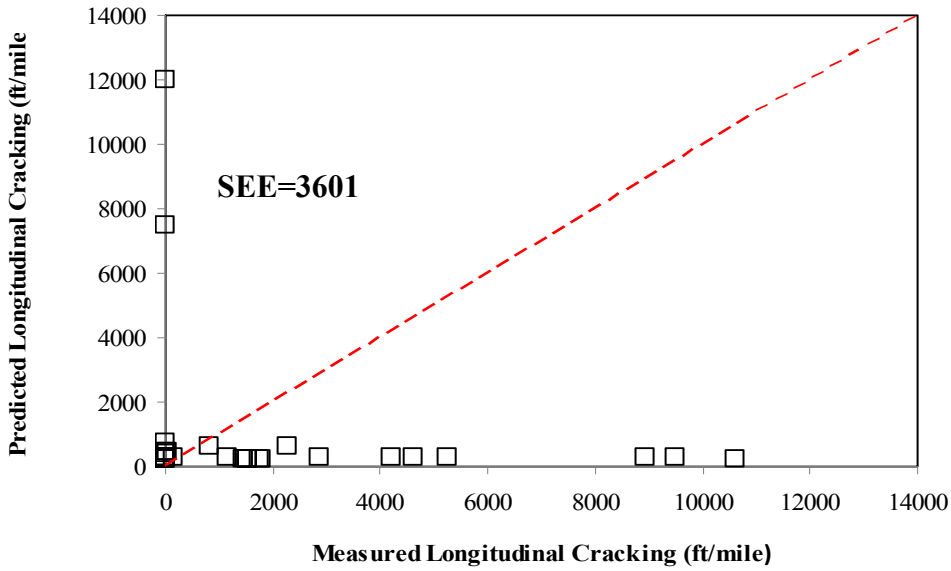

(a)

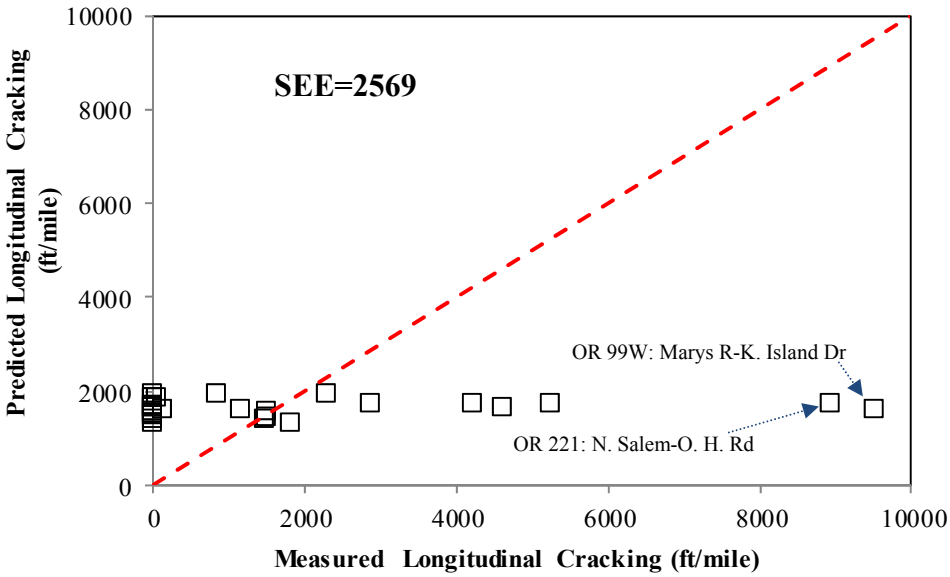

(b)

Figure 6.4: Comparisons of Predicted and Measured Longitudinal Cracking
(a) Before Calibration and (b) After Calibration

6.4 THERMAL CRACKING MODEL CALIBRATION

For the Darwin M-E, the amount of crack propagation induced by a given thermal cooling cycle is predicted using the equation 6.14 shown below (AASHTO 2008):

$$\Delta C = \left(k * \beta_t\right)^{n+1} * A * \left(\Delta K\right)^n \quad \textbf{(6.14)}$$

where,

ΔC = Change in the crack depth due to a cooling cycle

A, n = Fracture parameters for the HMA mixture

$n = 0.8\left[1 + \frac{1}{m}\right]$, where: m= Slope of the linear portion of the log compliance-log time relationship

ΔK = Change in the stress intensity factor due to a cooling cycle

β_t = Local or mixture calibration factor

k = Coefficient determined through field calibration for each input level (Level 1=1.5; Level 2 =0.5; and Level 3 =1.5)

Experimental results indicate that reasonable estimates of *A* and *n* can be obtained from the indirect tensile creep-compliance and strength of the HMA in accordance with equation 6.15 (AASHTO 2008).

$$A = 10^{(4.389 - 2.52 * Log(E_{AC} * \sigma_m * n))} \quad \textbf{(6.15)}$$

where,

A = Fracture parameter

$n = 0.8\left[1 + \frac{1}{m}\right]$, where: m= Slope of the linear portion of the log compliance-log time relationship

E_{AC} = HMA indirect tensile modulus, psi

σ_m = Mixture tensile strength, psi

The stress intensity factor, K, has been incorporated in the MEPDG through the use of a simplified equation developed from theoretical finite element studies (Equation 6.16).

$$K = \sigma_{tip}\left(0.45 + 1.99\left(C_0\right)^{0.56}\right) \quad \textbf{(6.16)}$$

where,

K = Stress intensity factor

σ_{tip} = Far-field stress from pavement response model at depth of crack tip, psi

C_0 = Current crack length, ft

The amount of thermal cracking is predicted by the Darwin M-E using an assumed relationship between the probability distribution of the log of the crack depth to HMA layer thickness ratio and the percent of cracking. Equation 6.17 shows the expression used to determine the amount of thermal cracking (AASHTO 2008).

$$C_f = 400 * N\left[\frac{1}{\sigma} Log\left(\frac{C}{h_{AC}}\right)\right] \quad \textbf{(6.17)}$$

where,

C_f = Amount of thermal cracking, ft/500 ft

$N[z]$ = Standard normal distribution evaluated at [z]

σ = Standard deviation of the log of the depth of cracks in the pavement

C = Crack depth, in.

h_{AC} = Thickness of AC surface layer, in.

There is one calibration factor (k) in thermal (transverse) cracking model. Iterative runs of the Darwin M-E using discrete coefficients were employed to optimize the thermal cracking model. The default (nationally calibrated) value of k for Level 3 is 1.5. In the iterative runs, the value of k ranged from 1.5 to 12.5, where most of the thermal cracking predicted were almost zero for k up to 7.5. At k=12, thermal cracks were highly over predicted by Darwin M-E, however, a reasonable estimate of thermal cracking were found at k=10. Figure 6.5 shows a comparison of the predicted and measured thermal cracking before and after calibration (k=10).

The locally calibrated model (SEE=751) did not improve the prediction as compared to the nationally calibrated model (SEE=121). It is important to point out that coastal and valley regions of Oregon do not experience thermal (transverse) cracking. Therefore, 15 projects from only eastern region were included in the calibration process which included 15 data points. Out of 15 projects, 10 projects had thermal cracking less than 100 ft/mile with 7 projects exhibiting no thermal cracking. It is recommended that more projects with variable degree of thermal cracking (low, medium, and high) be selected for future calibration effort.

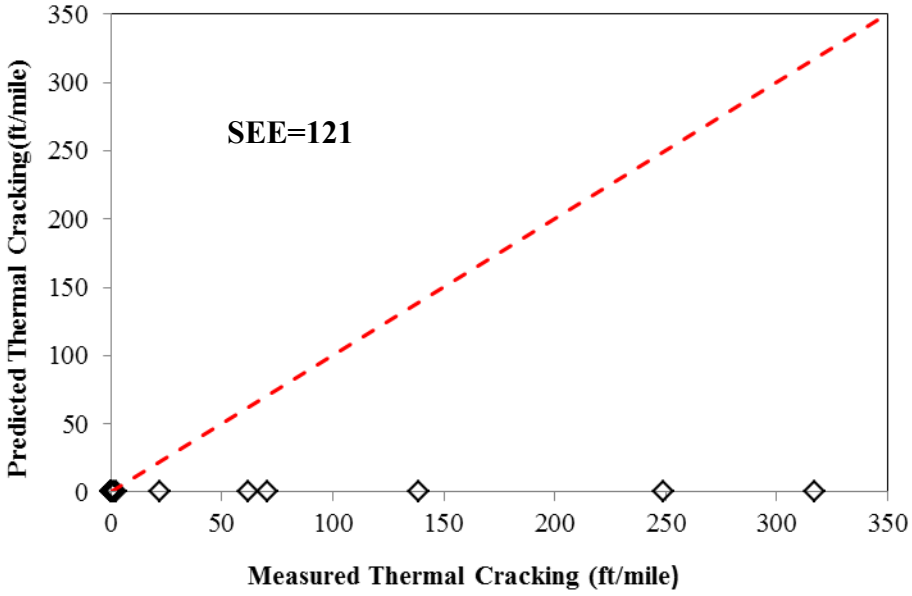

(a)

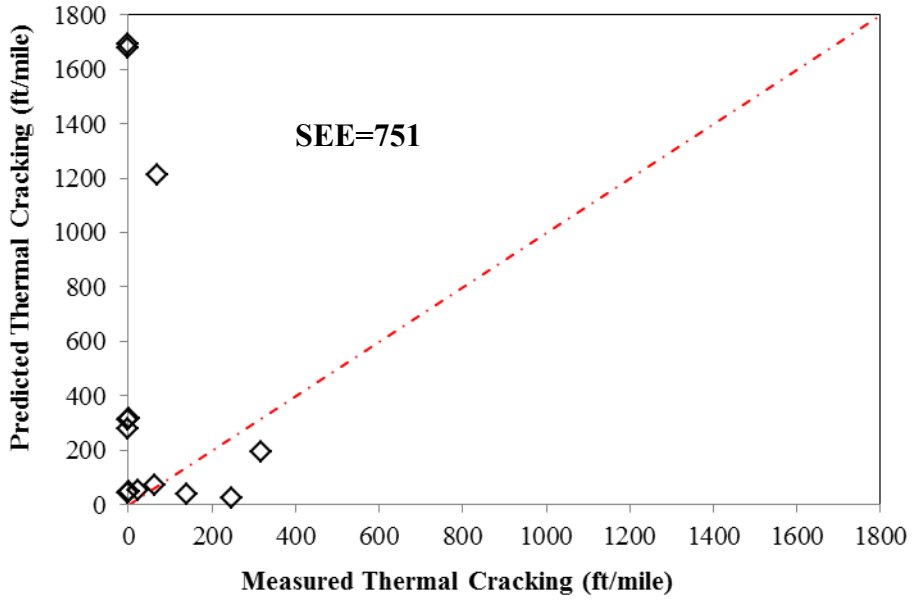

(b)

Figure 6.5: Comparisons of Predicted and Measured Thermal Cracking (a) Before Calibration and (b) After Calibration

6.5 VALIDATION

Calibrated models are needed to be validated to confirm that the locally calibrated performance prediction models can produce robust and accurate predictions for cases other than those used for model calibration.The calibrated models were validated by running the Darwin M-E on the remaining projects that were not included in the calibration process to compare predicted and measured performance. Figure 6-6 shows the comparison of the predicted and measured performance. It is observed that local calibration significantly reduced the difference between predicted and measured distresses. However, it is recommended that additional sites be established in the future calibration effort to further reduce this difference.

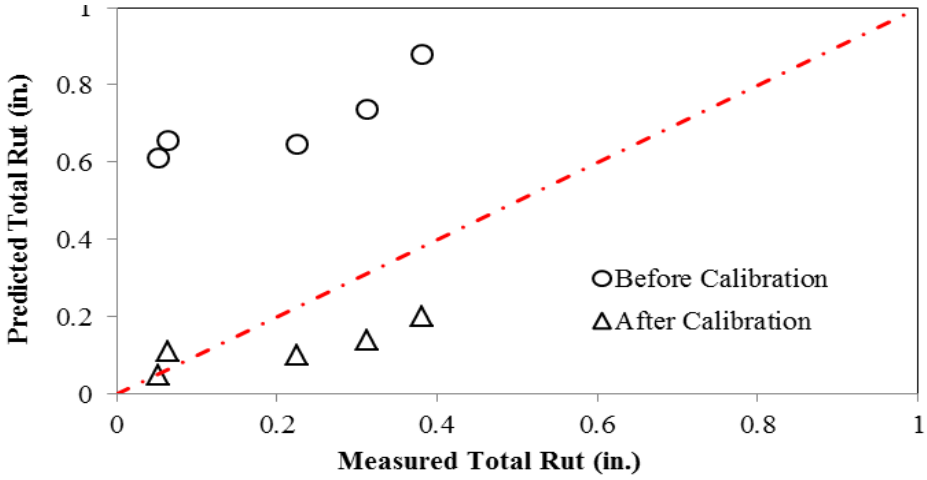

(a)

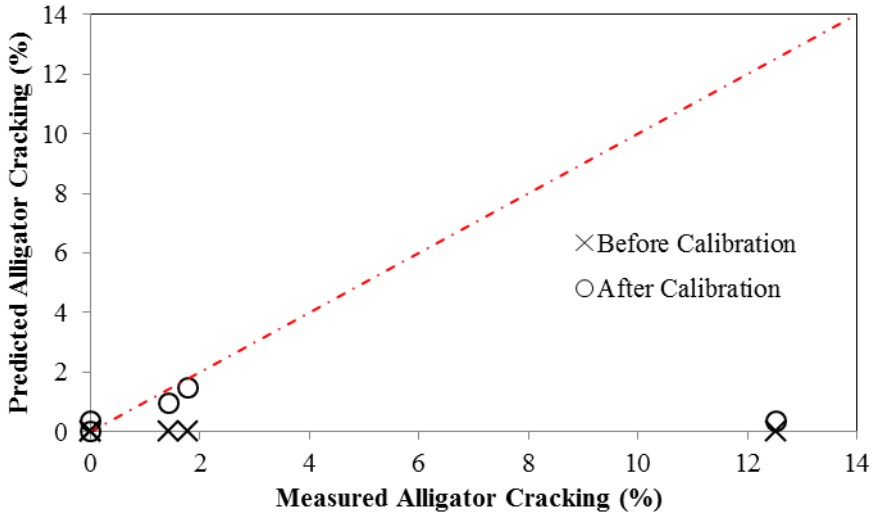

(b)

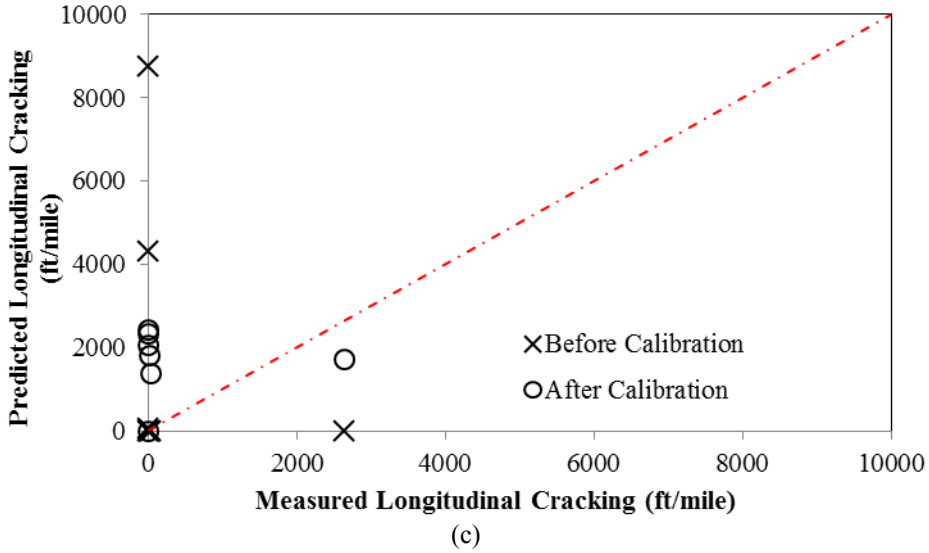

(c)

Figure 6.6: Comparisons of National and Calibrated Performance Models for (a) Rutting, (b) Alligator Cracking, and (c) Longitudinal Cracking.

7.0 SUMMARY, CONCLUSIONS, AND RECOMMENDATION

7.1 SUMMARY AND CONCLUSIONS

This paper presents the findings for calibration of the Darwin M-E performance prediction models for AC rehabilitation of existing pavements for Oregon. The following conclusions are made from this study:

- From the verification results, it was found that predicted distresses using the Darwin M-E default calibration coefficients did not match well with actual distresses observed during the condition surveys, suggesting extensive local calibration was required for Oregon conditions.

- Darwin M-E over predicted total rutting compared to the measured total rutting, as was evident from the verification runs using the Darwin M-E default calibration coefficients. Further, it was observed that most of the rutting predicted by Darwin M-E occurred in the subgrade.

- For alligator (bottom-up) cracking and thermal (transverse) cracking, the Darwin M-E underestimated the amount of cracking considerably as compared to the actual amount measured in the field. A high amount of variability between predicted and measured values was observed for longitudinal (top-down) cracking.

- From the verification runs on the four CRCP pavement sections, the Darwin M-E under predicted the number of punchouts per mile on the three CRCP sections while the remaining CRCP section's punchouts per mile were over predicted as compared to what was actually measured in the field. It is difficult to comment on the accuracy of the nationally calibrated punchout model based on only four pavement sections, however the initial assessment shows the nationally calibrated Darwin M-E model provided a reasonable estimate of the punchouts.

- From the calibration results, the locally calibrated models of rutting, alligator cracking, and longitudinal cracking provided better predictions with lower bias and standard error than the nationally (default) calibrated models. However, there was a high degree of variability between the predicted and measured distresses, especially for longitudinal cracking and thermal cracking, even after the calibration.

- From the validation results, both rutting and alligator cracking models provided reasonable predictions. Though the locally calibrated longitudinal cracking provided better predictions than the nationally calibrated model, a high degree of variability between the predicted and observed longitudinal cracking was found.

- It always remains a challenge to delineate between alligator (bottom-up) cracking and longitudinal (top-down) cracking as it is not practical to take cores or trenches at each single crack to distinguish between alligator cracking and longitudinal cracking. Therefore, there could be measurement error, which may affect the calibration effort related to these distresses.

7.2 RECOMMENDATIONS

The following recommendations are drawn from this study:

- The calibrated models of the MEPDG contained in Darwin M-E and summarized in Chapter 6 can be implemented. Continued assessment of the calibrated Darwin M-E should be done to ensure reasonable designs are being developed.

- Updates to the Darwin M-E will be needed in the future as new materials and newer pavement design strategies are being employed. One such set of materials and pavement design method are the use of interlayer mixes to mitigate reflective cracking as these mixes are high asphalt/low air void mixes using a highly polymerized asphalt binder.

- It is recommended that additional sites be established to include in future calibration efforts and thus, to further improve the accuracy of the rutting and alligator cracking models.

- The availability and quality of data (materials, construction, and performance data) required for Darwin M-E are critical for local calibration. It is recommended that more detailed inputs (Level 1 mostly) be established for future calibration efforts, which will help reduce a significant amount of input error and, thus, may improve the accuracy of prediction models.

- There remains a question regarding the usability of longitudinal cracking and thermal cracking models, as was supported by previous research. Currently, improved thermal cracking models are being developed through FHWA pooled-fund studies. And, a NCHRP project 01-52 is underway to improve the longitudinal cracking model (http://apps.trb.org/cmsfeed/TRBNetProjectDisplay.asp?ProjectID=3152). Therefore, it is recommended that longitudinal cracking and thermal cracking models be recalibrated once these models are improved by MEPDG.

- Only four CRCP pavement sections were included in the verification study. Therefore, it is recommended that additional CRCP pavement sections be established for future verification and subsequent calibration, if needed, to improve the accuracy of the punchout model.

8.0 REFERENCES

ARA, Inc., ERES Consultants Division. *Guide for Mechanistic–Empirical Design of New and Rehabilitated Pavement Structures.* Final report, NCHRP Project 1-37A. Transportation. Research Board of the National Academies, Washington, D.C., 2004. http://www.trb.org/ mepdg/guide.htm. Last accessed December 12, 2011.

Banaerjee, A., J.A. Prozzi, and J.P. Aguiar-Moya. Calibration of mechanistic-empirical pavement design guide permanent deformation models: Texas experience with long-term pavement performance. *Transportation Research Record,* No. 2094, Transportation Research Board, National Research Council, 12-20. Washington, D.C., 2009, pp. 12-20.

Banerjee, A., J.A. Prozzi, and J.P. Aguiar-Moya. Calibrating the MEPDG permanent deformation performance model for different maintenance and rehabilitation strategies, DVD. Presented at the 89th Annual Meeting of the Transportation Research Board. Washington, D.C., 2010.

Bustos, M. G., C. Cordo, P. Girardi, and M. Pereyra. Developing a methodology to calibrate Mechanistic-Empirical Pavement Design Guide procedures for rigid pavement design in Argentina, DVD. Presented at the 88th Annual Meeting of the Transportation Research Board. Washington, D.C., 2009.

Corley-Lay, J. B., F. Jadoun, J. Mastin, and R. Kim. Comparison of NCDOT and LTPP monitored flexible pavement distresses, DVD. Presented at the 89th Annual Meeting of the Transportation Research Board. Washington, D.C., 2010.

Galal, K. A., and G.R. Chehab. Implementing the mechanistic-empirical design guide procedure for a Hot-Mix Asphalt-rehabilitated pavement in Indiana. *Transportation Research Record,* No. 1919. Transportation Research Board, National Research Council,Washington, D.C., 2005, pp. 121-133.

Hall K.D., D.X. Xiao, and K.C.P. Wang. Calibration of the MEPDG for flexible pavement design in Arkansas. In Transportation Research Record: Journal of the Transportation Research Board, No. 2226, TRB, National Research Council, Washington, D.C., 2011, pp. 135-141.

Hoegh, K., L. Khazanovich, M.R. Jensen. Local calibration of MEPDG rutting model for MnROAD test sections, DVD. Presented at the 89th Annual Meeting of the Transportation Research Board. Washington, D.C., 2010.

Kang, M., T.M. Adams, and H. Bahia. *Development of a Regional Pavement Performance Database of the AASHTO Mechanistic-Empirical Pavement Design Guide: Part 2: Validations and Local Calibration*. MRUTC 07-01. Midwest Regional University Transportation Center, University of Wisconsin-Madison, Wisconsin, 2007.

Khazanovich, L., L. Yut, S. Husein, C. Turgeon, and T. Burnham. Adaptation of Mechanistic–Empirical Pavement Design Guide for design of Minnesota low-volume Portland Cement Concrete Pavements. *Transportation Research Record*, No. 2087. Transportation Research Board, National Research Council, Washington D.C., 2008, pp. 57-67.

Kim, S., H. Ceylan, K. Gopalakrishnan, O. Smadi, C. Brakke, and F. Behnami.Verification of MEPDG performance predictions using pavement management information system (PMIS), DVD. Presented at the 89th Annual Meeting of the Transportation Research Board. Washington, D.C., 2010.

Li, J., S.T. Muench, J.P. Mahoney, N. Sivaneswaran, and L.M. Pierce. Calibration of NCHRP 1-37A software for the Washington State Department of Transportation: rigid Pavement portion. *Transportation Research Record,* No. 1949, Transportation Research Board, National Research Council, Washington, D.C., 2006, pp. 43-53.

Li, J., L.M. Pierce, and J.S. Uhlmeyer, J. S. Calibration of flexible pavement in mechanistic-empirical pavement design guide for Washington State. *Transportation Research Record,* No. 2095, Transportation Research Board, National Research Council, Washington, D.C., 2009, pp. 73-83.

Li, J., D.R. Luhr, and J.S. Uhlmeyer. Pavement performance modeling using piecewise approximation, DVD. Presented at the 89th Annual Meeting of the Transportation Research Board. Washington, D.C., 2010.

Mamlouk, M. S., and C.E. Zapata. The Need to carefully assess use of State PMS data for MEPDG calibration process, DVD. Presented at the 89th Annual Meeting of the Transportation Research Board. Washington, D.C., 2010.

Miller, J. S. and W.Y. Bellinger. *Distress Identification Manual for the Long-Term Pavement Performance (LTPP) Project*. No. FHWA-RD-03-031 (4th edition). Federal Highway Administration. Mclean, Virginia, 2003.

Muthadi, N. R. 2007. Local Calibration of the MEPDG for Flexible Pavement Design. M.S thesis. North Carolina State University.

Muthadi, N. R., and Kim, R. 2008. Local calibration of mechanistic-empirical pavement design guide for flexible pavement design. *Transportation Research Record* 2087: 131-141. Washington DC: Transportation Research Board, National Research Council.

NCHRP. 2003a. *Jackknife Testing—An Experimental Approach to Refine Model Calibration and Validation*. Research Results Digest 283. National Cooperative Highway Research Program 9-30. Washington, DC: Transportation Research Board, National Research Council.

NCHRP. 2003b. *Refining the Calibration and Validation of Hot Mix Asphalt Performance Models: An Experimental Plan and Database*. Research Results Digest 284. National Cooperative Highway Research Program 9-30. Washington, DC: Transportation Research Board, National Research Council.

NCHRP. 2004. *Guide for Mechanistic-Empirical Design of New and Rehabilitated Pavement Structures*. www.trb.org/mepdg., National Cooperative Highway Research Program 1-37 A. Washington, DC: Transportation Research Board, National Research Council. Last Accessed December 5, 2011.

NCHRP. 2006a. *Independent Review of the Mechanistic-Empirical Pavement Design Guide and Software*. Research Results Digest 307. National Cooperative Highway Research Program 1-40 A. Washington, DC: Transportation Research Board, National Research Council.

NCHRP. 2006b. *Changes to The Mechanistic-Empirical Pavement Design Guide Software Through Version 0.900-July, 2006*. Research Results Digest 308. National Cooperative Highway Research Program 1-40 D. Washington, DC: Transportation Research Board, National Research Council.

NCHRP. 2007. *Recommended Practice for Local Calibration of the ME Pavement Design*

Guide. National Cooperative Highway Research Program 1-40B Draft. Texas: ARA, Inc.

NCHRP. 2009. *Standard Practice for Conducting Local or Regional Calibration Parameters for the MEPDG*. National Cooperative Highway Research Program Project 1- 40B Report (publication under review), Washington, DC: Transportation Research Board, National Research Council.

Schram, S., and Abdelrahman, M. 2006. Improving prediction accuracy in mechanistic-empirical pavement design guide. *Transportation Research Record* 1947: 59-68. Washington DC: Transportation Research Board, National Research Council.

Souliman, M. I., Mamlouk, M. S., El-Basyouny, M. M., and Zapata, C. E. 2010. Calibration of the AASHTO MEPDG for flexible pavement for Arizona conditions, DVD. *Presented at the 89th Annual Meeting of the Transportation Research Board*. Washington, DC: Transportation Research Board.

TRB. 2009. *NCHRP Projects*, http://www.trb.org/CRP/NCHRP/NCHRPProjects.asp, assessed by February, 2009.

TRB. 2010. *NCHRP 01-40B [Completed] User Manual and Local Calibration Guide for the Mechanistic-Empirical Pavement Design Guide and Software*, http://144.171.11.40/cmsfeed/TRBNetProjectDisplay.asp?ProjectID=223, assessed by April, 2010.

Von Quintus, H. L., Darter, M. I., and Mallela, J. 2005. *Phase I – Local Calibration Adjustments for the HMA Distress Prediction Models in the M-E Pavement Design Guide Software*. Interim Report. National Cooperative Highway Research Program 1-40 B. Washington, DC: Transportation Research Board, National Research Council.

Von Quintus, H. L. and Moulthrop, J. S. 2007. *Mechanistic-Empirical Pavement Design Guide Flexible Pavement Performance Prediction Models: Volume I- Executive Research Summar*y. FHWA/MT-07-008/8158-1. Texas: Fugro Consultants, Inc.

Von Quintus, H. L. 2008a. MEPDG Overview & National Perspective. *Presented at North-Central MEPDG User Group*, Ames, IA: February 19, 2008.

Von Quintus, H. L. 2008b. Local calibration of MEPDG—an overview of selected studies. *Presented at 2008 AAPT Symposium Session: Implementation of the New MEPDG*, Philadelphia, PA: April 29 2008.

Von Quintus, H. L., Darter, M. I., and Mallela, J. 2009a. *Recommended Practice for Local Calibration of the M-E Pavement Design Guide*. National Cooperative Highway Research Program Project 1- 40B Manual of Practice (under review), Washington, DC: Transportation Research Board, National Research Council.

Von Quintus, H. L., Darter, M. I., and Mallela, J. 2009a. *Examples Using the Recommended Practice for Local Calibration of the MEPDG Software*. National Cooperative Highway Research Program Project 1- 40B Manual of Practice (under review), Washington, DC: Transportation Research Board, National Research Council.

APPENDIX A:
OREGON MAP WITH PAVEMENT SECTIONS SURVEYED

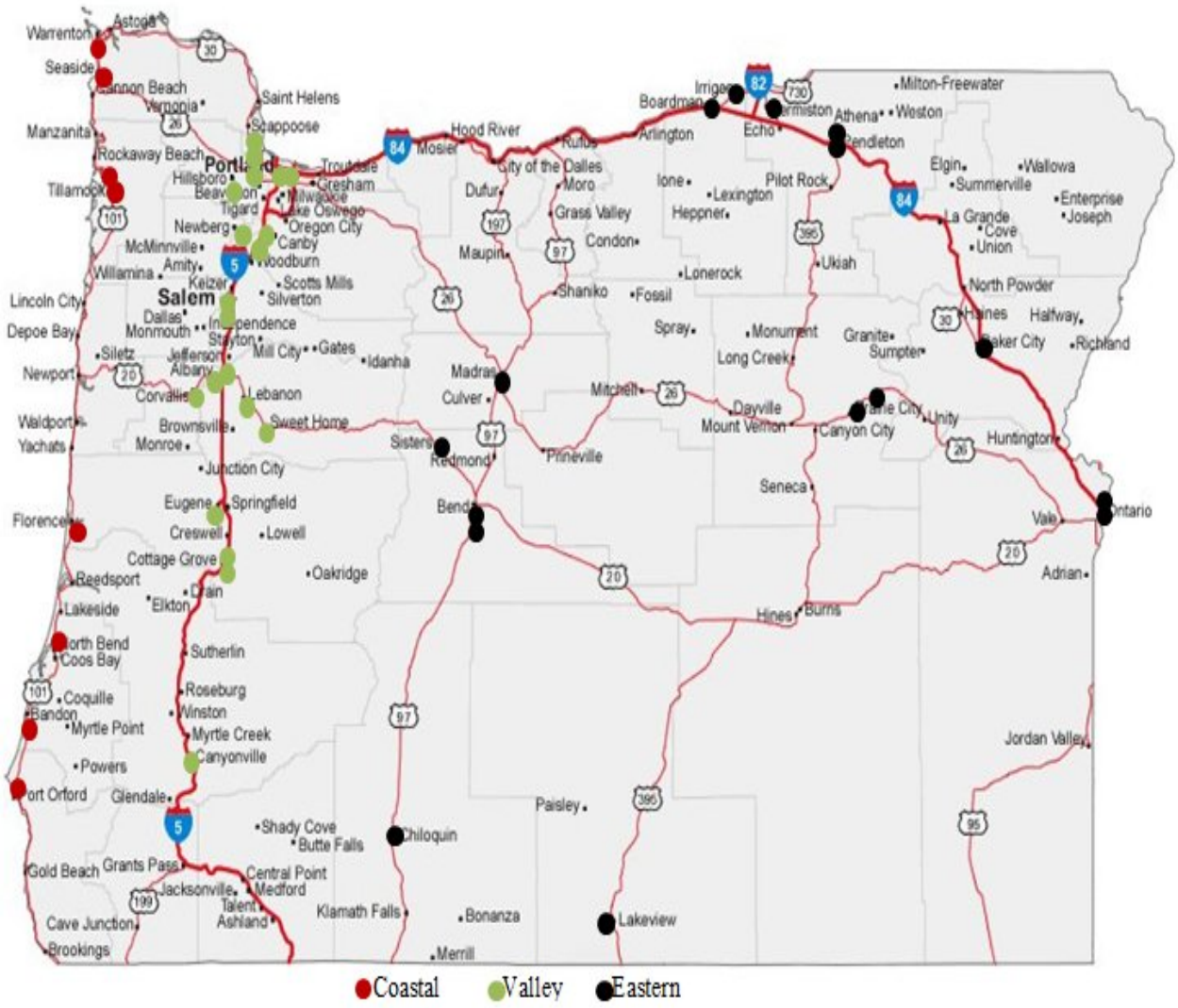

Figure A-1 Locations of Pavement Sections Surveyed

APPENDIX B:
SCREEN SHOTS OF DARWIN M-E

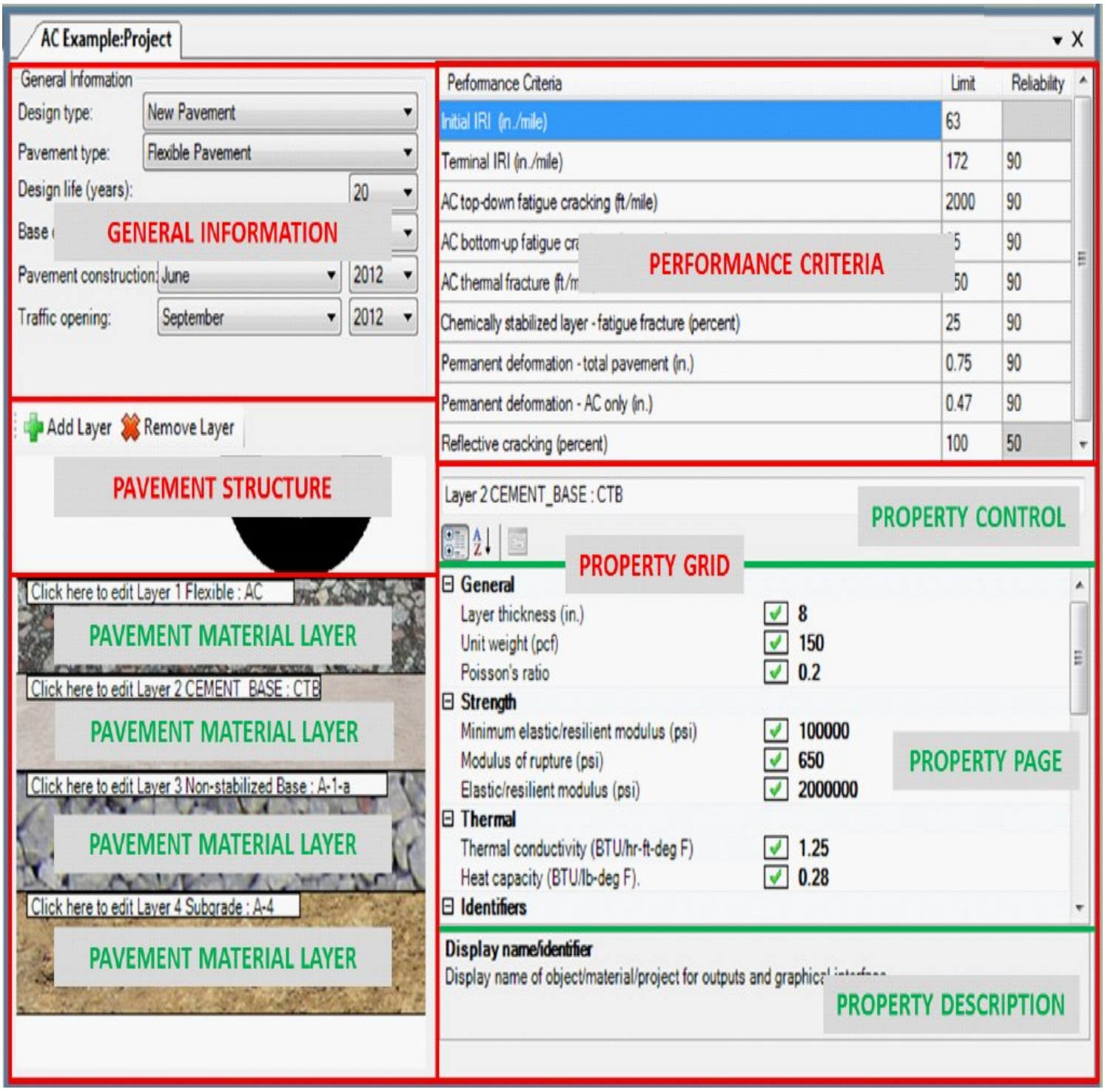

Figure B.1: Project Tab Showing General Information and Performance Criteria

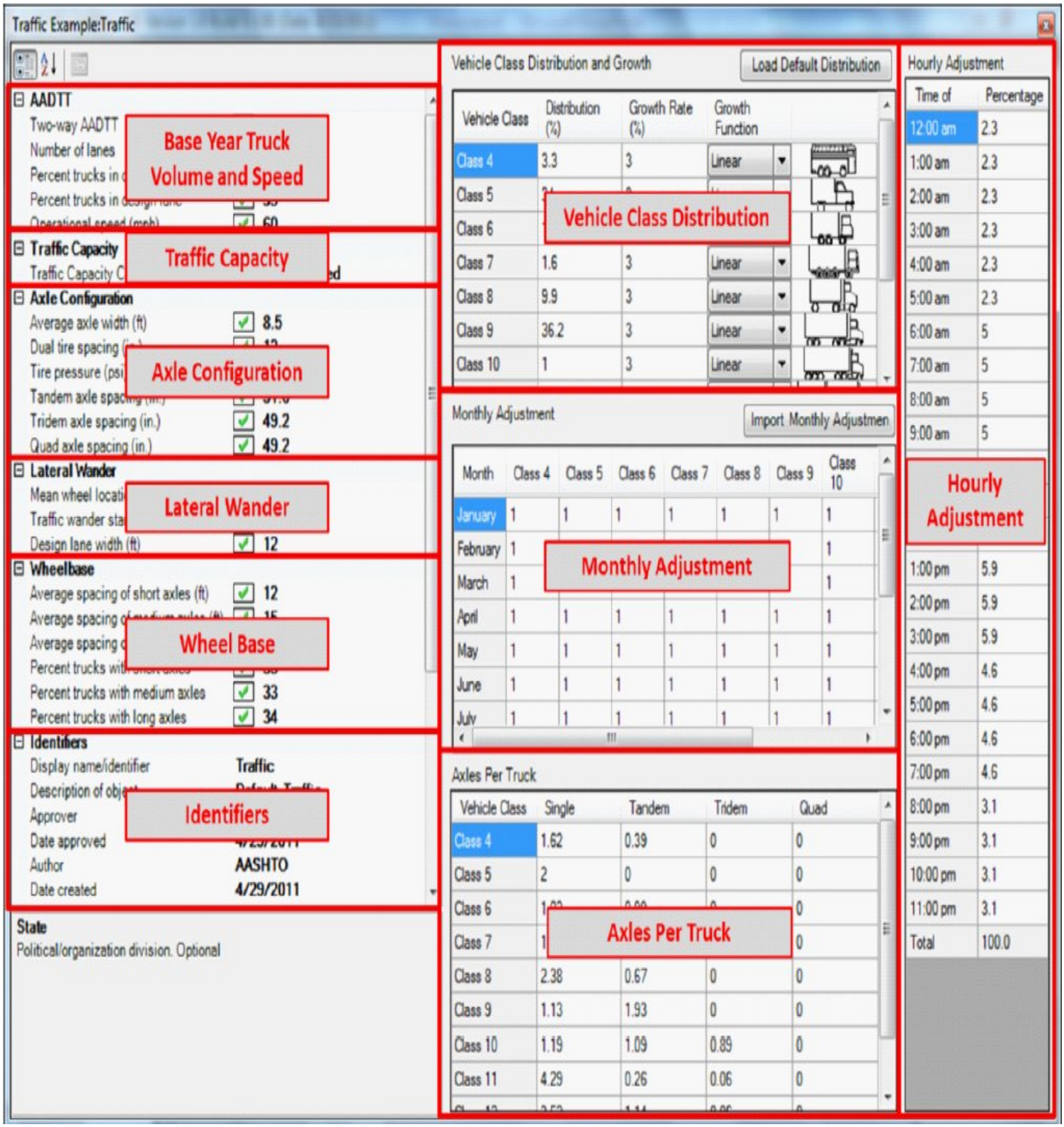

Figure B.2: Traffic Inputs Consisting of Traffic Tab

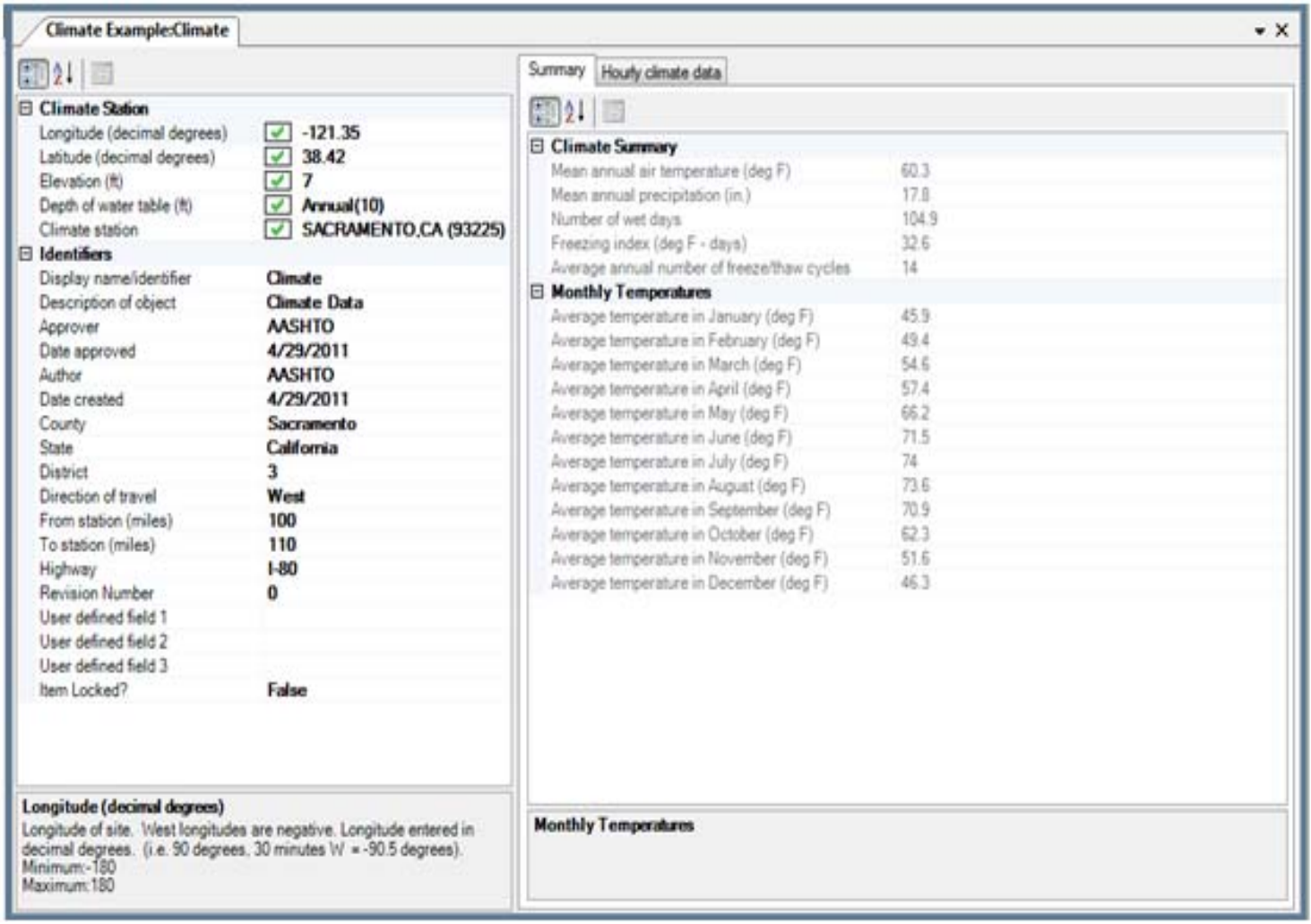

Figure B.3 Climate Tab

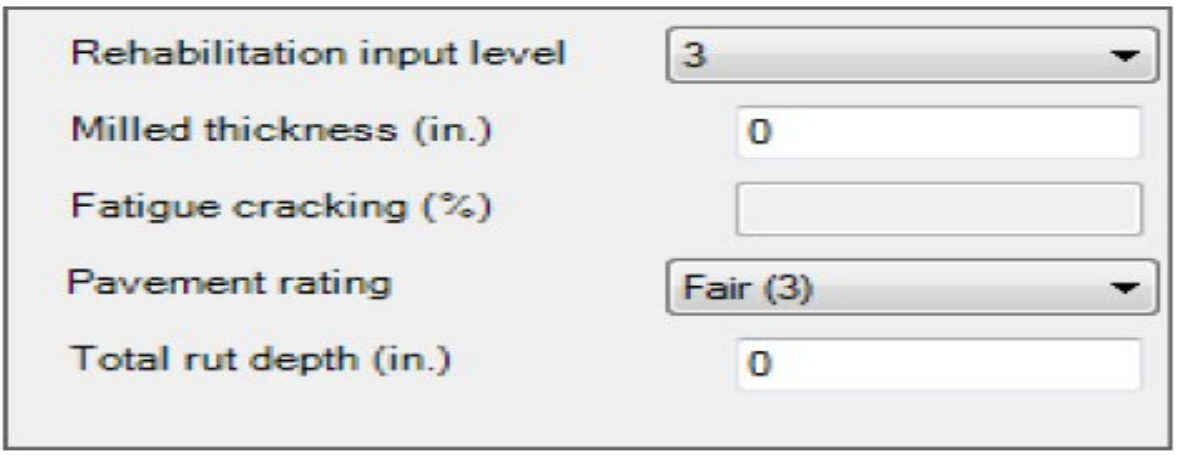

Figure B.4 AC Rehabilitation (Level 3)

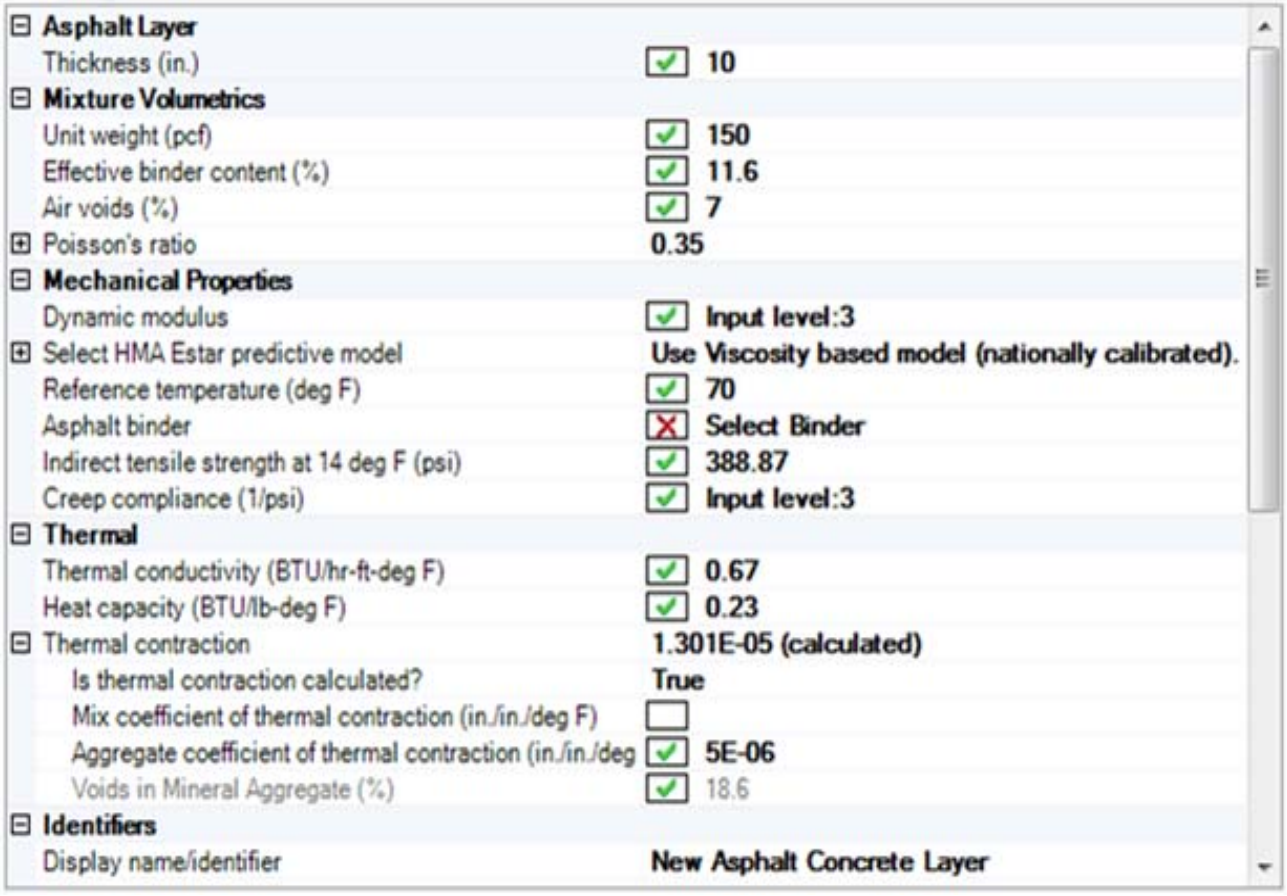

Figure B.5 HMA Layer Properties

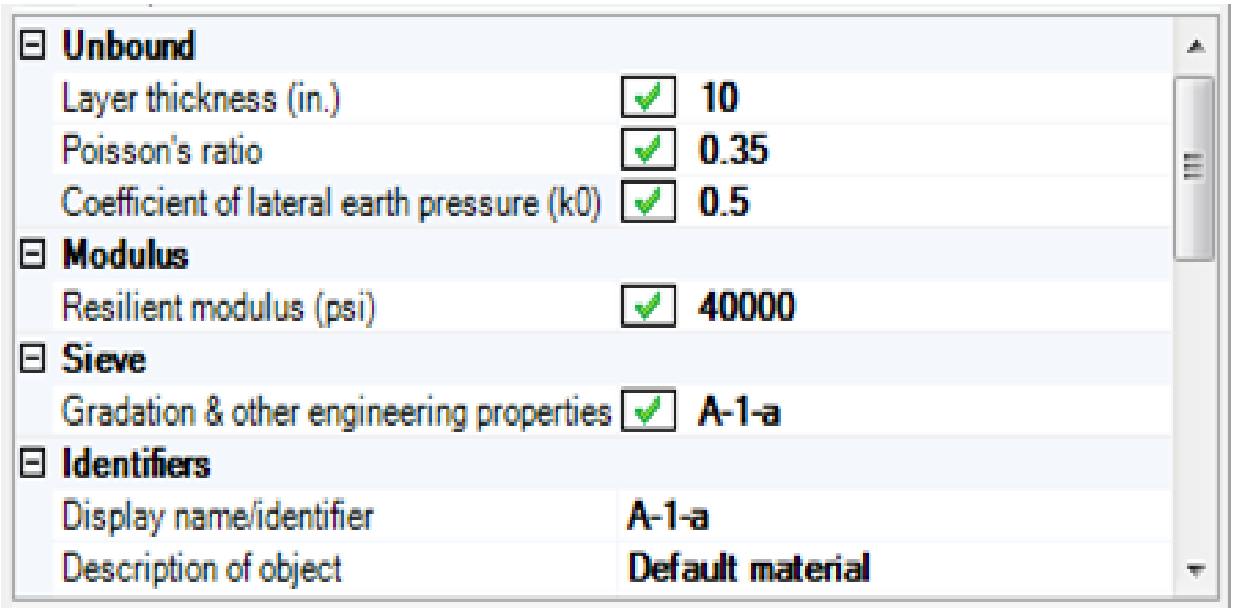

Figure B.6 Layer Properties of Non-stabilized Base

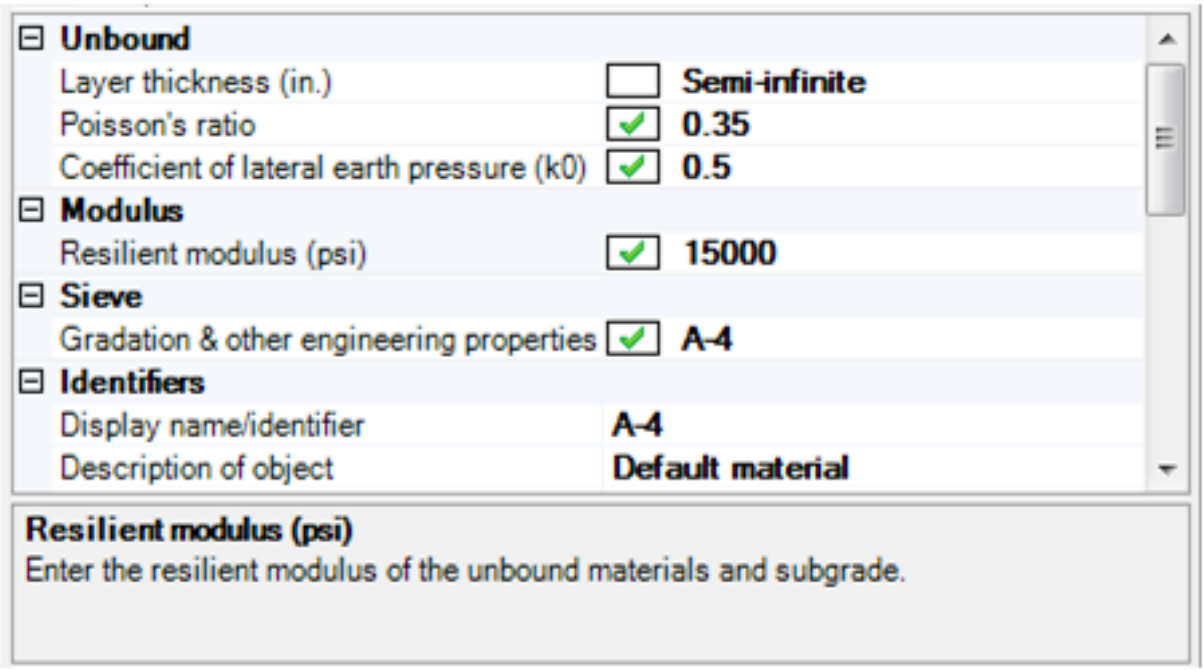

Figure B.7 Layer Properties of Subgrade

APPENDIX C:
INPUTS FOR PAVEMENT SECTIONS UNDER STUDY

US 101: NEPTUNE DR-CAMP RILEA

Traffic Info		Climatic Info	
Initial Two-way AADTT	2300	Latitude	46.159198
No of Lanes in Design Direction	1	Longitude	-123.90206
Growth Rate (%)	0	Elevation	22.586
Lane Distribution Factor	1	Depth to Water Table (ft)	1.02
Speed Limit (MPH)	45		

HMA Layer Properties				
Aggregate Gradation (% passing)		Asphalt Binder Grade	Volumetric Properties (In place)	
3/4 in. Sieve	100	PG 64-22	Effective Binder Content, Pbe (%)	11.93
3/8 in. Sieve	81		Air Voids (%)	5
#4 Sieve	56		Unit Weight (lb/ft^3)	151.64
#200 Sieve	5.5		Pbe (%) by Wt	5.1

Other Layer Properties					
Subgrade		Aggregate Base		Chemically-Stabilized Base	
Type	A-4	Type	A-1-a	Type	-
Resilient Modulus (psi)	5500	Resilient Modulus (psi)	25000	Other Values	-

US 101: Tillamook Couplet

Traffic Info		Climatic Info	
Initial Two-way AADTT	1220	Latitude	45.45552
No of Lanes in Design Direction	1	Longitude	-123.843062
Growth Rate (%)	0	Elevation	25.094
Lane Distribution Factor	1	Depth to Water Table (ft)	10
Speed Limit (MPH)	25		

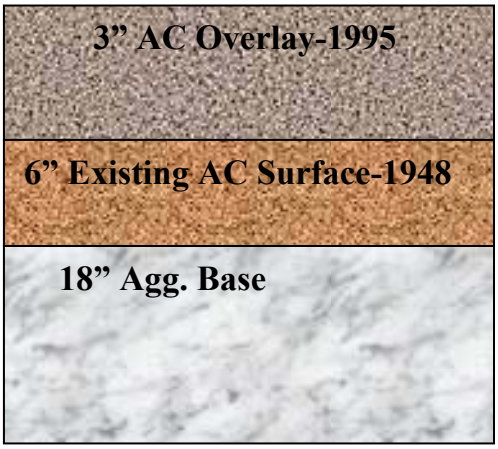

HMA Layer Properties				
Aggregate Gradation (% passing)		Asphalt Binder Grade	Volumetric Properties (In place)	
3/4 in. Sieve	96	PG 64-22	Effective Binder Content, Pbe (%)	9.9
3/8 in. Sieve	68		Air Voids (%)	4.4
#4 Sieve	46		Unit Weight (lb/ft^3)	163.92
#200 Sieve	4.1		Pbe (%) by Wt	3.9

Other Layer Properties					
Subgrade		Aggregate Base		Chemically-Stabilized Base	
Type	A-4	Type	A-1-a	Type	-
Resilient Modulus (psi)	5500	Resilient Modulus (psi)	25000	Other Values	-

US 101: DOOLEY BR-JCT HWY 047

Traffic Info		Climatic Info	
Initial Two-way AADTT	1852	Latitude	45.94336
No of Lanes in Design Direction	1	Longitude	-123.920167
Growth Rate (%)	0	Elevation	35.128
Lane Distribution Factor	1	Depth to Water Table (ft)	4
Speed Limit (MPH)	50		

HMA Layer Properties				
Aggregate Gradation (% passing)		Asphalt Binder Grade	Volumetric Properties (In place)	
3/4 in. Sieve	100	PG 64-22	Effective Binder Content, Pbe (%)	11.01
3/8 in. Sieve	88		Air Voids (%)	5.49
#4 Sieve	57		Unit Weight (lb/ft^3)	148.01
#200 Sieve	6.5		Pbe (%) by Wt	4.7

Other Layer Properties					
Subgrade		Aggregate Base		Chemically-Stabilized Base	
Type	A-4	Type	A-1-a	Type	-
Resilient Modulus (psi)	5500	Resilient Modulus (psi)	25000	Other Values	-

US 101: NCL BANDON-JUNE AVE

Traffic Info		Climatic Info	
Initial Two-way AADTT	1680	Latitude	43.11893
No of Lanes in Design Direction	2	Longitude	-124.403407
Growth Rate (%)	0	Elevation	65.799
Lane Distribution Factor	0.90	Depth to Water Table (ft)	4
Speed Limit (MPH)	30		

HMA Layer Properties				
Aggregate Gradation (% passing)		Asphalt Binder Grade	Volumetric Properties (In place)	
3/4 in. Sieve	100	PG 64-22	Effective Binder Content, Pbe (%)	11.19
3/8 in. Sieve	87		Air Voids (%)	4
#4 Sieve	57		Unit Weight (lb/ft^3)	149.34
#200 Sieve	5.9		Pbe (%) by Wt	4.86

Other Layer Properties					
Subgrade		Aggregate Base		Chemically-Stabilized Base	
Type	A-7-5	Type	-	Type	Cement Stabilized
Resilient Modulus (psi)	4000	Resilient Modulus (psi)	-	Other Values	Default

US 101: WILSON R.-TILLAMOOK COUPLET

Traffic Info		Climatic Info	
Initial Two-way AADTT	3090	Latitude	45.472916
No of Lanes in Design Direction	2	Longitude	-123.844162
Growth Rate (%)	0	Elevation	13.494
Lane Distribution Factor	0.90	Depth to Water Table (ft)	10
Speed Limit (MPH)	45		

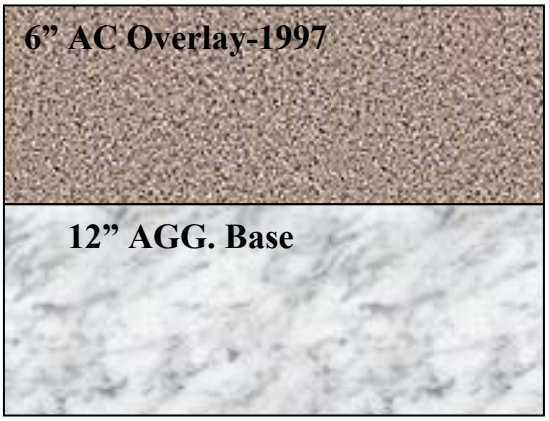

HMA Layer Properties				
Aggregate Gradation (% passing)		Asphalt Binder Grade	Volumetric Properties (In place)	
3/4 in. Sieve	95	PG 64-22	Effective Binder Content, Pbe (%)	10.94
3/8 in. Sieve	69		Air Voids (%)	4.2
#4 Sieve	45		Unit Weight (lb/ft^3)	150.95
#200 Sieve	4.7		Pbe (%) by Wt	4.7

Other Layer Properties					
Subgrade		Aggregate Base		Chemically-Stabilized Subgrade	
Type	A-4	Type	A-1-a	Type	-
Resilient Modulus (psi)	5500	Resilient Modulus (psi)	Default	Other Values	-

US 101: FLORIDA AVE-WASHINGTON AVE

Traffic Info		Climatic Info	
Initial Two-way AADTT	1410	Latitude	43.410704
No of Lanes in Design Direction	3	Longitude	-124.223529
Growth Rate (%)	0	Elevation	44.496
Lane Distribution Factor	0.50	Depth to Water Table (ft)	10
Speed Limit (MPH)	45		

HMA Layer Properties				
Aggregate Gradation (% passing)		Asphalt Binder Grade	Volumetric Properties (In place)	
3/4 in. Sieve	100	PG 64-22	Effective Binder Content, Pbe (%)	11.93
3/8 in. Sieve	81		Air Voids (%)	5
#4 Sieve	56		Unit Weight (lb/ft^3)	151.64
#200 Sieve	5.5		Pbe (%) by Wt	5.1

Other Layer Properties					
Subgrade		Aggregate Base		Chemically-Stabilized Base	
Type	A-7-5	Type	A-1-a	Type	-
Resilient Modulus (psi)	4000	Resilient Modulus (psi)	Default	Other Values	-

US 101: SUTTON CREEK-MUNSEL LAKE RD

Traffic Info		Climatic Info	
Initial Two-way AADTT	1170	Latitude	43.970103
No of Lanes in Design Direction	1	Longitude	-124.096968
Growth Rate (%)	0	Elevation	17.136
Lane Distribution Factor	1	Depth to Water Table (ft)	10
Speed Limit (MPH)	55		

HMA Layer Properties (AC Wearing Course)				
Aggregate Gradation (% passing)		Asphalt Binder Grade	Volumetric Properties (In place)	
3/4 in. Sieve	100	PG 64-22	Effective Binder Content, Pbe (%)	11.23
3/8 in. Sieve	86		Air Voids (%)	4
#4 Sieve	44		Unit Weight (lb/ft^3)	148.64
#200 Sieve	5.5		Pbe (%) by Wt	4.9
HMA Layer Properties (AC Base Course)				
Aggregate Gradation (% passing)		Asphalt Binder Grade	Volumetric Properties (In place)	
3/4 in. Sieve	99	PG 64-22	Effective Binder Content, Pbe (%)	13.43
3/8 in. Sieve	47		Air Voids (%)	4
#4 Sieve	17		Unit Weight (lb/ft^3)	150.18
#200 Sieve	3.4		Pbe (%) by Wt	5.8

Other Layer Properties					
Subgrade		Aggregate Base		Chemically-Stabilized Base	
Type	A-7-5	Type	A-1-a	Type	Cement
Resilient Modulus (psi)	4000	Resilient Modulus (psi)	Default	Other Values	Default

US 20: SWEET HOME-18 TH AVE

Traffic Info		Climatic Info	
Initial Two-way AADTT	1172	Latitude	44.398201
No of Lanes in Design Direction	2	Longitude	-122.726715
Growth Rate (%)	0	Elevation	544.404
Lane Distribution Factor	0.90	Depth to Water Table (ft)	2
Speed Limit (MPH)	35		

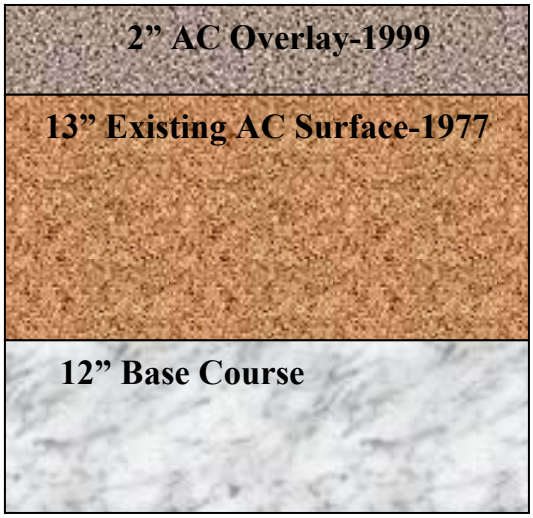

HMA Layer Properties				
Aggregate Gradation (% passing)		Asphalt Binder Grade	Volumetric Properties (In place)	
3/4 in. Sieve	100	PG 64-22	Effective Binder Content, Pbe (%)	10.53
3/8 in. Sieve	87		Air Voids (%)	5.1
#4 Sieve	54		Unit Weight (lb/ft^3)	151.69
#200 Sieve	6		Pbe (%) by Wt	4.5

Other Layer Properties					
Subgrade		Aggregate Base		Chemically-Stabilized Base	
Type	A-6	Type	A-1-a	Type	-
Resilient Modulus (psi)	4500	Resilient Modulus (psi)	Default	Other Values	-

OR 99E: ALBANY AVE-CALAPOOIA ST

Traffic Info		Climatic Info	
Initial Two-way AADTT	2366	Latitude	44.624824
No of Lanes in Design Direction	2	Longitude	-123.108543
Growth Rate (%)	2	Elevation	220.115
Lane Distribution Factor	0.90	Depth to Water Table (ft)	1
Speed Limit (MPH)	35		

HMA Layer Properties				
Aggregate Gradation (% passing)		Asphalt Binder Grade	Volumetric Properties (In place)	
3/4 in. Sieve	100	PG 64-22	Effective Binder Content, Pbe (%)	10.77
3/8 in. Sieve	79		Air Voids (%)	2.4
#4 Sieve	51		Unit Weight (lb/ft^3)	148.54
#200 Sieve	5		Pbe (%) by Wt	4.7

Other Layer Properties					
Subgrade		Aggregate Base		Chemically-Stabilized Base	
Type	A-4	Type	A-1-a	Type	-
Resilient Modulus (psi)	5500	Resilient Modulus (psi)	Default	Other Values	-

OR 34: WCL LEBANON-RXR X-ING

Traffic Info		Climatic Info	
Initial Two-way AADTT	1580	Latitude	44.545045
No of Lanes in Design Direction	2	Longitude	-122.910956
Growth Rate (%)	0	Elevation	345.532
Lane Distribution Factor	0.90	Depth to Water Table (ft)	2
Speed Limit (MPH)	35		

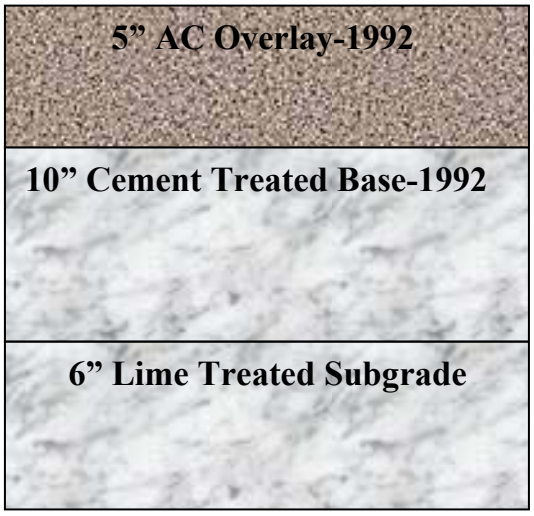

HMA Layer Properties				
Aggregate Gradation (% passing)		Asphalt Binder Grade	Volumetric Properties (In place)	
3/4 in. Sieve	100	PG 64-22	Effective Binder Content, Pbe (%)	10.44
3/8 in. Sieve	87		Air Voids (%)	4.4
#4 Sieve	54		Unit Weight (lb/ft^3)	144.1
#200 Sieve	4.6		Pbe (%) by Wt	4.7

Other Layer Properties					
Subgrade		Aggregate Base		Chemically-Stabilized Base	
Type	A-6	Type	-	Type	Cement
Resilient Modulus (psi)	4000	Resilient Modulus (psi)	-	Other Values	Default

OR 221: N. SALEM-ORCHARD HEIGHTS RD

Traffic Info		Climatic Info	
Initial Two-way AADTT	1850	Latitude	44.953147
No of Lanes in Design Direction	2	Longitude	-123.052461
Growth Rate (%)	2.5	Elevation	178.247
Lane Distribution Factor	0.90	Depth to Water Table (ft)	3.5
Speed Limit (MPH)	35		

HMA Layer Properties				
Aggregate Gradation (% passing)		Asphalt Binder Grade	Volumetric Properties (In place)	
3/4 in. Sieve	96	PG 64-22	Effective Binder Content, Pbe (%)	10.84
3/8 in. Sieve	72		Air Voids (%)	4.5
#4 Sieve	49		Unit Weight (lb/ft^3)	146.5
#200 Sieve	5.7		Pbe (%) by Wt	4.8

Other Layer Properties					
Subgrade		Aggregate Base		Chemically-Stabilized Base	
Type	A-4	Type	A-1-a	Type	-
Resilient Modulus (psi)	5500	Resilient Modulus (psi)	Default	Other Values	-

OR 22: END HWY 072-I-5 NB RAMPS

Traffic Info		Climatic Info	
Initial Two-way AADTT	7042	Latitude	44.913469
No of Lanes in Design Direction	2	Longitude	-122.982268
Growth Rate (%)	1	Elevation	214.157
Lane Distribution Factor	0.90	Depth to Water Table (ft)	2
Speed Limit (MPH)	55		

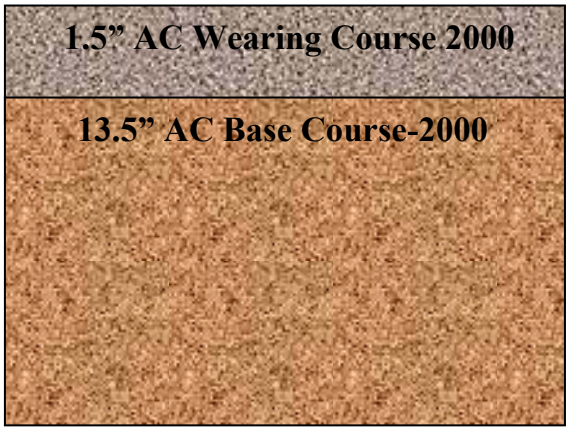

HMA Layer Properties				
Aggregate Gradation (% passing)		Asphalt Binder Grade	Volumetric Properties (In place)	
3/4 in. Sieve	96	PG 64-28	Effective Binder Content, Pbe (%)	9.81
3/8 in. Sieve	76		Air Voids (%)	4
#4 Sieve	49		Unit Weight (lb/ft^3)	147.9
#200 Sieve	4.6		Pbe (%) by Wt	4.3

Other Layer Properties					
Subgrade		Aggregate Base		Chemically-Stabilized Base	
Type	A-4	Type	-	Type	-
Resilient Modulus (psi)	5500	Resilient Modulus (psi)	-	Other Values	-

I-5: AZALEA-CANYONVILLE

Traffic Info		Climatic Info	
Initial Two-way AADTT	13286	Latitude	42.8838
No of Lanes in Design Direction	2	Longitude	-123.24059
Growth Rate (%)	1.5	Elevation	1030.166
Lane Distribution Factor	0.90	Depth to Water Table (ft)	10
Speed Limit (MPH)	65		

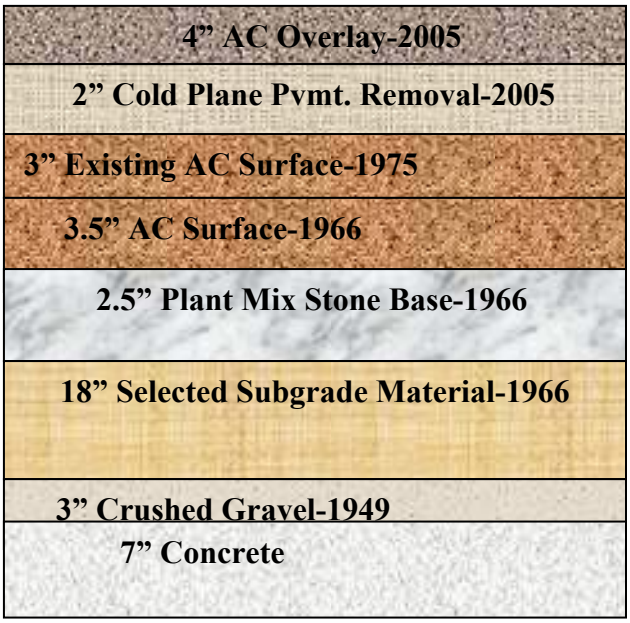

HMA Layer Properties				
Aggregate Gradation (% passing)		Asphalt Binder Grade	Volumetric Properties (In place)	
3/4 in. Sieve	100	PG 76-22	Effective Binder Content, Pbe (%)	10.62
3/8 in. Sieve	80		Air Voids (%)	4
#4 Sieve	50		Unit Weight (lb/ft^3)	160.7
#200 Sieve	6.1		Pbe (%) by Wt	4.3

Other Layer Properties					
Subgrade		Aggregate Base		Chemically-Stabilized Base	
Type	A-4	Type	A-1-a	Type	-
Resilient Modulus (psi)	5500	Resilient Modulus (psi)	Default	Other Values	-

I-5: I-5 Haysville Intch to Woodburn

Traffic Info		Climatic Info	
Initial Two-way AADTT	29270	Latitude	45.013501
No of Lanes in Design Direction	2	Longitude	-122.991968
Growth Rate (%)	0.5	Elevation	143.410
Lane Distribution Factor	0.90	Depth to Water Table (ft)	2
Speed Limit (MPH)	65		

HMA Layer Properties (2007 AC Overlay)				
Aggregate Gradation (% passing)		Asphalt Binder Grade	Volumetric Properties (In place)	
3/4 in. Sieve	93	PG 70-28	Effective Binder Content, Pbe (%)	9.68
3/8 in. Sieve	47		Air Voids (%)	14.4
#4 Sieve	23		Unit Weight (lb/ft^3)	130.1
#200 Sieve	2.3		Pbe (%) by Wt	4.818
HMA Layer Properties (1998 Existing AC Overlay)				
Aggregate Gradation (% passing)		Asphalt Binder Grade	Volumetric Properties (In place)	
3/4 in. Sieve	100	PG 64-22	Effective Binder Content, Pbe (%)	10.45
3/8 in. Sieve	86		Air Voids (%)	4.2
#4 Sieve	52		Unit Weight (lb/ft^3)	147.3
#200 Sieve	6		Pbe (%) by Wt	4.6

Other Layer Properties					
Subgrade		Aggregate Base		Chemically-Stabilized Base/Subgrade	
Type	A-4	Type	A-1-a	Type	-
Resilient Modulus (psi)	5500	Resilient Modulus (psi)	Default	Other Values	-

I-5: Corvallis/Lebanon Interchange

Traffic Info		Climatic Info	
Initial Two-way AADTT	21730	Latitude	44.560965
No of Lanes in Design Direction	2	Longitude	-123.062016
Growth Rate (%)	0	Elevation	261.947
Lane Distribution Factor	0.90	Depth to Water Table (ft)	2
Speed Limit (MPH)	65		

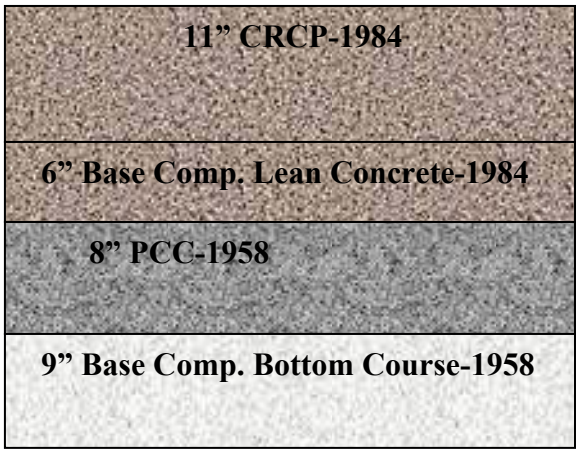

CRCP		
Steel Reinforcement	Steel (%)	0.60
	Steel Diameter (in.)	0.63
	Steel Depth (in.)	4.0
Other Properties	Default	
Other Layer Properties		Default

Unbound Layer Properties					
Subgrade		Aggregate Base		Chemically-Stabilized Base	
Type	A-4	Type	A-1-a	Type	-
Resilient Modulus (psi)	5500	Resilient Modulus (psi)	Default	Other Values	-

I-5: I-5 Wilsonville Intch - Tualatin R

Traffic Info		Climatic Info	
Initial Two-way AADTT	35560	Latitude	45.314104
No of Lanes in Design Direction	4	Longitude	-122.769525
Growth Rate (%)	0.7	Elevation	218.278
Lane Distribution Factor	0.12	Depth to Water Table (ft)	2
Speed Limit (MPH)	65		

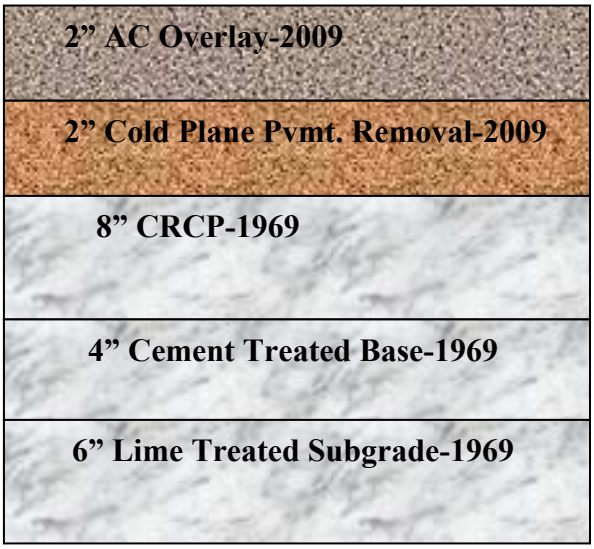

HMA Layer Properties				
Aggregate Gradation (% passing)		Asphalt Binder Grade	Volumetric Properties (In place)	
3/4 in. Sieve	93	PG 70-28	Effective Binder Content, Pbe (%)	9.68
3/8 in. Sieve	47		Air Voids (%)	14.4
#4 Sieve	23		Unit Weight (lb/ft^3)	130.1
#200 Sieve	2.3		Pbe (%) by Wt	4.818

Other Layer Properties					
Subgrade		Aggregate Base		Chemically-Stabilized Base/Subgrade	
Type	A-4	Type	-	Type/Type	Cement/Lime
Resilient Modulus (psi)	6000	Resilient Modulus (psi)	-	Other Values	Default

I-84: N. Powder-Baldock Slough

Traffic Info		Climatic Info	
Initial Two-way AADTT	8000	Latitude	44.953623
No of Lanes in Design Direction	2	Longitude	-117.857208
Growth Rate (%)	0	Elevation	3451.530
Lane Distribution Factor	0.90	Depth to Water Table (ft)	10
Speed Limit (MPH)	55		

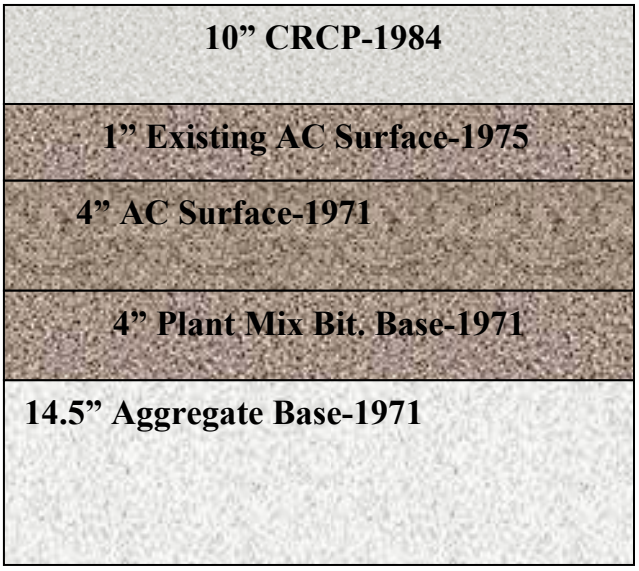

CRCP		
Steel Reinforcement	Steel (%)	0.60
	Steel Diameter (in.)	0.63
	Steel Depth (in.)	4.0
Other Properties	Default	

HMA Layer Properties					
Aggregate Gradation (% passing)		Asphalt Binder Grade	Volumetric Properties (In place)		
3/4 in. Sieve	100	PG 70-22	Effective Binder Content, Pbe (%)	11.96	
3/8 in. Sieve	84		Air Voids (%)	4.1	
#4 Sieve	58		Unit Weight (lb/ft^3)	146.14	
#200 Sieve	5.7		Pbe (%) by Wt	5.3	

Unbound Layer Properties					
Subgrade		Aggregate Base		Chemically-Stabilized Base	
Type	A-6	Type	A-1-a	Type	-
Resilient Modulus (psi)	6000	Resilient Modulus (psi)	Default	Other Values	-

I-84: I-84 NE Union Ave - S. Banfield Intch

Traffic Info		Climatic Info	
Initial Two-way AADTT	18820	Latitude	45.531068
No of Lanes in Design Direction	3	Longitude	-122.597988
Growth Rate (%)	1.5	Elevation	205.778
Lane Distribution Factor	0.50	Depth to Water Table (ft)	10
Speed Limit (MPH)	55		

HMA Layer Properties				
Aggregate Gradation (% passing)		Asphalt Binder Grade	Volumetric Properties (In place)	
3/4 in. Sieve	100	PG 70-22	Effective Binder Content, Pbe (%)	11.96
3/8 in. Sieve	84		Air Voids (%)	4.1
#4 Sieve	58		Unit Weight (lb/ft^3)	146.14
#200 Sieve	5.7		Pbe (%) by Wt	5.3

Other Layer Properties					
Subgrade		Aggregate Base		Chemically-Stabilized Base	
Type	A-4	Type	-	Type	Default
Resilient Modulus (psi)	5500	Resilient Modulus (psi)	-	Other Values	Default

US 730: I-84-Canal Rd

Traffic Info		Climatic Info	
Initial Two-way AADTT	1500	Latitude	45.867421
No of Lanes in Design Direction	1	Longitude	-119.559059
Growth Rate (%)	0	Elevation	331.366
Lane Distribution Factor	1	Depth to Water Table (ft)	10
Speed Limit (MPH)	55		

HMA Layer Properties				
Aggregate Gradation (% passing)		Asphalt Binder Grade	Volumetric Properties (In place)	
3/4 in. Sieve	100	PG 70-28	Effective Binder Content, Pbe (%)	11.08
3/8 in. Sieve	86		Air Voids (%)	4
#4 Sieve	64		Unit Weight (lb/ft^3)	149.5
#200 Sieve	5.8		Pbe (%) by Wt	4.8

Other Layer Properties					
Subgrade		Aggregate Base		Chemically-Stabilized Base	
Type	A-1-a	Type	A-1-a	Type	-
Resilient Modulus (psi)	8000	Resilient Modulus (psi)	Default	Other Values	-

I-84: Stanfield Int-Pendleton

Traffic Info		Climatic Info	
Initial Two-way AADTT	9380	Latitude	45.747881
No of Lanes in Design Direction	2	Longitude	-119.110336
Growth Rate (%)	1	Elevation	877.991
Lane Distribution Factor	0.90	Depth to Water Table (ft)	10
Speed Limit (MPH)	65		

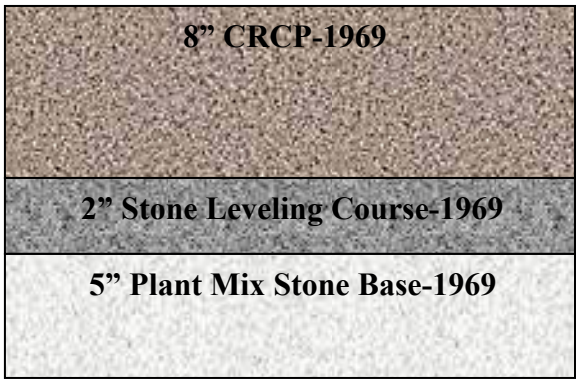

CRCP		
Steel Reinforcement	Steel (%)	0.60
	Steel Diameter (in.)	0.63
	Steel Depth (in.)	4.0
Other Properties	Default	

Unbound Layer Properties					
Subgrade		Aggregate Base		Chemically-Stabilized Base	
Type	A-4	Type	A-1-a	Type	-
Resilient Modulus (psi)	5500	Resilient Modulus (psi)	Default	Other Values	-

US 730: Canal Rd-Umatilla Bridge

Traffic Info		Climatic Info	
Initial Two-way AADTT	2766	Latitude	45.915751
No of Lanes in Design Direction	1	Longitude	-119.352722
Growth Rate (%)	0	Elevation	269.120
Lane Distribution Factor	1	Depth to Water Table (ft)	10
Speed Limit (MPH)	45		

HMA Layer Properties				
Aggregate Gradation (% passing)		Asphalt Binder Grade	Volumetric Properties (In place)	
3/4 in. Sieve	100	PG 70-28	Effective Binder Content, Pbe (%)	11.08
3/8 in. Sieve	86		Air Voids (%)	4
#4 Sieve	64		Unit Weight (lb/ft^3)	149.5
#200 Sieve	5.8		Pbe (%) by Wt	4.8

Other Layer Properties					
Subgrade		Aggregate Base		Chemically-Stabilized Base	
Type	A-2-4	Type	A-1-a	Type	-
Resilient Modulus (psi)	7500	Resilient Modulus (psi)	Default	Other Values	-

US 97: Madras Couplet-Hwy360

Traffic Info		Climatic Info	
Initial Two-way AADTT	4510	Latitude	44.619463
No of Lanes in Design Direction	1	Longitude	-121.132722
Growth Rate (%)	0	Elevation	2323.570
Lane Distribution Factor	1	Depth to Water Table (ft)	10
Speed Limit (MPH)	35		

HMA Layer Properties				
Aggregate Gradation (% passing)		Asphalt Binder Grade	Volumetric Properties (In place)	
3/4 in. Sieve	97	PG 64-28	Effective Binder Content, Pbe (%)	11.12
3/8 in. Sieve	74		Air Voids (%)	4.2
#4 Sieve	49		Unit Weight (lb/ft^3)	153.5
#200 Sieve	6.4		Pbe (%) by Wt	4.7

Other Layer Properties					
Subgrade		Aggregate Base		Chemically-Stabilized Base	
Type	A-2-4	Type	-	Type	Cement
Resilient Modulus (psi)	5800	Resilient Modulus (psi)	-	Other Values	Default

US 97: S. Century Drive-MP 161

Traffic Info		Climatic Info	
Initial Two-way AADTT	3044	Latitude	43.837622
No of Lanes in Design Direction	2	Longitude	-121.422272
Growth Rate (%)	2.5	Elevation	4210.241
Lane Distribution Factor	0.9	Depth to Water Table (ft)	4
Speed Limit (MPH)	55		

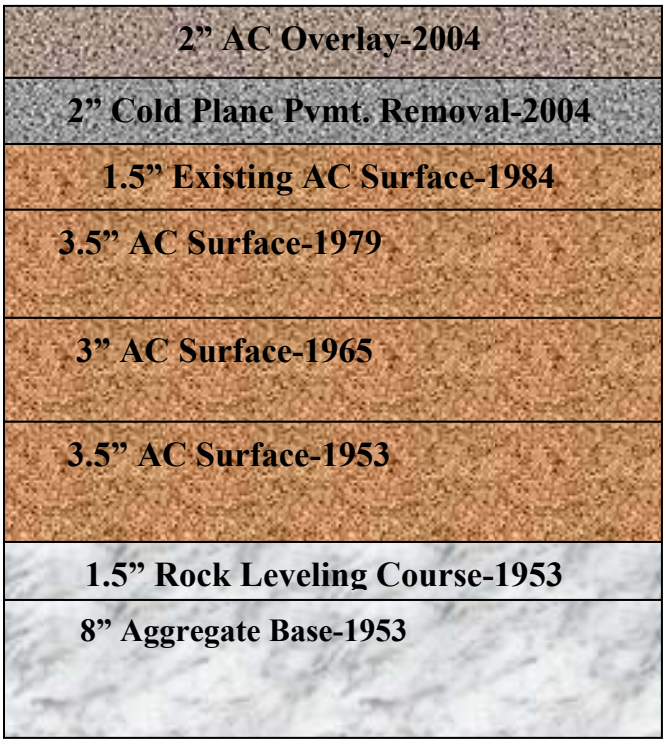

HMA Layer Properties				
Aggregate Gradation (% passing)		Asphalt Binder Grade	Volumetric Properties (In place)	
3/4 in. Sieve	100	PG 70-28	Effective Binder Content, Pbe (%)	10.89
3/8 in. Sieve	85		Air Voids (%)	4
#4 Sieve	57		Unit Weight (lb/ft^3)	146.9
#200 Sieve	7		Pbe (%) by Wt	4.8

Other Layer Properties					
Subgrade		Aggregate Base		Chemically-Stabilized Base	
Type	A-7-5	Type	A-1-a	Type	-
Resilient Modulus (psi)	4000	Resilient Modulus (psi)	Default	Other Values	-

US 97: Weighb Station-Crawford Road

Traffic Info		Climatic Info	
Initial Two-way AADTT	3282	Latitude	43.917124
No of Lanes in Design Direction	2	Longitude	-121.349401
Growth Rate (%)	0	Elevation	4522.131
Lane Distribution Factor	0.90	Depth to Water Table (ft)	4
Speed Limit (MPH)	55		

SB

NB

HMA Layer Properties				
Aggregate Gradation (% passing)		Asphalt Binder Grade	Volumetric Properties (In place)	
3/4 in. Sieve	98	PG 64-28	Effective Binder Content, Pbe (%)	10.34
3/8 in. Sieve	80		Air Voids (%)	4
#4 Sieve	53		Unit Weight (lb/ft^3)	152.2
#200 Sieve	5.8		Pbe (%) by Wt	4.4

Other Layer Properties					
Subgrade		Aggregate Base		Chemically-Stabilized Base	
Type	A-4	Type	A-1-a	Type	Cement
Resilient Modulus (psi)	7000	Resilient Modulus (psi)	Default	Other Values	Default

US 26: Prairie City-Dixie Summit

Traffic Info		Climatic Info	
Initial Two-way AADTT	762	Latitude	44.460924
No of Lanes in Design Direction	2	Longitude	-118.672342
Growth Rate (%)	2.5	Elevation	3608.283
Lane Distribution Factor	0.90	Depth to Water Table (ft)	4
Speed Limit (MPH)	55		

HMA Layer Properties				
Aggregate Gradation (% passing)		Asphalt Binder Grade	Volumetric Properties (In place)	
3/4 in. Sieve	96	PG 64-28	Effective Binder Content, Pbe (%)	10.85
3/8 in. Sieve	71		Air Voids (%)	5.3
#4 Sieve	47		Unit Weight (lb/ft^3)	143.5
#200 Sieve	4.4		Pbe (%) by Wt	4.9

Other Layer Properties					
Subgrade		Aggregate Base		Chemically-Stabilized Base	
Type	A-4	Type	A-1-a	Type	-
Resilient Modulus (psi)	5500	Resilient Modulus (psi)	Default	Other Values	-

US 26: Prairie City Section

Traffic Info		Climatic Info	
Initial Two-way AADTT	792	Latitude	44.462563
No of Lanes in Design Direction	1	Longitude	-118.710752
Growth Rate (%)	3	Elevation	3540.107
Lane Distribution Factor	1	Depth to Water Table (ft)	4
Speed Limit (MPH)	25		

HMA Layer Properties				
Aggregate Gradation (% passing)		Asphalt Binder Grade	Volumetric Properties (In place)	
3/4 in. Sieve	96	PG 64-28	Effective Binder Content, Pbe (%)	10.85
3/8 in. Sieve	71		Air Voids (%)	5.3
#4 Sieve	47		Unit Weight (lb/ft^3)	143.5
#200 Sieve	4.4		Pbe (%) by Wt	4.9

Other Layer Properties					
Subgrade		Aggregate Base		Chemically-Stabilized Base	
Type	A-4	Type	A-1-a	Type	-
Resilient Modulus (psi)	5500	Resilient Modulus (psi)	Default	Other Values	-

I-84: N. FK Jocobsen Gulch-Malheur River (EB)

Traffic Info		Climatic Info	
Initial Two-way AADTT	9648	Latitude	44.072540
No of Lanes in Design Direction	2	Longitude	-117.001648
Growth Rate (%)	1.5	Elevation	2293.092
Lane Distribution Factor	0.90	Depth to Water Table (ft)	10
Speed Limit (MPH)	55		

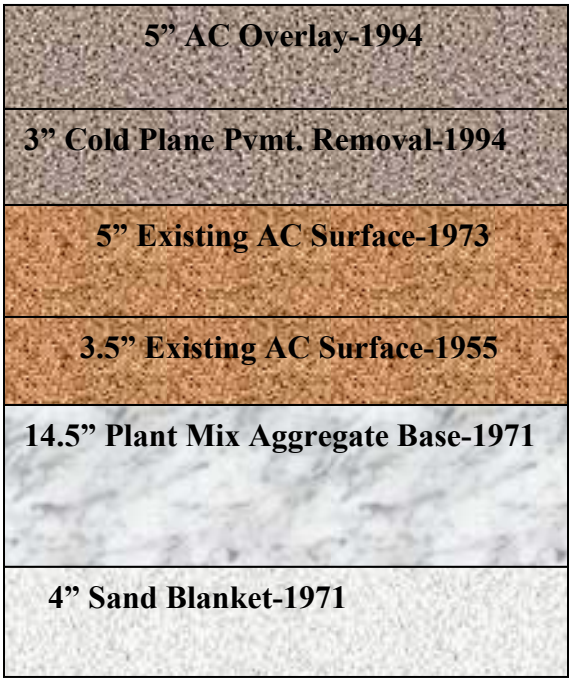

HMA Layer Properties				
Aggregate Gradation (% passing)		Asphalt Binder Grade	Volumetric Properties (In place)	
3/4 in. Sieve	89	PG 70-28	Effective Binder Content, Pbe (%)	9.70
3/8 in. Sieve	44		Air Voids (%)	14.2
#4 Sieve	27		Unit Weight (lb/ft^3)	130.5
#200 Sieve	3		Pbe (%) by Wt	4.818

Other Layer Properties					
Subgrade		Aggregate Base		Chemically-Stabilized Base	
Type	A-4	Type	A-1-a	Type	-
Resilient Modulus (psi)	7000	Resilient Modulus (psi)	Default	Other Values	-

I-84: N. FK Jocobsen Gulch-Malheur River (WB)

Traffic Info		Climatic Info	
Initial Two-way AADTT	8200	Latitude	44.072540
No of Lanes in Design Direction	2	Longitude	-117.001648
Growth Rate (%)	1.5	Elevation	2293.092
Lane Distribution Factor	0.90	Depth to Water Table (ft)	10
Speed Limit (MPH)	55		

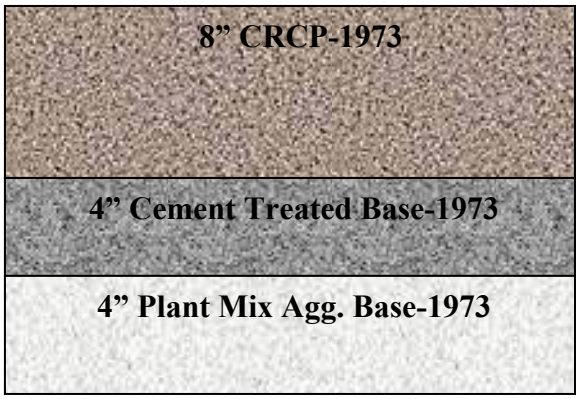

CRCP		
Steel Reinforcement	Steel (%)	0.60
	Steel Diameter (in.)	0.63
	Steel Depth (in.)	3.5

Unbound Layer Properties					
Subgrade		Aggregate Base		Chemically-Stabilized Base	
Type	A-4	Type	A-1-a	Type	-
Resilient Modulus (psi)	5500	Resilient Modulus (psi)	Default	Other Values	-

US 20: MP 10.3-MP 12.5

Traffic Info		Climatic Info	
Initial Two-way AADTT	1706	Latitude	44.181096
No of Lanes in Design Direction	2	Longitude	-121.379871
Growth Rate (%)	2	Elevation	3334.959
Lane Distribution Factor	0.90	Depth to Water Table (ft)	10
Speed Limit (MPH)	55		

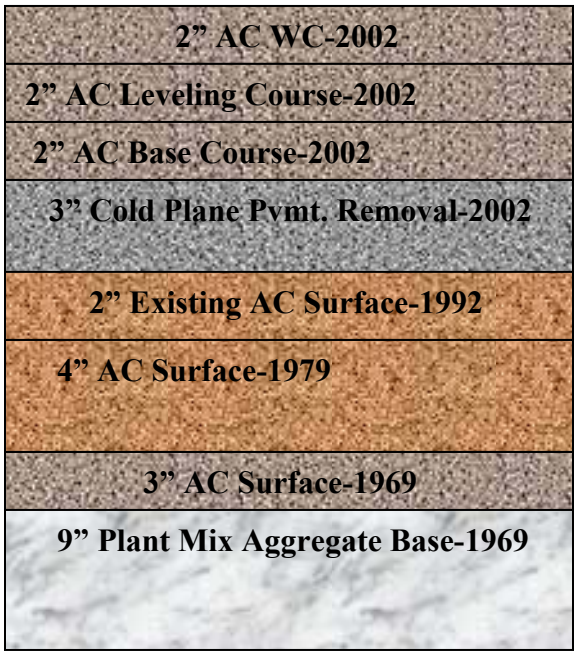

HMA Layer Properties (2002 AC Wearing Course)				
Aggregate Gradation (% passing)		Asphalt Binder Grade	Volumetric Properties (In place)	
3/4 in. Sieve	98	PG 64-28	Effective Binder Content, Pbe (%)	10.29
3/8 in. Sieve	80		Air Voids (%)	4.1
#4 Sieve	53		Unit Weight (lb/ft^3)	151.7
#200 Sieve	6.4		Pbe (%) by Wt	4.4
HMA Layer Properties (2002 AC Base Course)				
Aggregate Gradation (% passing)		Asphalt Binder Grade	Volumetric Properties (In place)	
3/4 in. Sieve	92	PG 70-28	Effective Binder Content, Pbe (%)	9.28
3/8 in. Sieve	41		Air Voids (%)	14.1
#4 Sieve	15		Unit Weight (lb/ft^3)	136.7
#200 Sieve	3.1		Pbe (%) by Wt	4.4

Other Layer Properties					
Subgrade		Aggregate Base		Chemically-Stabilized Base	
Type	A-2-5	Type	A-1-a	Type	-
Resilient Modulus (psi)	7000	Resilient Modulus (psi)	Default	Other Values	-

US 395: Jct Hwy2-Hwy33 (Elm Ave)

Traffic Info		Climatic Info	
Initial Two-way AADTT	2186	Latitude	45.914736
No of Lanes in Design Direction	2	Longitude	-119.305172
Growth Rate (%)	0	Elevation	463.668
Lane Distribution Factor	0.90	Depth to Water Table (ft)	2.5
Speed Limit (MPH)	55		

HMA Layer Properties				
Aggregate Gradation (% passing)		Asphalt Binder Grade	Volumetric Properties (In place)	
3/4 in. Sieve	100	PG 58-28	Effective Binder Content, Pbe (%)	9.97
3/8 in. Sieve	82		Air Voids (%)	5.1
#4 Sieve	55		Unit Weight (lb/ft^3)	153.6
#200 Sieve	4.9		Pbe (%) by Wt	4.2

Other Layer Properties					
Subgrade		Aggregate Base		Chemically-Stabilized Base	
Type	A-4	Type	A-1-a	Type	-
Resilient Modulus (psi)	5500	Resilient Modulus (psi)	Default	Other Values	-

OR 569: Hwy 091 Williamette R E/B

Traffic Info		Climatic Info	
Initial Two-way AADTT	11650	Latitude	44.097542
No of Lanes in Design Direction	2	Longitude	-123.114935
Growth Rate (%)	1	Elevation	-393.701
Lane Distribution Factor	0.90	Depth to Water Table (ft)	10
Speed Limit (MPH)	55		

HMA Layer Properties (1999 AC Wearing Course)				
Aggregate Gradation (% passing)		Asphalt Binder Grade	Volumetric Properties (In place)	
3/4 in. Sieve	92	PG 70-28	Effective Binder Content, Pbe (%)	9.743
3/8 in. Sieve	40		Air Voids (%)	14
#4 Sieve	20		Unit Weight (lb/ft^3)	131.5
#200 Sieve	3.1		Pbe (%) by Wt	4.8
HMA Layer Properties (1999 AC Base Course)				
Aggregate Gradation (% passing)		Asphalt Binder Grade	Volumetric Properties (In place)	
3/4 in. Sieve	95	PG 64-22	Effective Binder Content, Pbe (%)	10.02
3/8 in. Sieve	65		Air Voids (%)	4.4
#4 Sieve	40		Unit Weight (lb/ft^3)	147.6
#200 Sieve	5.2		Pbe (%) by Wt	4.4
HMA Layer Properties (1993 AC Surface)				
Aggregate Gradation (% passing)		Asphalt Binder Grade	Volumetric Properties (In place)	
3/4 in. Sieve	92	PG 64-22	Effective Binder Content, Pbe (%)	9.743
3/8 in. Sieve	48		Air Voids (%)	14.5
#4 Sieve	17		Unit Weight (lb/ft^3)	132.9
#200 Sieve	3.3		Pbe (%) by Wt	4.8

Other Layer Properties					
Subgrade		Aggregate Base		Chemically-Stabilized Base	
Type	A-4	Type	A-1-a	Type	-
Resilient Modulus (psi)	5500	Resilient Modulus (psi)	Default	Other Values	-

OR 99W: Marys R-Kiger Island Dr

Traffic Info		Climatic Info	
Initial Two-way AADTT	2450	Latitude	44.519931
No of Lanes in Design Direction	2	Longitude	-123.276689
Growth Rate (%)	0	Elevation	239.624
Lane Distribution Factor	0.90	Depth to Water Table (ft)	2
Speed Limit (MPH)	35		

HMA Layer Properties (AC Wearing Course)				
Aggregate Gradation (% passing)		Asphalt Binder Grade	Volumetric Properties (In place)	
3/4 in. Sieve	100	PG 70-22	Effective Binder Content, Pbe (%)	10.90
3/8 in. Sieve	83		Air Voids (%)	5.6
#4 Sieve	50		Unit Weight (lb/ft^3)	147.20
#200 Sieve	5		Pbe (%) by Wt	4.8
HMA Layer Properties (AC Base Course)				
Aggregate Gradation (% passing)		Asphalt Binder Grade	Volumetric Properties (In place)	
3/4 in. Sieve	95	PG 64-22	Effective Binder Content, Pbe (%)	10.723
3/8 in. Sieve	71		Air Voids (%)	4.6
#4 Sieve	45		Unit Weight (lb/ft^3)	144.83
#200 Sieve	5		Pbe (%) by Wt	4.8

Other Layer Properties					
Subgrade		Aggregate Base		Chemically-Stabilized Base	
Type	A-4	Type	-	Type	-
Resilient Modulus (psi)	5500	Resilient Modulus (psi)	-	Other Values	-

OR 99W: Brutschr St. Jct. Hwy. 151

Traffic Info		Climatic Info	
Initial Two-way AADTT	4522	Latitude	45.303512
No of Lanes in Design Direction	2	Longitude	-122.940909
Growth Rate (%)	0	Elevation	199.047
Lane Distribution Factor	0.90	Depth to Water Table (ft)	1.5
Speed Limit (MPH)	40		

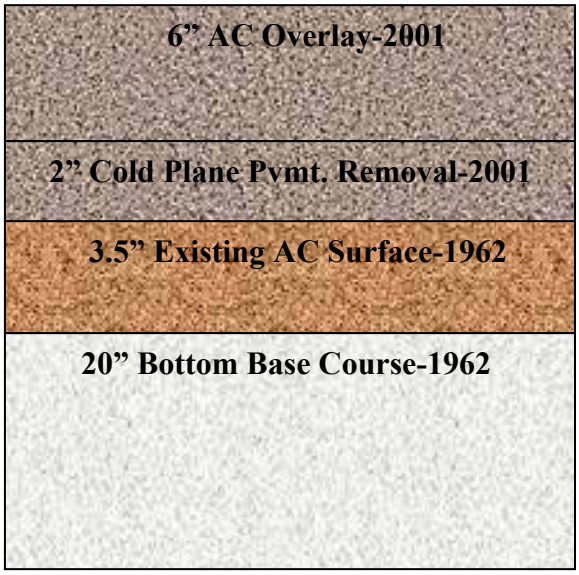

HMA Layer Properties				
Aggregate Gradation (% passing)		Asphalt Binder Grade	Volumetric Properties (In place)	
3/4 in. Sieve	100	PG 70-22	Effective Binder Content, Pbe (%)	9.93
3/8 in. Sieve	85		Air Voids (%)	4
#4 Sieve	54		Unit Weight (lb/ft^3)	146.3
#200 Sieve	5.4		Pbe (%) by Wt	4.4

Other Layer Properties					
Subgrade		Aggregate Base		Chemically-Stabilized Base	
Type	A-4	Type	A-1-a	Type	-
Resilient Modulus (psi)	5500	Resilient Modulus (psi)	Default	Other Values	-

OR 99W: N Sherwood to SW 12th Street

Traffic Info		Climatic Info	
Initial Two-way AADTT	4750	Latitude	45.369778
No of Lanes in Design Direction	3	Longitude	-122.843731
Growth Rate (%)	1.5	Elevation	205.145
Lane Distribution Factor	0.50	Depth to Water Table (ft)	10
Speed Limit (MPH)	45		

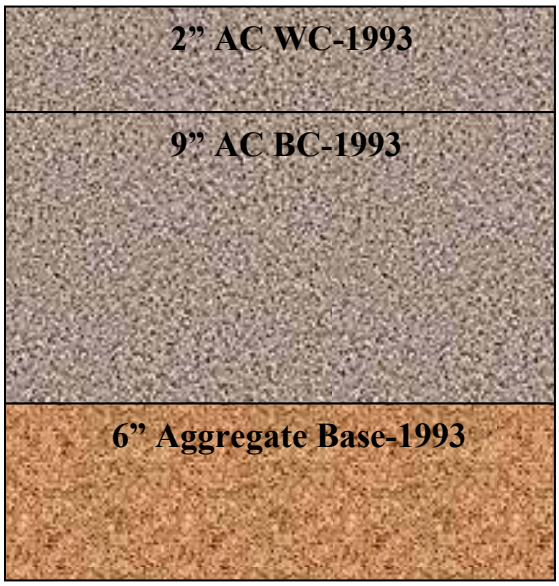

HMA Layer Properties (AC WC)				
Aggregate Gradation (% passing)		Asphalt Binder Grade	Volumetric Properties (In place)	
3/4 in. Sieve	93	PG 64-22	Effective Binder Content, Pbe (%)	10.91
3/8 in. Sieve	46		Air Voids (%)	15.2
#4 Sieve	15		Unit Weight (lb/ft^3)	133.54
#200 Sieve	3.2		Pbe (%) by Wt	5.3
HMA Layer Properties (AC Base Course)				
Aggregate Gradation (% passing)		Asphalt Binder Grade	Volumetric Properties (In place)	
3/4 in. Sieve	95	PG 64-22	Effective Binder Content, Pbe (%)	12.53
3/8 in. Sieve	68		Air Voids (%)	4.6
#4 Sieve	45		Unit Weight (lb/ft^3)	147.70
#200 Sieve	4.8		Pbe (%) by Wt	5.5

Other Layer Properties					
Subgrade		Aggregate Base		Chemically-Stabilized Base	
Type	A-4	Type	A-1-a	Type	-
Resilient Modulus (psi)	5500	Resilient Modulus (psi)	Default	Other Values	-

US 30: Cornelius Pass Rd

Traffic Info		Climatic Info	
Initial Two-way AADTT	5540	Latitude	44.560937
No of Lanes in Design Direction	2	Longitude	-123.25716
Growth Rate (%)	0	Elevation	208.118
Lane Distribution Factor	0.90	Depth to Water Table (ft)	10
Speed Limit (MPH)	55		

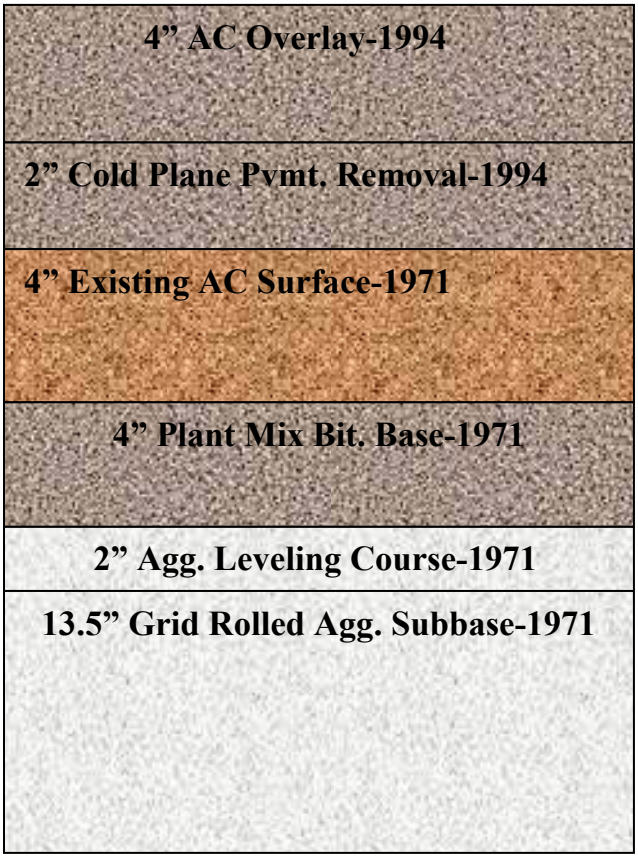

HMA Layer Properties				
Aggregate Gradation (% passing)		Asphalt Binder Grade	Volumetric Properties (In place)	
3/4 in. Sieve	96	PG 58-28	Effective Binder Content, Pbe (%)	10.03
3/8 in. Sieve	71		Air Voids (%)	4.4
#4 Sieve	49		Unit Weight (lb/ft^3)	147.6
#200 Sieve	6.4		Pbe (%) by Wt	4.4

Other Layer Properties					
Subgrade		Aggregate Base		Chemically-Stabilized Base	
Type	A-4	Type	A-1-a	Type	-
Resilient Modulus (psi)	5500	Resilient Modulus (psi)	Default	Other Values	-

OR 120: End Jcp-Beg Hwy 081

Traffic Info		Climatic Info	
Initial Two-way AADTT	7010	Latitude	45.607822
No of Lanes in Design Direction	2	Longitude	-122.687225
Growth Rate (%)	0	Elevation	22.391
Lane Distribution Factor	0.90	Depth to Water Table (ft)	10
Speed Limit (MPH)	45		

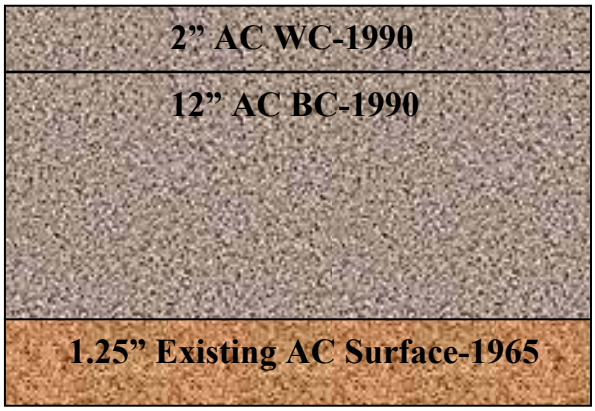

HMA Layer Properties				
Aggregate Gradation (% passing)		Asphalt Binder Grade	Volumetric Properties (In place)	
3/4 in. Sieve	99	PG 64-28	Effective Binder Content, Pbe (%)	11.53
3/8 in. Sieve	69		Air Voids (%)	4
#4 Sieve	48		Unit Weight (lb/ft^3)	143.8
#200 Sieve	4.9		Pbe (%) by Wt	5.2

Other Layer Properties					
Subgrade		Aggregate Base		Chemically-Stabilized Base	
Type	A-4	Type	-	Type	-
Resilient Modulus (psi)	5500	Resilient Modulus (psi)	-	Other Values	-

OR 201: Washington Ave-Airport Way

Traffic Info		Climatic Info	
Initial Two-way AADTT	620	Latitude	44.032197
No of Lanes in Design Direction	1	Longitude	-117.002935
Growth Rate (%)	5	Elevation	2151.704
Lane Distribution Factor	1	Depth to Water Table (ft)	10
Speed Limit (MPH)	55		

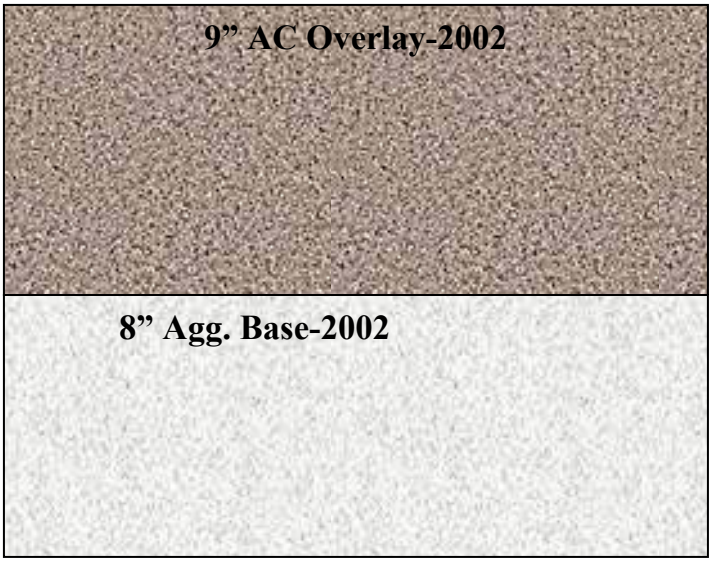

HMA Layer Properties				
Aggregate Gradation (% passing)		Asphalt Binder Grade	Volumetric Properties (In place)	
3/4 in. Sieve	99	PG 64-28	Effective Binder Content, Pbe (%)	11.53
3/8 in. Sieve	69		Air Voids (%)	4
#4 Sieve	48		Unit Weight (lb/ft^3)	143.8
#200 Sieve	4.9		Pbe (%) by Wt	5.2

Other Layer Properties					
Subgrade		Aggregate Base		Chemically-Stabilized Base	
Type	A-4	Type	A-1-a	Type	-
Resilient Modulus (psi)	5500	Resilient Modulus (psi)	-	Other Values	-

OR 140: Jct Hwy 019-Bowers Bridges Creek

Traffic Info		Climatic Info	
Initial Two-way AADTT	160	Latitude	42.188772
No of Lanes in Design Direction	1	Longitude	-120.345792
Growth Rate (%)	0	Elevation	4794.002
Lane Distribution Factor	1	Depth to Water Table (ft)	10
Speed Limit (MPH)	40		

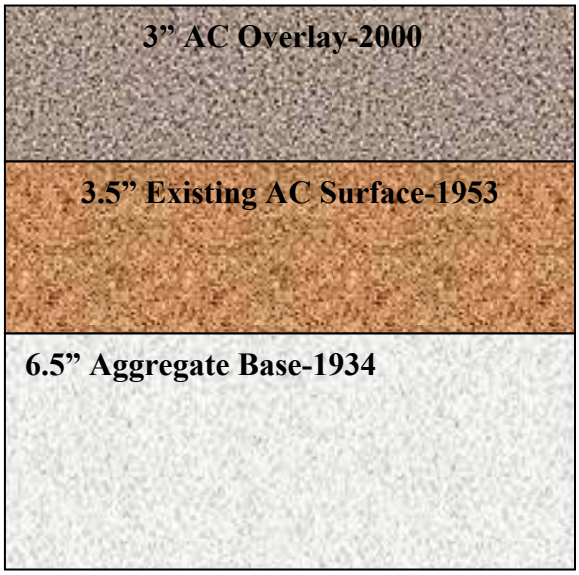

HMA Layer Properties				
Aggregate Gradation (% passing)		Asphalt Binder Grade	Volumetric Properties (In place)	
3/4 in. Sieve	100	PG 64-28	Effective Binder Content, Pbe (%)	13.95
3/8 in. Sieve	81.5		Air Voids (%)	3.84
#4 Sieve	50.5		Unit Weight (lb/ft^3)	153.32
#200 Sieve	6		Pbe (%) by Wt	5.9

Other Layer Properties					
Subgrade		Aggregate Base		Chemically-Stabilized Base	
Type	A-4	Type	A-1-a	Type	-
Resilient Modulus (psi)	5500	Resilient Modulus (psi)	Default	Other Values	-

US 97: N. Chiloquin Intch-Williamson Dr

Traffic Info		Climatic Info	
Initial Two-way AADTT	3570	Latitude	42.577636
No of Lanes in Design Direction	1	Longitude	-121.866126
Growth Rate (%)	0	Elevation	4179.410
Lane Distribution Factor	1	Depth to Water Table (ft)	5
Speed Limit (MPH)	40		

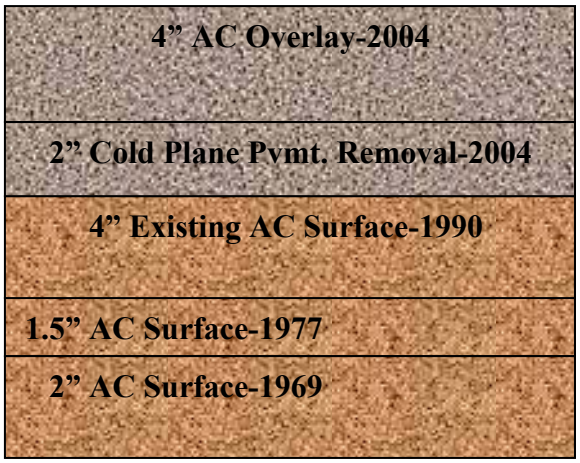

HMA Layer Properties				
Aggregate Gradation (% passing)		Asphalt Binder Grade	Volumetric Properties (In place)	
3/4 in. Sieve	100	PG 70-28	Effective Binder Content, Pbe (%)	12.42
3/8 in. Sieve	75		Air Voids (%)	3.93
#4 Sieve	40		Unit Weight (lb/ft^3)	146.27
#200 Sieve	6.7		Pbe (%) by Wt	5.5

Other Layer Properties					
Subgrade		Aggregate Base		Chemically-Stabilized Base	
Type	A-4	Type	-	Type	-
Resilient Modulus (psi)	5500	Resilient Modulus (psi)	-	Other Values	-